ABSTRACT

DEYESO III, ROBERT LEONARD. Obstructing Exceptional Surgeries using Immersed Curves. (Under the direction of Tye Lidman).

We study toroidal and reducible surgeries along knots in S^3 using Heegaard Floer homology via immersed curves techniques. Surgeries that contain a Klein bottle are often examples of the former type, and are presentable as a gluing of the twisted I-bundle over the Klein bottle to a knot manifold. We use a genus bound on the surgery slope due to Ichihara and Teragaito to study such gluings with a knot complement of S^3. Toward reducible surgeries, the Cabling Conjecture of González-Acuña and Short holds that only cable knots admit them. It is one of the largest open problems in low-dimensional topology, and has been verified for many types of knots. We show that almost all thin knots satisfy the conjecture, with possible exception coming from a (possibly non-existent) collection of thin, hyperbolic, L-space knots. This also serves as a reproof that the Cabling Conjecture is satisfied by alternating knots.

Obstructing Exceptional Surgeries using Immersed Curves

by
Robert Leonard DeYeso III

A dissertation submitted to the Graduate Faculty of
North Carolina State University
in partial fulfillment of the
requirements for the Degree of
Doctor of Philosophy

Mathematics

Raleigh, North Carolina
2022

APPROVED BY:

Radmila Sazdanovic	Ernest Stitzinger
Adam Levine	Tye Lidman Chair of Advisory Committee

DEDICATION

To my family.

BIOGRAPHY

The author grew up in a military family, regularly moving between states with a brief period in Japan. He followed both of his sisters in attending the University of Tennessee at Martin, graduating in 2015. He then moved to Raleigh, North Carolina to begin a graduate program in mathematics at North Carolina State University. At the time of writing, he is overjoyed to join the topology group at the University of Iowa as an RTG-postdoctoral researcher.

ACKNOWLEDGEMENTS

I would like to thank my parents, Bob and Lynn, for instilling within me a desire to think critically. They were regular practitioners of this throughout my upbringing, providing the perfect environment for the mathematically-minded. I am appreciative of the inseparable bond I have with my two sisters, Cheryl and Jennifer. When at my lowest, they did not hesitate to lift me up even when encumbered by their own duties.

I am grateful for the very talented mathematics department at the University of Tennessee at Martin for fostering the best undergraduate environment that any student could want. The full sequences in algebra and analysis by Louis Kolitsch and Chris Caldwell were excellent preparation for the graduate level. Additionally, I am indebted to Jason DeVito for being the perfect mentor for undergraduate research.

I benefited greatly from joining the topology group at NC State. This decision came after the immaculate introductory sequence by Radmila Sazdanovic, who continued to encourage me even after I foolishly mentioned not wanting to study knot theory. In close proximity at Duke, Adam Levine was greatly helpful both by welcoming me to their weekly seminar and by demystifying various aspects of bordered Heegaard Floer homology. I also thank Jonathan Hanselman for showcasing the immersed curves formulation of bordered invariants during a serendipitous Duke seminar, and for setting aside time to field my questions about the construction.

Outside of the research triangle, I must thank Jen Hom for aiding me with the nuances of the mapping cone formula connecting knot Floer and Heegaard Floer homology. As one of the organizers of the excellent Tech Topology conferences and workshops, Jen has often given me the opportunity to speak and develop. Likewise I am grateful to Ken Baker, Robert Lipshitz, and Liam Watson for their interest in my work and comments on preprints, as well as inviting me to speak in their seminars. The topology community has been more welcoming and compassionate than I ever could have anticipated.

I wholeheartedly thank Tye Lidman for taking me on as a student. Tye went above and beyond even generous levels of mentorship to guide me through graduate school, contending with my initial tendencies of apathy and unreliability. With seemingly unending patience and enthusiasm, Tye introduced me to a multitude of fascinating areas in low-dimensional topology with the utmost expertise. It is not an understatement to say that I likely would have left if not for their support. I was partially supported by NSF grant DMS-1709702.

TABLE OF CONTENTS

LIST OF FIGURES

CHAPTER

1

INTRODUCTION

1.1 Background

Following the success of the h-cobordism theorem of Smale for large dimensions (≥ 5) [Sma61] and classical results for small dimensions, current classification efforts in geometric topology focus on 3- and 4-dimensional manifolds. This is the domain of low-dimensional topology, and the strategy for studying 3-manifolds often involves decomposing them along submanifolds into more understood pieces. They may be decomposed along 2-spheres, annuli, and tori [JS79, Joh79], resulting in pieces with specific geometries due to Thurston's Geometrisation conjecture [Thu82], established by Perelman [KL08].

Such pieces often arise from a construction called Dehn surgery, which is a process of constructing a 3-manifold using a knot as follows. Given $K \subset S^3$, excise its solid torus neighborhood from S^3 to obtain its exterior $S^3 \setminus \nu K$, and then glue a solid torus back in along a map between their boundaries. The homology class of the attaching solid torus's meridian in $\partial(S^3 \setminus \nu K)$, represented as a slope $r \in \mathbb{Q} \cup \left\{\frac{1}{0}\right\}$, determines the resulting manifold. We denote the result of r-surgery along K by $S^3_r(K)$, and say that a manifold is realizable as surgery if it may be obtained in this way.

Lickorish and Wallace showed that all closed, connected, orientable 3-manifolds may be obtained by integral Dehn surgery on a link in S^3 [Lic62, Wal60]. It is then important to understand surgery descriptions of 3-manifolds that arise as surgery on just a knot. A 3-manifold that contains an essential 2-sphere is called reducible, and the knots which admit reducible surgeries are the subject of the Cabling Conjecture [GAnS86]. On the other hand, Thurston's hyperbolic Dehn surgery theorem shows that a hyperbolic knot K, which is a knot whose exterior has hyperbolic geometry, admits surgeries $S^3_r(K)$ that are hyperbolic for all but finitely many slopes r [Thu78]. Dubbed exceptional, these non-hyperbolic surgeries of K are then rare enough to warrant classification. Surgeries along a hyperbolic knot containing a Klein bottle are exceptional, and together with reducible surgeries these are our two main focuses. In order to study these surgeries, we use various invariants of knots and manifolds.

Denoted *HF*, Ozsváth's and Szabó's Heegaard Floer homology is a collection of various "flavors" of graded homology theories that utilize Lagrangian Floer homology [OS04d]. These invariants have applications to knot theory [OS04a, OS04e, Ni07, Ghi08], contact topology [OS05a], 4-manifold topology [OS04e], and Dehn surgery [OS08, OS11]. Knot Floer homology, due to [OS04b, Ras03], is an invariant for knots similar to the hat-flavor $\widehat{HF}$ of Heegaard Floer homology. The Heegaard Floer homology of a given surgery is determined by the knot Floer homology of the surgery knot [OS08], and this connection has led to fruitful approaches in three big open problems in Dehn surgery; the Berge Conjecture [OS05b, BGH08, Hed11], the Cosmetic Surgery Conjecture [Wan06, NW15, Han19], and the Cabling Conjecture [HLZ15, Jab15]. We will involve this connection in an alternate way, by using bordered Heegaard Floer homology.

Lipshitz, Ozsváth, and Thurston introduced bordered Heegaard Floer invariants for manifolds with torus boundary in [LOT18b]. With $M_0 \cup_h M_1$ denoting a gluing of two manifolds along their torus boundaries, they prove a pairing theorem involving the two bordered invariants that recovers the Heegaard Floer homology of the glued 3-manifold. Hanselman, Rasmussen, and Watson reinterpreted these bordered invariants as collections of immersed curves in the punctured torus, and proved an analogous pairing theorem for these curve invariants. Their construction trades the difficulty of computing Floer homology for that of determining the form of the curve invariant associated to the bordered manifolds. For our purposes however, it will be straightforward to determine the requisite curve invariants. These homology theories are presented in more detail later in Chapter 2.

1.2 Main Results

Our objective is to use Heegaard Floer homology to study surgeries that contain either a Klein bottle or an essential 2-sphere, primarily accomplished via immersed curves techniques. We address the former type first before turning to the latter.

1.2.1 Klein Bottle Surgeries

Much is known about surgeries $S^3_r(K)$ containing Klein bottles. Gordon and Luecke [GL95] showed that the surgery slope r is integral when K is hyperbolic, and Teragaito [Ter01] extended this condition to K non-cabled and showed that r is divisible by four. In [IT03], Ichihara and Teragaito gave bounds for $|r|$ in terms of the knot genus $g(K)$ when K is non-cabled, and shortly after showed the same bound holds when K is cabled, albeit allowing rational slopes [IT05]. Their combined results show that if $S^3_r(K)$ contains a Klein bottle with K non-trivial then $|r| \leq 4g(K) + 4$, with equality only occurring for specific knots. If K is hyperbolic then $S^3_r(K)$ is exceptional, and the surgery slope satisfies the tighter bound $|r| \leq 4g(K)$.

Looking at increasing knot genus, we see that the lens spaces containing a Klein bottle are $L(4n, 2n \pm 1)$ [BW69], and Teragaito proved that a genus one knot admitting a surgery containing a Klein bottle is either a trefoil or a Whitehead double [Ter01]. However less is known when $g(K) = 2$. In this case the largest surgeries containing a Klein bottle are $S^3_{\pm 12}(K)$, for $K = T(2, \pm 5)$ or $K = T(2, \pm 3) \# T(2, \pm 3)$ due to [IT05, Theorem 1]. The next largest slope to consider is then $|r| = 8$, which is where we specialize.

Suppose X is realizable as 8-surgery along a genus two knot K, and contains a Klein bottle. There is a convenient torus along which to decompose X, that arises as the boundary of the twisted I-bundle over the Klein bottle. Denoted N, this object is the regular neighborhood of a Klein bottle in X. While X can then be decomposed as a gluing of N to a knot manifold, or rational homology solid torus, we will focus on gluings with S^3 knot complements so that $X = (S^3 \setminus \nu J) \cup_h N$ for some knot $J \subset S^3$. The gluing h and its effects on X are studied in Subsection 3.1. Through mostly bordered Heegaard Floer methods, we prove

Theorem 1.2.1. *Let $X = S^3_8(K)$ with $g(K) = 2$ contain a Klein bottle, and write $X = M \cup_h N$. If $M = S^3 \setminus \nu J$, then X is the Seifert fibered manifold $(-1; \frac{1}{2}, \frac{1}{2}, \frac{2}{5})$ with base orbifold S^2, J is the unknot, and $K = T(2, 5)$.*

The theorem is stated in terms of positive surgery, but the analogous result for negative

surgery holds with $K = T(2, -5)$. In order to obstruct the complements $S^3 \setminus \nu J$ in gluing, we use the large surgery theorem of Osváth-Szabó and Rasmussen [OS04b, Ras03] for Heegaard Floer homology; bordered Heegaard Floer invariants due to Lipshitz, Osváth, and Thurston [LOT18b]; and their immersed curves formulation developed by Hanselman, Rasmussen, and Watson [HRW16, HRW18]. The versatility of the immersed curves package lends itself toward studying Dehn surgery problems, and has already led to fruitful results towards the cosmetic surgery conjecture (see [Han19]).

The results in Theorem 1.2.1 actually hold for complements of knots J in integer homology sphere L-spaces Y. These are integer homology spheres Y with the simplest Heegaard Floer homology, which is to say dim $\widehat{HF}(Y) = |H_1(Y, \mathbb{Z})|$. Figure 1.1 shows the immersed curves machinery for $(S^3 \setminus \nu T(2, 3)) \cup_h N$, where the count of intersection points corresponds to dim $\widehat{HF}(X)$. This manifold (along with an integral family depending on h) are toroidal L-spaces, and were known to Hanselman, Rasmussen, and Watson in [HRW18]. Theorem 1.2.1 shows that these toroidal manifolds cannot be realized as surgery along a knot.

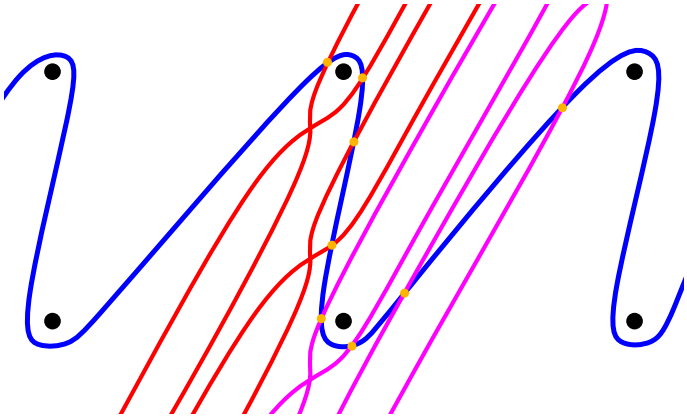

Figure 1.1: The pairing of immersed curves for $S^3 \setminus \nu T(2, 3)$ in blue and N in red and purple, that computes $\widehat{HF}((S^3 \setminus \nu T(2, 3)) \cup_h N)$.

Ichihara and Teragaito remark that the 2-bridge knot 6_2 admits an 8-surgery containing a Klein bottle [IT03, Example 5.6]. This knot is not an L-space knot, and so Theorem 1.2.1 then implies that $S^3_8(6_2)$ is obtained as $Y \setminus \nu J$ glued to N, with Y not an integer homology sphere L-space. This example highlights that gluing along integer homology sphere L-space complements is special. Additionally, there are many examples of genus

two cabled knots in S^3 admitting rational surgeries $S^3_{8/q}(K)$ that contain Klein bottles. When K is a torus knot, the only example arises from the dihedral manifold obtained by Dehn filling N stated in Theorem 1.2.1. Otherwise K is the $(2,1)$-cable of a genus one knot, and there are many rationally sloped fillings of the associated cable space for $S^3 \setminus \nu K$ that yield Klein bottles [Gor83, Corollary 7.3].

1.2.2 Reducible Surgeries

If $S^3_r(K)$ is a reducible manifold, meaning it contains an essential 2-sphere, we will call r a reducing slope. The primary example of a reducible surgery to keep in mind is when K is the (p,q)-cable of some knot K' and r is given by the cabling annulus. In this case, we have $S^3_{pq}(K) \cong L(p,q) \# S^3_{\frac{1}{p}}(K')$. The Cabling Conjecture asserts that this is the only example of a reducible surgery.

Conjecture 1.2.2 (Cabling Conjecture, Gonzalez-Acuña – Short [GAnS86])**.** *If K is a knot in S^3 which has a reducible surgery, then K is a cabled knot and the reducing slope is given by the cabling annulus.*

The Cabling Conjecture is satisfied by many classes of knots. Torus knots, as cables of the unknot, were shown to satisfy the conjecture in [Mos71]. Additionally, satellite [Sch90] and alternating knots [MT92] satisfy the conjecture as well. To establish this conjecture in full, it remains to show that it is satisfied by hyperbolic knots. Our aim is shorter, as we consider thin, hyperbolic knots.

We will present knot Floer homology in more detail in Section 2.2, but for now recall that $\widehat{HFK}(K)$ with coefficients in $\mathbb{F}_2$ is bigraded with Alexander and Maslov gradings, respectively A and M. A knot K is *Floer homologically thin* if the generators of $\widehat{HFK}(K)$ all have the same $\delta = A - M$ grading. This family contains alternating knots [OS03b], and the more generalized quasi-alternating knots [OS05c]. We say K is an *L-space knot* if it admits a surgery to a (Heegaard Floer) L-space, which is a manifold with the simplest Heegaard Floer homology. Using Heegaard Floer homology via immersed curves techniques, we show that

Theorem 1.2.3. *If a thin, hyperbolic knot K in S^3 admits a reducible surgery, then K is an L-space knot and the reducing slope must be $r = 2g(K) - 1$ after mirroring K if necessary.*

It is conjectured that the only thin, L-space knots are the torus knots $T(2,n)$. Provided this is true, there would not exist thin, hyperbolic, L-space knots and so Theorem

1.2.3 would show that all thin knots satisfy the Cabling Conjecture. While stated for thin, hyperbolic knots, this theorem holds more generally for non-cabled knots. This is because we use the Matignon-Sayari genus bound, stated blow, to only need to consider $r \leq 2g(K) - 1$. The case where $r > 2g(K) - 1$ can be handled using our proof strategy to conclude that $K = T(2, n)$, but perhaps more immediate is the result of Dey that cables of non-trivial knots are not thin [Dey19]. The only alternating, L-space knots are the $T(2, n)$'s [OS05b], and so Theorem 1.2.3 also provides an immersed curves reproof that alternating knots satisfy the Cabling Conjecture.

Corollary 1.2.4. *Alternating knots satisfy the Cabling Conjecture.*

The next corollary follows because the only thin, slice, L-space knot is the unknot.

Corollary 1.2.5. *Thin, slice knots satisfy the Cabling Conjecture.*

Corollary 1.2.6. *Thin knots cannot admit two reducible surgeries.*

Part of the proof strategy for Theorem 1.2.3 involves obstructing an $\mathbb{R}P^3$ connected summand, and so we get the following corollary with identical proof to that of [HLZ15, Corollary 1.5].

Corollary 1.2.7. *If K is a thin, hyperbolic knot, then $S^3 \setminus \nu K$ does not contain properly embedded punctured projective planes.*

When K is a non-trivial knot in S^3 with reducible surgery $S^3_r(K)$, the surgery decomposes as a connected sum and the reducing slope satisfies $r \neq 0$ [Gab87]. We saw from the cabled knot example that the reducing slope is an integer and one of the connected summands is a lens space. The former and latter conditions occur for all reducible surgeries due to [GL87] and [GL89], respectively. A reducible surgery can admit at most three connected summands due to the combined efforts of [Say98, VS99, How02], in which case two summands are lens spaces and the remaining summand is an integer homology sphere. Since $S^3_r(K)$ must have a non-trivial lens space summand, the integral reducing slope r satisifes $r \neq -1, 0, 1$. In [MS03], Matignon and Sayari provide the following genus bound if K is non-cabled:

$$1 < |r| \leq 2g(K) - 1.$$

Heegaard Floer homology satisfies a Künneth formula for connected sums, and has proved very useful for studying Dehn surgery. If surgery along K produces precisely a connected sum of two lens spaces, then K must be a cabled knot due to [Gre15]. Further,

[Gre15] together with [BZ98] shows that a hyperbolic knot in S^3 cannot admit both a lens space surgery and a reducible surgery. Hom, Lidman, and Zufelt showed that a hyperbolic, L-space knot can admit at most one reducing slope, and the slope must be $2g(K) - 1$ after mirroring the knot to make the slope positive [HLZ15]. To obtain this result they established a periodicity structure to the Heegaard Floer homology of a reducible surgery, which will be invaluable to the proof strategy of Theorem 1.2.3. Inspired by Hanselman's approach to the Cosmetic Surgery Conjecture using immersed curves techniques [Han19], we will leverage this periodicity structure to severely constrain the types of permissible curve invariants.

1.3 Organization

Unless stated otherwise, all manifolds are assumed to be compact, connected, and orientable 3-manifolds and coefficients in Floer homology belong to $\mathbb{F} = \mathbb{F}_2$. We denote closed manifolds by X or Y, and manifolds with (typically torus) boundary by M. Also knots $J \subset Y$ bounding a disk are said to be trivial, and figures will have the immersed curves invariant for knot complements in blue and the filling manifold in red. All surgeries are assumed to be positively-sloped, achieved by mirroring the knot if necessary.

The thesis is organized as follows. Chapter 2 summarizes the relevant background from Heegaard Floer, knot Floer, and bordered Heegaard Floer homology. Readers familiar with these homology theories are encouraged to skip to Subsection 2.3.2 for the overview of immersed curves invariants, their general properties and form, as well as their associated pairing theorem and Maslov grading.

In Chapter 3 we approach Klein bottle surgeries by introducing the possible gluings h, and establish two of the three lemmas on the way to proving Theorem 1.2.1. We handle the case that J is trivial in Lemma 3.2.1, showing that X must be a dihedral manifold that falls under Doig's classification of finite, non-cyclic surgeries for $p \leq 9$ in [Doi15]. We then consider gluings with J non-trivial in Lemma 3.3.1, showing that J must be a trefoil in order to possibly have the right Floer homology for X. Chapter 4 provides a brief overview of the refined grading on bordered invariants and their relation to the relative $\mathbb{Q}$-grading on $\widehat{HF}$ under pairing. This extra structure is sufficient to establish the final lemma needed to complete the proof of Theorem 1.2.1, showing that the toroidal gluings involving trefoil complements are obstructed.

Chapter 5 changes pace to reducible surgeries along thin knots. It expands on the

relative Maslov grading for immersed curves invariants of complements of thin knots, and along the way we set up formulas for components of the grading difference formula in terms of $\tau(K)$. The proof of Theorem 1.2.3 is divided into a collection of lemmas depending on r in relation to $\tau(K)$ and $g(K)$. In particular, the cases with $|\tau(K)| < g(K)$ are handled here. Chapter 6 resolves the remaining cases, with some requiring absolute grading information, before addressing the proof of Theorem 1.2.3.

CHAPTER

2

HEEGAARD FLOER HOMOLOGY AND IMMERSED CURVES

Our method of studying Dehn surgery involves generating obstructions using the simplest flavor of Heegard Floer homology. This is primarily accomplished using immersed curves techniques, which are related to bordered Heegaard Floer invariants. We will need the curve invariant associated to a knot complement, which will require some knot Floer homology to a small degree. We briefly introduce each of these homology theories to the extent they are ultimately called upon.

2.1 Heegaard Floer Homology

Let Y be a closed, connected, orientable 3-manifold equipped with a spin^c structure $\mathfrak{s}$. Our immediate goal is to define our primary invariant: the "hat"-flavor of Heegaard Floer homology $\widehat{HF}(Y, \mathfrak{s})$. This was introduced by Ozsváth and Szabó in [OS04d] among a family of graded homology theories, and will be taken to be graded vector space over $\mathbb{F} = \mathbb{F}_2$. The "Heegaard" part of the invariant comes from a Heegaard splitting of Y and

provides us with the generators of its chain complex, while the "Floer" part determines the differential between them.

Definition 2.1.1. A genus g handlebody is a regular neighborhood of $\vee_g S^1$ in $\mathbb{R}^3$. A Heegaard splitting of a 3-manifold Y is a decomposition $Y = H_1 \cup_f H_2$, where H_1 and H_2 are handlebodies of equal genus and f is an orientation-reversing homeomorphism from ∂H_2 to ∂H_1.

It is straightforward to show that any 3-manifold Y admits a Heegaard splitting. Since Y is triangulable, we may consider H_1 to be a regular neighborhood of its 1-skeleton, which in turn gives H_2 as the regular neighborhood of the dual 1-skeleton. We will typically describe a Heegaard splitting via a Heegaard diagram, which is characterized by a collection of curves in $\partial H_1 = \partial H_2 = \Sigma$ that encode handle attachments to rebuild Y from $\Sigma \times [0, 1]$.

Definition 2.1.2. A Heegaard diagram associated to a Heegaard splitting $Y = H_1 \cup_f H_2$ is a triple $\mathcal{H} = (\Sigma, \alpha, \beta)$ such that

1. Σ is a closed, oriented surface of genus g.
2. $\alpha = \{\alpha_1, \ldots, \alpha_g\}$ is a collection of linearly-independent, pairwise disjoint attaching circles that each bound a disk in H_1.
3. $\beta = \{\beta_1, \ldots, \beta_g\}$ is a collection of linearly-independent, pairwise disjoint attaching circles that each bound a disk in H_2.

We will need to consider *pointed* Heegaard diagrams, which incorporate an extra decoration in the form of a basepoint z in $\Sigma - \alpha - \beta$. To a pointed Heegaard diagram $(\Sigma, \alpha, \beta, z)$ of a 3-manifold Y, Ozsváth and Szabó associate a chain complex $\widehat{CF}(\mathcal{H})$ as follows. Consider the g-dimensional tori $\mathbb{T}_\alpha = \alpha_1 \times \cdots \times \alpha_g$ and $\mathbb{T}_\beta = \beta_1 \times \cdots \times \beta_g$ contained in the g-fold symmetric product $\mathrm{Sym}^g(\Sigma)$. The chain complex $\widehat{CF}(\mathcal{H})$ is freely generated by the intersections between $\mathbb{T}_\alpha$ and $\mathbb{T}_\beta$, and its differential $\partial : \widehat{CF}(\mathcal{H}) \to \widehat{CF}(\mathcal{H})$ counts pseudoholomorphic Whitney disks between them in $\mathrm{Sym}^g(\Sigma)$ that avoid $\{z\} \times \mathrm{Sym}^{g-1}(\Sigma)$.

Definition 2.1.3. Let $\mathbf{x}, \mathbf{y} \in \mathbb{T}_\alpha \cap \mathbb{T}_\beta$ and $\mathbb{D} \subset \mathbb{C}$. A *Whitney disk* from $\mathbf{x}$ to $\mathbf{y}$ is a continuous map $\phi : \mathbb{D} \to \mathrm{Sym}^g(\Sigma)$ satisfying

1. $\phi(-i) = \mathbf{x}$,
2. $\phi(i) = \mathbf{y}$,

3. $\phi(\mathrm{Re}(\partial\mathbb{D}) \geq 0) \subset \mathbb{T}_\alpha$,

4. $\phi(\mathrm{Re}(\partial\mathbb{D}) \leq 0) \subset \mathbb{T}_\beta$.

The set of homotopy classes of Whitney disks from $\mathbf{x}$ to $\mathbf{y}$ will be denoted by $\pi_2(\mathbf{x}, \mathbf{y})$.

A choice of complex structure on Σ induces a complex structure on $\mathrm{Sym}^g(\Sigma)$. For $\phi \in \pi_2(\mathbf{x}, \mathbf{y})$, let $\mathcal{M}(\phi)$ be the moduli space of holomorphic representatives of ϕ. This space is shown to be generically smooth [OS04d], and the Maslov index $\mu(\phi)$ denotes the expected dimension of $\mathcal{M}(\phi)$. The automorphisms of $\mathbb{D}$ that preserve i and $-i$ provide an $\mathbb{R}$-action on $\mathcal{M}(\phi)$, and so $\widehat{\mathcal{M}}(\phi) = \mathcal{M}(\phi)/\mathbb{R}$ is a compact, zero-dimensional manifold when $\mu(\phi) = 1$. Finally, by letting $n_z(\phi)$ denote the algebraic intersection between $\phi(\mathbb{D})$ and $\{z\} \times \mathrm{Sym}^{g-1}(\Sigma)$, the differential $\partial : \widehat{CF}(\mathcal{H}) \to \widehat{CF}(\mathcal{H})$ is given by

$$\partial \mathbf{x} = \sum_{\mathbf{y} \in \mathbb{T}_\alpha \cap \mathbb{T}_\beta} \sum_{\substack{\phi \in \pi_2(\mathbf{x}, \mathbf{y}) \\ \mu(\phi) = 1 \\ n_z(\phi) = 0}} \#\widehat{\mathcal{M}}(\phi)\mathbf{y}.$$

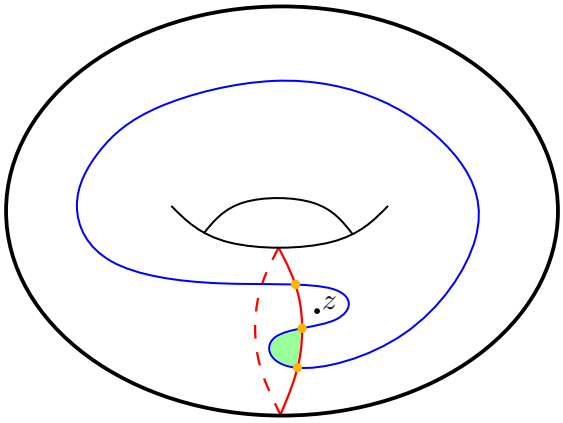

Figure 2.1: A Whitney disk between generators associated to an atypical Heegaard diagram for S^3.

We will think of $\mathrm{Spin}^c(Y)$ in terms of homology classes of vector fields on Y (see [**?**]), which are in one-to-one correspondence with $H^2(Y; \mathbb{Z})$. Ozsváth and Szabó show in [OS04d] that the intersections $\mathbb{T}_\alpha \cap \mathbb{T}_\beta$ may be placed in equivalence classes in bijection with $\mathrm{Spin}^c(Y)$ as follows. Let f be a self-indexing Morse function compatible with the Heegaard diagram $\mathcal{H}$, meaning $f^{-1}([0, \frac{3}{2}]) = H_1$, $f^{-1}([\frac{3}{2}, 3]) = H_2$, and $f^{-1}(\frac{3}{2}) = \Sigma$. An

intersection $\mathbf{x} \in \mathbb{T}_\alpha \cap \mathbb{T}_\beta$ connects the index one critical points to the index two critical points along a g-tuple of gradient flow lines of f. The index zero and index three critical points are connected by a flow line determined by the basepoint z, and deleting these neighborhoods of these $g+1$ flow lines yields a non-vanishing gradient vector field Δf. The flow lines connect critical points of opposite parities, so the vector field may be extended as a non-vanishing vector field over Y.

The homology class of this vector field is the Spin^c structure $\mathfrak{s}(\mathbf{x})$, and two intersections $\mathbf{x}$ and $\mathbf{y}$ describe the same spin^c structures if $\mathfrak{s}(\mathbf{y}) - \mathfrak{s}(\mathbf{x}) = 0 \in H^2(Y, \mathbb{Z})$. This implies that the Heegaard Floer chain complex decomposes over spin^c structures as

$$\widehat{CF}(\mathcal{H}) = \bigoplus_{\mathfrak{s} \in \mathrm{Spin}^c(Y)} \widehat{CF}(\mathcal{H}, \mathfrak{s}).$$

Ozsváth and Szabó prove that $H_*(\widehat{CF}(\mathcal{H}, \mathfrak{s}), \partial)$ is an invariant of $(Y, \mathfrak{s})$ by showing that it is ultimately independent of the choice of Heegaard diagram $\mathcal{H}$, basepoint z, and complex structure on Σ [OS04d]. Accordingly, we will use $\widehat{HF}(Y, \mathfrak{s})$ to denote them going forward.

While we will primarily use $\widehat{HF}$, various other flavors of Heegaard Floer homology are constructed by considering the larger chain complex $CF^\infty(Y, \mathfrak{s})$. It is freely-generated by intersections $\mathbb{T}_\alpha \cap \mathbb{T}_\beta$ over $\mathbb{F}[U, U^{-1}]$ instead of just $\mathbb{F}$, where U is a formal variable associated to $n_z(\phi)$ and the differential ∂ is suitably modified. Denoted HF^-, HF^+, and $\widehat{HF}$, these flavors arise as the homology of quotient complexes of $CF^\infty(Y, \mathfrak{s})$. They are all equipped with a relative $\mathbb{Z}$-grading given by

$$\mathrm{gr}(\mathbf{x}) - \mathrm{gr}(\mathbf{y}) = \mu(\phi) - 2n_z(\phi), \qquad \mathrm{gr}(U) = -1$$

This relative grading, called the Maslov grading, will be crucial to the approach for both Theorems 1.2.1 and 1.2.3.

If Y is a rational homology sphere, then $\dim \widehat{HF}(Y, \mathfrak{s}) \geq 1$ for each $\mathfrak{s}$. When we have equality for all $\mathfrak{s}$, we say Y is a (Heegaard Floer) L-space, generalizing the behavior exhibited by lens spaces. Further, the relative $\mathbb{Z}$-grading on Y may be lifted to an absolute $\mathbb{Q}$-grading [OS03a]. For the "plus" flavor, we may write $HF^+(Y, \mathfrak{s}) \cong \mathcal{T}^+ \oplus HF_{red}(Y, \mathfrak{s})$, where $\mathcal{T}^+ \cong \mathbb{F}[U, U^{-1}]/\mathbb{F}[U]$ denotes the tower submodule. The *d-invariants* $d(Y, \mathfrak{s})$, sometimes called the *Heegaard Floer correction terms*, record the smallest absolutely graded element of $\mathcal{T}^+ \subseteq HF^+(Y, \mathfrak{s})$ [OS03a]. These invariants satisfy a few symmetries, such as spin^c conjugation symmetry $d(Y, \mathfrak{s}) = d(Y, \bar{\mathfrak{s}})$ and orientation-reversal $d(-Y, \mathfrak{s}) = -d(Y, \mathfrak{s})$, as well as additivity for connected sums. It is normalized so that $d(S^3, \mathfrak{s}_0) = 0$, and is

recursively determined for lens spaces in [OS03a, Proposition 4.8]. Presently, we only make use of $\widehat{HF}$ and lightly appeal to $d(Y,\mathfrak{s})$ when necessary. It is difficult to compute $\widehat{HF}(Y,\mathfrak{s})$ using a Heegaard diagram in general, and so we will use an alternate method later on that utilizes a complex related to knot Floer homology.

2.2 Knot Floer Homology

Let K be a knot in S^3. Ozsváth and Szabó [OS04c], and independently Rasmussen [Ras03], associate a bigraded, finitely-generated vector space over $\mathbb{F}$ that decomposes as

$$\widehat{HFK}(K) = \bigoplus_{M,A} \widehat{HFK}_M(K,A).$$

The integers M and A denote the Maslov (or homological) and Alexander gradings, respectively. Knot Floer homology categorifies the Alexander polynomial [OS04b] via

$$\Delta_K(t) = \sum_{M,A} (-1)^M \dim \widehat{HFK}_M(K,A) t^A.$$

The degree of $\Delta_K(t)$ provides a lower bound for $g(K)$ [Sei35], but knot Floer homology strengthens this property. Due to [OS04b], knot Floer homology precisely detects knot genus by

$$g(K) = \max\{A \geq 0 \mid \widehat{HFK}(K,A) \neq 0\}.$$

Together with work of Ghiggini and Ni, knot Floer homology also detects precisely if a knot is fibered [OS04e, Ghi08, Ni07] by

$$K \subset S^3 \text{ fibered } \Leftrightarrow \widehat{HFK}(K, g(K)) \cong \mathbb{F}.$$

Further, these detection results were used in [Ghi08] to show that knot Floer homology precisely detects the figure-eight knot 4_1 and the right- and left-handed trefoils $T(2,\pm 3)$.

Similar to Heegaard Floer homology, the chain complex for knot Floer homology consists of intersections between $\mathbb{T}_\alpha$ and $\mathbb{T}_\beta$ associated to a doubly-pointed Heegaard diagram $(\Sigma, \alpha, \beta, z, w)$ for S^3. The knot K is realized as the union of arcs connecting z and w that avoid the attaching circles and are pushed slightly into the two handlebodies. The differential looks for Whitney disks that avoid both basepoints, while the new Alexander grading determined by $n_z(\phi)$ and $n_w(\phi)$. It ends up being more useful to track disks that

cross either type of basepoint however, resulting in the full knot Floer complex $CFK^\infty(K)$.

Following [OS04c], we can view $CFK^\infty(K)$ as freely-generated over $\mathbb{Z}$ by triples $[\mathbf{x}, i, j]$, where $\mathbf{x} \in \mathbb{T}_\alpha \cap \mathbb{T}_\beta$, $i, j \in \mathbb{Z}$, and $A(\mathbf{x}) = j - i$. Each generator $U^{-i}\mathbf{x}$ corresponds to a triple $[\mathbf{x}, i, j]$, and can be presented in the plane as a dot with coordinates (i, j). Suppose $\phi \in \pi_2(\mathbf{x}, \mathbf{y})$ contributes to $\mathbf{y} \in \partial\mathbf{x}$. In CFK^∞, the differential is given by an arrow between these generators, where the change in horizontal and vertical components are $-n_w(\phi)$ and $-n_z(\phi)$, respectively. Figure 2.2 provides an example of such a diagram for $CFK^\infty(4_1)$.

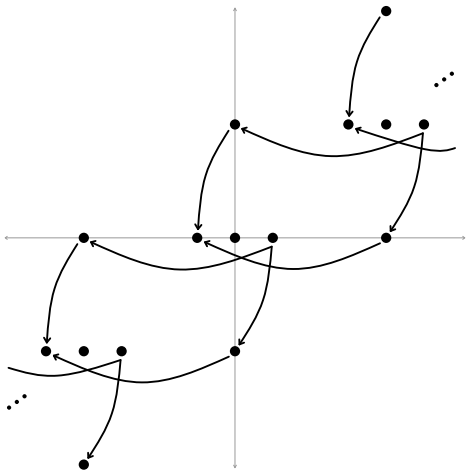

Figure 2.2: A portion of the full knot Floer complex for the figure-eight knot 4_1.

A typical strategy for determining the Heegaard Floer homology of Dehn surgery involves using the Mapping Cone Formula of [OS08]. We will not make full use of this object, but will need its primary components in order to define integral invariants of K useful later on. These components are the following subcomplexes and quotient complexes of CFK^∞:

$$\mathcal{A}_s^+ = C\left\{\max\left\{i, j - s\right\} \geq 0\right\},$$
$$\mathcal{B}_s^+ = C\left\{i \geq 0\right\}.$$

By a careful look at the two constructions, we can see $\mathcal{B}_s^+ \cong CF^+(S^3)$. Additionally, there are chain maps $\mathfrak{v}_s^+ : \mathcal{A}_s^+ \to \mathcal{B}_s^+$ and $\mathfrak{h}_s^+ : \mathcal{A}_s^+ \to \mathcal{B}_{s+r}^+$ between these subcomplexes. Take homology to obtain $A_s^+ = H_*(\mathcal{A}_s^+)$ and $B_s^+ = H_*(\mathcal{B}_s^+) \cong HF^+(S^3)$, and induced maps v_s^+ and h_s^+. As before, $\mathcal{T}^+$ denotes the tower submodule $HF^+(S^3)$. Observe that

$U^N(A_s^+) \cong \mathcal{T}^+$ for arbitrarily large N. By restricting both v_s^+ and h_s^+ to this submodule, we obtain the restrictions $\overline{v}_s^+$ and $\overline{h}_s^+$. The integral invariants of K that we desire are due to [OS08], and are defined by

$$V_s = \text{rank}(\ker \overline{v}_s^+),$$
$$H_s = \text{rank}(\ker \overline{h}_s^+).$$

These terms will play a large role when studying potential reducible surgeries when K is thin. We will determine them using an alternative geometric method later in Section 5.1. By [HLZ15, Lemma 2.3] the maps v_s^+ and h_{-s}^+ agree on homology after identifying $A_s^+ \cong A_{-s}^+$ (essentially reversing the roles of i and j above), so that $V_s = H_{-s}$. They are by definition non-negative, and also satisfy the following lemma.

Lemma 2.2.1 ([NW15, Lemma 2.4])**.** *The V_s form a non-increasing sequence and the H_s form a non-decreasing sequence, so that*

$$V_s \geq V_{s+1} \text{ and } H_s \leq H_{s+1} \text{ for all } s \in \mathbb{Z}.$$

2.2.1 Heegaard Floer Homology of Dehn Surgery

Equipped with these two Floer homology theories, we can establish a few preliminary propositions and lemmas. We collect ones relevant for Klein bottle surgeries before doing the same for reducible surgeries. Let us identify $\text{Spin}^c(S_r^3(K))$ with $\mathbb{Z}/r\mathbb{Z}$ as in [OS08, Subsection 2.4], and denote the correspondence using $[s] \in \text{Spin}^c(S_r^3(K))$ for $[s] \in \mathbb{Z}/r\mathbb{Z}$. We will also choose equivalence classes for elements of $\mathbb{Z}/r\mathbb{Z}$ as centered about 0, so that for example $\mathbb{Z}/r\mathbb{Z} = \left\{-\frac{r-1}{2}, \ldots, 0, \ldots, \frac{r-1}{2}\right\}$ if r is odd. As an abuse of notation, we will commonly use s for the representative of $[s]$ that falls within this range.

The following theorem shows that $\widehat{HF}(S_r^3(K), [s])$ and $\widehat{A}_s$ are relatively-graded isomorphic if r is large relative to s.

Theorem 2.2.2 ([OS04b, Ras03])**.** *For integral $r \gg 0$ and any $s \in \mathbb{Z}$ with $|s| \leq r/2$, there is an isomorphism*

$$\widehat{HF}(S_r^3(K)), [s]) \cong \widehat{A}_s.$$

Useful for obstructing Klein bottle surgeries in Chapter 3, we may apply this theorem for all spin^c structures of $S_8^3(K)$ with $g(K) = 2$.

Proposition 2.2.3. Let $K \subset S^3$ have $g(K) = 2$. Then $\dim \widehat{HF}(S^3_8(K), [s]) = 1$ for at least five of the eight $[s] \in \mathrm{Spin}^c(S^3_8(K))$.

Proof. We have that $\widehat{A}_{-s}$ and $\widehat{A}_s$ are isomorphic due to Lemma 2.3 of [HLW15], following from the fact that $CFK^\infty(K)$ is filtered chain homotopy equivalent to itself under reversing the roles of i and j. Since $\widehat{HFK}$ detects the knot genus, we have $\widehat{A}_s = \widehat{HF}(S^3) = \mathbb{F}$ for $|s| \geq g(K)$. The surgery slope is sufficiently large ($> 2g(K) - 1$), and so Theorem 2.2.2 implies $\widehat{HF}(S^3_8(K), [s]) \cong \mathbb{F}$ for $s \in \mathbb{Z}$ satisfying $[s] \neq 0, \pm 1 \in \mathbb{Z}/8\mathbb{Z}$. □

This simple structure of $\widehat{HF}(S^3_8(K))$ is the first major constraint toward proving Theorem 1.2.1. If $(S^3 \setminus \nu J) \cup_h N$ is realizable as $S^3_8(K)$ with $g(K) = 2$, we will appeal to the number of $\mathfrak{t} \in \mathrm{Spin}^c(X)$ supporting $\dim \widehat{HF}(X, \mathfrak{t}) > 1$ to constrain J. This large surgery is also particularly special because of the following proposition.

Proposition 2.2.4. $S^3_8(K)$ is irreducible for any knot K with $g(K) = 2$.

Proof. To generate a contradiction, suppose that $S^3_8(K)$ is reducible. From [MS03], we see that $S^3_r(K)$ reducible implies $1 < |r| \leq 2g(K) - 1$ for K non-cabled. So it must be the case that K is the (p, q)-cable of some knot K', where p and q are coprime and positive with $p > 1$. The cabling conjecture holds for cable knots, and so the slope $r = pq$ provided by the cabling annulus is the only reducing slope for $S^3_r(K)$. In this case we have $S^3_{pq}(K) \cong L(p, q) \# S^3_{\frac{q}{p}}(K')$, and so $H_1(S^3_8(K))$ cyclic forces

$$S^3_8(K) \cong L(8, 1) \# S^3_{\frac{1}{8}}(K')$$

Let $[\mathfrak{s}_i] \in \mathrm{Spin}^c(S^3_8(K))$ restrict to $[\mathfrak{s}'_j] \times [\mathfrak{s}_0]$, where $[\mathfrak{s}'_j] \in \mathrm{Spin}^c(L(8, 1))$ and $[\mathfrak{s}_0] \in \mathrm{Spin}^c(S^3_{\frac{1}{8}}(K'))$. The Künneth formula for the hat-flavor of Heegaard Floer homology [OS04c, Theorem 1.5] implies

$$\begin{aligned} \widehat{HF}(S^3_8(K), [\mathfrak{s}_i]) &= H_*(\widehat{CF}(L(8, 1), [\mathfrak{s}'_j]) \otimes_{\mathbb{F}} \widehat{CF}(S^3_{\frac{1}{8}}(K'), [\mathfrak{s}])) \\ &= \widehat{HF}(S^3_{\frac{1}{8}}(K'), [\mathfrak{s}]), \end{aligned}$$

since $L(8, 1)$ is a lens space. Theorem 2.2.2 forces $\dim \widehat{HF}(S^3_8(K), [\mathfrak{s}_i]) = \dim \widehat{A}_i$, and since $\dim \widehat{A}_s = 1$ for $|s| \geq g(K)$, we see that $S^3_8(K)$ is an L-space and K' is an L-space knot. From [OS11, Proposition 9.5], the ν invariant for K' must be trivial, which implies K' is the unknot by [OS11, Proposition 9.6]. Therefore K is trivial as the $(8, 1)$-cable of the unknot, and so $S^3_8(K) \cong L(8, 1)$, yielding the desired contradiction. □

We also have the following immediate corollary, which is used in Section 3.2.

Corollary 2.2.5. *Let $M = Y \setminus \nu J$ be a knot manifold. If $X = M \cup_h N$ is realizable as $S^3_8(K)$ for $g(K) = 2$, then M is irreducible.*

For reducible surgeries, we will make extensive use of the following lemma. It is a simplified version of a more general Floer homology periodicity result for HF^+ of a general reducible 3-manifold from [HLZ15], and a special case of it was used in the proof strategy for Proposition 2.2.4. Essentially, we should expect to see repeated behavior among the spin^c summands of $\widehat{HF}(S^3_r(K))$ of a reducible surgery.

Lemma 2.2.6. *Suppose $S^3_r(K) \cong X \# Y$, where X is an L-space and $|H^2(Y)| = k < \infty$. Then for any $[s] \in Spin^c(S^3_r(K))$ and $\alpha \in H^2(S^3_r(K)) \cong \mathbb{Z}/r\mathbb{Z}$, we have $\widehat{HF}(S^3_r(K), [s + k\alpha]) \cong \widehat{HF}(S^3_r(K), [s])$ as relatively-graded $\mathbb{F}$ vector spaces.*

Proof. Let $[s] \in \mathrm{Spin}^c(S^3_r(K))$ restrict to $[s_i] \in \mathrm{Spin}^c(X)$ and $[s_j] \in \mathrm{Spin}^c(Y)$. We see that $\widehat{HF}(X, [s_i]) \cong \mathbb{F}$ since X is an L-space, and so the Künneth formula for $\widehat{HF}$ [OS04c, Theorem 1.5] implies

$$\begin{aligned}\widehat{HF}(S^3_r(K), [s]) &\cong H_*(\widehat{CF}(X, [s_i]) \otimes_{\mathbb{F}} \widehat{CF}(Y, [s_j])) \\ &\cong \widehat{HF}(Y, [s_j]).\end{aligned}$$

For any $\alpha \in \mathbb{Z}/r\mathbb{Z}$, we have that $[s + k\alpha]$ restricts to $[s_j]$ in $\mathrm{Spin}^c(Y)$. Then because $\widehat{HF}(S^3_r(K), [s])$ is independent of $[s_i]$, we obtain

$$\widehat{HF}(S^3_r(K), [s + k\alpha]) \cong \widehat{HF}(Y, [s_j]) \cong \widehat{HF}(S^3_r(K), [s])$$

as relatively-graded $\mathbb{F}$ vector spaces. □

Toward both Klein bottle and reducible surgeries, we will need to appeal to $d(S^3_r(K), [s])$ when relative grading information is insufficient. In [NW15], the d-invariants of rational surgeries are related to those of $d(L(p, q), [s])$ and the H's and V's. We state a special case of the more general result for our purposes.

Proposition 2.2.7 ([NW15, Proposition 1.6])**.** Suppose r is integral and positive, and fix $0 \leq s < r - 1$. Then

$$d(S^3_r(K), [s]) = d(L(r, 1), [s]) - 2 \max\{V_s, V_{r-s}\}.$$

Among many of its applications, this result enables the following lemma.

Lemma 2.2.8 ([HLZ15, Lemma 2.5]). *For all $s \in \mathbb{Z}$, the integers V_s and H_s are related by*

$$H_s - V_s = s.$$

2.3 Bordered Heegaard Floer homology

Bordered Heegaard Floer homology, introduced by Lipshitz, Ozsváth, and Thurston, provides a cut-and-paste style of computing $\widehat{HF}$ for a 3-manifold. This is done by decomposing along a surface, and then recovering Floer homology by a suitable means of pairing the relative Floer invariants for the decomposed pieces [LOT18b]. While defined for general manifolds with connected boundary, we will only be interested in applying the theory to manifolds with torus boundary.

Let M be an orientable 3-manifold with torus boundary and choose α, β in ∂M with $\beta \cdot \alpha = 1$, so that (α, β) forms a parameterization of ∂M. A bordered 3-manifold is such a triple (M, α, β). For a bordered 3-manifold M_2, they associate a differential module called a type D structure $\widehat{CFD}(M_2, \alpha_2, \beta_2)$. For another bordered 3-manifold M_1, they associate a suitably dual object $\widehat{CFA}(M_1, \alpha_1, \beta_1)$, and prove Theorem 2.3.1 below showing that $\widehat{CF}(M_1 \cup_h M_2)$ is modeled by something called the box tensor product between these modules (with corresponding parameterizations).

Theorem 2.3.1 ([LOT18b, Theorem 10.42]). *Consider the pairing $X = M_1 \bigcup_h M_2$, where the M_i are compact, oriented 3-manifolds with torus boundary and $h : \partial M_2 \to \partial M_1$ is an orientation reversing homeomorphism. Then*

$$\widehat{HF}(X) \cong H_*(\widehat{CFA}(M_1, \alpha_1, \beta_1) \boxtimes \widehat{CFD}(M_2, h^{-1}(\beta_1), h^{-1}(\alpha_1))),$$

where the isomorphism is one of relatively graded vector spaces that respects the Spin^c decomposition.

The type A and D structures decompose over spin^c structures on the respective M_i's, and so this implies that

$$\bigoplus_{\substack{\mathfrak{t} \in \mathrm{Spin}^c(X) \\ \mathfrak{t}|_{M_i} = \mathfrak{s}_i}} \widehat{HF}(X, \mathfrak{t}) \cong H_*(\widehat{CFA}(M_1, \alpha_1, \beta_1, \mathfrak{s}_1) \boxtimes \widehat{CFD}(M_2, h^{-1}(\beta_1), h^{-1}(\alpha_1), \mathfrak{s}_2))$$

We will invoke the pairing theorem for all future computations of $\widehat{HF}$ and its relative Maslov grading, albeit in immersed curves form due to Hanselman, Rasmussen, and Watson [HRW16, HRW18] (presented at the end of this section).

2.3.1 The Bordered Invariants

The type A and type D structures are types of modules over the differential graded torus algebra $\mathcal{A} = \mathcal{A}(\mathbb{T})$. This algebra is generated over $\mathbb{F}$ by the elements ρ_1, ρ_2, ρ_3 and idempotents ι_0 and ι_1, and multiplication in $\mathcal{A}$ is described by the quiver in Figure 2.3 and further satisfies the relations $\rho_2\rho_1 = \rho_3\rho_2 = 0$. We will concatenate the multiplication using the common shorthand notation of $\rho_{12} = \rho_1\rho_2$, $\rho_{23} = \rho_2\rho_3$, and $\rho_{123} = \rho_1\rho_2\rho_3$. In this way, $\{\iota_0, \iota_1, \rho_1, \rho_2, \rho_3, \rho_{12}, \rho_{23}, \rho_{123}\}$ is an $\mathbb{F}$-basis for $\mathcal{A}$. Finally, let $\mathcal{I}$ denote the subring of idempotents.

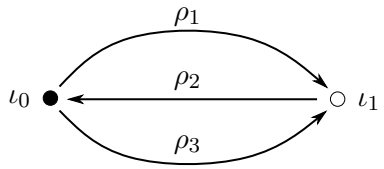

Figure 2.3: A quiver for $\mathcal{A}(\mathbb{T})$.

The module $\widehat{CFA}(M)$ is a type A structure, which is a right-$\mathcal{A}_\infty$ module over $\mathcal{A}$. The module structure comes with a family of maps

$$m_{k+1} : \widehat{CFA}(M) \otimes_{\mathcal{I}} \mathcal{A} \otimes_{\mathcal{I}} \cdots \otimes_{\mathcal{I}} \mathcal{A} \to \widehat{CFA}(M),$$

and we will use commas to separate the tensor factors of m_{k+1} in the future. A type D structure over $\mathcal{A}$ is a left $\mathcal{I}$-module V with a splitting over a left action of the idempotents $V \cong \iota_0 V \oplus \iota_1 V$, equipped with an $\mathcal{I}$-linear map $\delta^1 : V \to \mathcal{A} \otimes V$. The map δ^1 satisfies a compatibility condition that ensures $\partial(a \otimes \mathbf{x}) = a \cdot \delta^1\mathbf{x}$ is a differential on $\mathcal{A} \otimes_{\mathcal{I}} V$. This gives $\mathcal{A} \otimes_{\mathcal{I}} V$ a left differential module structure over $\mathcal{A}$, and we will typically view $\widehat{CFD}(M)$ as this differential module. This type D structure also comes with a collection of recursively defined maps $\delta^k : V \to \mathcal{A}^{\otimes k} \otimes V$ with $\delta^0 : V \to V$ the identity and $\delta^k = (\mathrm{id}_{\mathcal{A}^{\otimes(k-1)}} \otimes \delta^1) \circ \delta^{(k-1)}$.

The chain complex $\widehat{CFA}(M_1, \alpha_1, \beta_1) \boxtimes \widehat{CFD}(M_2, h^{-1}(\beta_1), h^{-1}(\alpha_1))$ in Theorem 2.3.1 is obtained from $\widehat{CFA}(M_1, \alpha_1, \beta_1) \otimes_{\mathcal{I}} \widehat{CFD}(M_2, h^{-1}(\beta_1), h^{-1}(\alpha_1))$, and has differential $\partial^{\boxtimes}$

given by

$$\partial^{\boxtimes}(\mathbf{x}\otimes\mathbf{y}) = \sum_{k=0}^{\infty}(m_{k+1}\otimes \mathrm{id})(\mathbf{x}\otimes\partial^k(\mathbf{y}).$$

This sum is finite if the type D structure is *bounded*, which is to say δ^k vanishes for sufficiently large k. We will refer to it as the box tensor product of the type A and D structures involved. This is a computable model of the $\mathcal{A}_\infty$ tensor product and enables a proof of Theorem 2.3.1. Computations with the box tensor product are cumbersome, and so we will use a geometric interpretation of these invariants as often as possible.

2.3.2 Bordered Invariants as Immersed Curves

In [HRW16, HRW18], Hanselman, Rasmussen, and Watson give a geometric construction of $\widehat{CFD}(M)$ as a collection of immersed curves, and prove an analogue of the pairing theorem that uses these objects. Denoted $\widehat{HF}(M)$, this invariant lives in the punctured torus, which we now define.

Definition 2.3.2. Let the punctured torus T_M be defined as $(H_1(\partial M;\mathbb{R})/H_1(\partial M;\mathbb{Z}))\setminus\{z\}$, where $z=(1-\epsilon,1-\epsilon)$ for ϵ small. We refer to z as the marked point, and orient T_M so that the y-axis projects to α and the x-axis projects to β, with α,β specifying the handle decomposition of $\partial M\setminus z$.

The prototype immersed curves invariant is a type of train track in T_M, a construction we briefly introduce. Along the way, we will apply these concepts to $\widehat{CFD}(N)$, for N the twisted I-bundle over the Klein bottle. Given a type D structure $\widehat{CFD}(M,\alpha,\beta)$ we can conveniently express it as a decorated graph, with vertex set generating V and edge set describing δ^1. Length k directed paths are associated to δ^k, and correspondingly the type D structure is bounded if it admits no directed cycles. The vertices labeled $\bullet$ correspond to ι_0 generators, and those labeled $\circ$ correspond to ι_1 generators. For the edges, a term $\rho_I\otimes\mathbf{x}_2\in\delta^1\mathbf{x}_1$ gives a directed edge labeled $\{I\}$ from $\mathbf{x}_1$ to $\mathbf{x}_2$.

The bordered invariant for N is computed in [BGW13] from a bordered Heegaard diagram (we caution the reader that the opposite idempotent decomposition of the torus algebra $\mathcal{A}(\mathbb{T})$ is used in this reference). Supporting two different Seifert structures, ∂N is parameterized by the dual slopes ϕ_0 and ϕ_1 that correspond to the fiber slope of the structure with base orbifold a Möbius band and $D^2(2,2)$, respectively. The slope ϕ_0 is the rational longitude of N, or the unique slope in ∂N that includes in $H_1(N)$ with finite order [Wat12]. The curve ϕ_1 includes in $H_1(N)$ as twice the generator of the $\mathbb{Z}$ factor, and

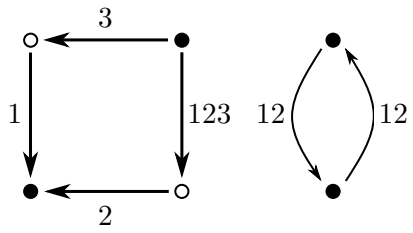

Figure 2.4: Left: $\widehat{CFD}(N, \phi_1, \phi_0, \mathfrak{s}_1)$. Right: $\widehat{CFD}(N, \phi_1, \phi_0, \mathfrak{s}_0)$.

for this reason N admits two torsion spin^c structures $\mathfrak{s}_0$ and $\mathfrak{s}_1$. We will always assume this (standard) parameterization is taken before acting on ∂N. The decorated graph for $\widehat{CFD}(N, \phi_1, \phi_0)$ is shown in Figure 2.4.

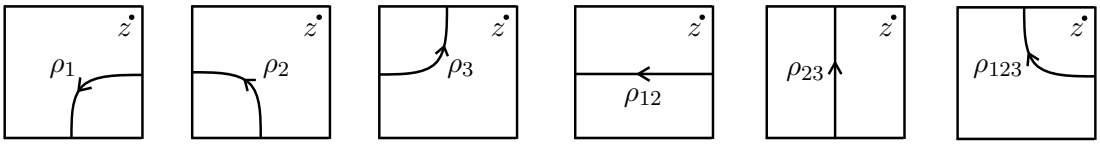

Figure 2.5: Train track segments in T_M corresponding to the $\rho_I \otimes$ terms appearing in δ^1.

Given a decorated graph for $\widehat{CFD}(M, \alpha, \beta)$, we may construct a train track $A(\theta_M)$ in T_M as follows. First, embed the $\bullet$ vertices corresponding to $V_0 = \iota_0 V$ generators along α in the interval $0 \times [\frac{1}{4}, \frac{3}{4}]$, and the $\circ$ vertices corresponding to $V_1 = \iota_1 V$ generators along β in the interval $[\frac{1}{4}, \frac{3}{4}] \times 0$. Next, the edges describing δ^1 are embedded in T_M according to Figure 2.5. We refer to such an $A(\theta_M)$ as a type A realization of $\widehat{CFD}(M, \alpha, \beta)$. For example, this process for $\widehat{CFD}(N)$ is shown in Figure 2.6. For pairing, we will also need the dual type D realization $D(\theta_M)$, which is generated by reflecting $A(\theta_M)$ across the anti-diagonal in T_M.

Now we describe the prototype geometric analogue of Theorem 2.3.1 for a gluing $M_1 \cup_h M_2$ from [HRW16]. Divide T_{M_1} into four quadrants, and include $A(\theta_{M_1})$ in the first quadrant and extend horizontally and vertically. Likewise, include $D(\theta_{M_2})$ into the third quadrant and extend horizontally and vertically. This is shown on the left side of Figure 4.9. Let $\mathcal{C}(A(\theta_{M_1}), D(\theta_{M_2}))$ be the vector space over $\mathbb{F}$ generated by intersections between $A(\theta_{M_1})$ and $D(\theta_{M_2})$, and d^θ a linear map counting bigons analogous to the Whitney disks

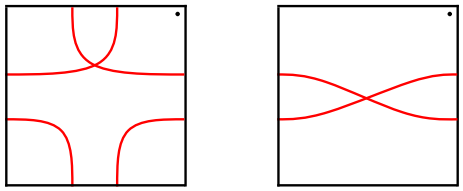

Figure 2.6: The type A realizations for both components of $\widehat{CFD}(N, \phi_1, \phi_0)$.

of Heegaard Floer homology. Hanselman, Rasmussen, and Watson show that under mild hypotheses, $\mathcal{C}(A(\theta_{M_1}), D(\theta_{M_2}), d^\theta)$ forms a chain complex that may be identified with $\mathcal{C}(\widehat{CFA}(M_1, \alpha_1, \beta_1) \boxtimes \widehat{CFD}(M_2, h^{-1}(\beta_1), h^{-1}(\alpha_1)), \partial^{\boxtimes})$ [HRW16, Theorem 16].

2.3.3 Heegaard Floer Homology via Immersed Curves

In general, intersecting train tracks as previously described is not an invariant. This happens for instance if the decorated graph for $\widehat{CFD}(M_i, \alpha_i, \beta_i)$ is not valence 2, so that extended type D structures and local systems need to be employed. However in the examples we encounter, $\widehat{HF}(M)$ is given by $A(\theta_M)$ and requires no extra decoration. This is the case when M is *loop type*, a class of manifold first introduced by Hanselman and Watson in [HW15]. In the course of studying Klein bottle surgeries, we will show that the knot complement $S^3 \setminus \nu J$ is loop type since it admits multiple L-space Dehn fillings [HRW18, Proposition 15]. The twisted I-bundle over the Klein bottle N, as well as knot complements $S^3 \setminus \nu K$ with K thin, have type D structures with the usual boundary parameterization representable as a valence 2 decorated graph. Due to [HW15], this ensures they are loop type as well.

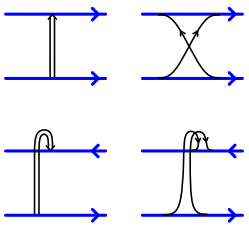

Figure 2.7: Edges of a grading arrow either follow or oppose the orientations of the attached curve components.

If the invariant has multiple curve components, then they are connected by pairs of edges which we denote with a grading arrow. These are presented in Figure 2.7, and they carry an integral weight m useful for determining Maslov grading differences. When considering $M = S^3 \setminus \nu K$, we may lift $\widehat{HF}(M)$ to the infinite cylindrical cover $\pi : \overline{T}_M \to T_M$. This cover is realized as $[-\frac{1}{2}, \frac{1}{2}] \times \mathbb{R}$ with $[-\frac{1}{2}, t]$ and $[\frac{1}{2}, t]$ identified, and where $\pi^{-1}(z) = \left\{(0, \frac{1}{2} + n) \,|\, n \in \mathbb{Z}\right\}$. These lifted marked points reside within a neighborhood of the lift of the meridian $\overline{\mu}$. One of the curves wraps around the cylinder, and we will use $\overline{\gamma}$ to denote this component. Figure 2.8 shows a centered lift of the invariant for the complement of a hypothetical example of a thin knot K with $g(K) = 2$ and $\tau(K) = 1$.

The lifts of the marked points will be taken to lie at purely half-integral heights, so that curve components cross at integral heights. With this at hand, the lifted curve invariant also encodes a few numerical and concordance invariants of K. For example, the Seifert genus is given by the height of the tallest curve component. Additionally, the height around which $\overline{\gamma}$ wraps is precisely the Oszváth-Szabó invariant $\tau(K)$. Hom's ϵ invariant may also be determined by observing what $\overline{\gamma}$ does next. It curve turns downwards, upwards, or continues straight corresponding to $\epsilon(K)$ being 1, -1, and 0, respectively. Notice that $\overline{\gamma}$ is horizontal if $\epsilon(K) = 0$. These two invariants determine the slope $\overline{\gamma}$ outside of a thin vertical strip surrounding the lifts of the marked point, given by $2\tau(K) - \epsilon(K)$. Recall that $\widehat{HFK}(K)$ detects $g(K)$ due to [OS04a]. Looking in $\overline{T}_M$, genus detection manifests itself in $\widehat{HF}(M)$ by ensuring that some curve component crosses at height $g(K)$.

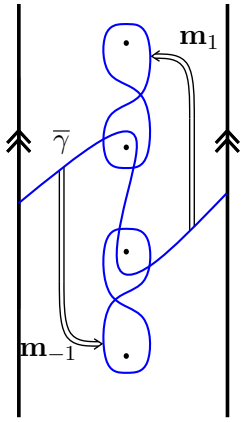

Figure 2.8: An example of $\widehat{HF}(M)$ for $g(K) = 2$ and $\tau(K) = 1$.

The curve invariant (as unlabelled curves) for a general manifold with torus boundary M is invariant under the action by the elliptic involution, with z fixed, of ∂M [HRW18, Theorem 7]. More concretely, Hanselman, Rasmussen, and Watson show that $\widehat{CFD}(M, c(\mathfrak{s})) \cong \mathbf{E} \boxtimes \widehat{CFD}(M, \mathfrak{s})$, meaning that Spin^c conjugation on the level of bordered invariants achieves the same resulting curve invariant as what would arise from the box tensor product with a particular type DA structure associated with elliptic involution. In the form we often use it, this means the curve invariant in $\overline{T}_M$ is unchanged by rotation by π about $(0, 0)$.

Theorem 2.3.3 ([HRW18, Theorem 7]). *The invariant $\widehat{HF}(M)$ is symmetric under the elliptic involution of ∂M. Here, the involution is chosen so that z is a fixed point.*

If K admits either a horizontally or vertically simplified basis for $CFK^-(K)$, then the procedure of [HRW18, Proposition 47] allows one to construct $\widehat{HF}(M)$ from $CFK^-(K)$. The special case when $CFK^-(K)$ is both horizontally and vertically simplified enables us to quickly generate these curves. This condition holds if K is a thin knot, and in particular we have that every arrow encoding the differential in $CFK^-(K)$ has length one. These properties imply two features of $\widehat{HF}(M)$, which are effectively the immersed curves analog of [Pet13, Lemma 7]:

- The essential component $\overline{\gamma}$ winds between adjacent basepoints determined by $\tau(K)$, before ultimately wrapping around the cylinder.
- Any other component is a simple figure-eight, enclosing vertically adjacent lifts of z.

Definition 2.3.4. We say a simple figure-eight component of $\widehat{HF}(M)$ is at height i if it encloses vertically adjacent lifts of z at heights $(0, i \pm \frac{1}{2})$, viewed in $\overline{T}_M$. Further, let e_i denote the number of simple figure-eight components at height i.

We have $e_{-i} = e_i$ due to Theorem 2.3.3, and Figure 2.8 provides an example with $e_0 = 0$ and $e_{-1} = e_1 = 1$. With individual properties of the curve invariants handled, we turn to the main reason for their involvement.

Theorem 2.3.5 ([HRW18, Theorem 2]). *Consider the gluing $M_1 \cup_h M_2$, where the M_i are compact, oriented 3-manifolds with torus boundary and $h : \partial M_2 \to \partial M_1$ is an orientation reversing homeomorphism for which $h(z_2) = z_1$. Then*

$$\widehat{HF}(M_1 \cup_h M_2) \cong HF(\widehat{HF}(M_1), h(\widehat{HF}(M_2))),$$

where intersection Floer homology is computed in T_{M_1} and the isomorphism is one of relatively graded vector spaces that respects the Spin^c decomposition.

More precisely, $HF(\widehat{HF}(M_1), h(\widehat{HF}(M_2)))$ decomposes over spin^c structures on $M_1 \cup_h M_2$ and carries a relative Maslov grading on each spin^c summand. Theorem 2.3.5 places these in correspondence with the spin^c decomposition on $\widehat{HF}(M_1 \cup_h M_2)$, and also ensures the relative Maslov gradings agree. This is best seen when viewing Dehn surgery as such a

gluing, continuing to use M for $S^3 \setminus \nu K$. We have $S^3_r(K) = M \cup_{h_r} (D^2 \times S^1)$ with h_r the slope-r gluing map. Then Theorem 2.3.5 provides

$$\widehat{HF}(S^3_r(K)) \cong HF(\widehat{HF}(M), h_r(\widehat{HF}(D^2 \times S^1)).$$

The spin^c decomposition is recovered by using r vertically-adjacent lifts of $h_r(\widehat{HF}(D^2 \times S^1))$, which is the precise number required to lift every intersection from T_M to $\overline{T}_M$ without duplicates. This is motivated by the example in Figure 2.9, showing the pairing of curves that recovers $\widehat{HF}(S^3_4(T(2,5)))$. The invariant for the solid torus simply consists of a horizontal essential curve, and so $h_4(\widehat{HF}(D^2 \times S^1))$ is a slope 4 curve in the punctured torus. We have four lifts of $h_4(\widehat{HF}(D^2 \times S^1))$, each generating intersections in correspondence with the four spin^c summands of $\widehat{HF}(S^3_4(K))$. These lifts are selected at heights in correspondence with the selected representatives of $\mathbb{Z}/r\mathbb{Z}$ from Subsection 2.2.1. These are $-1, 0, 1$, and 2 for the example in Figure 2.9, and motivate the following definition when lifting further to the tiled-plane cover $\widetilde{T}$.

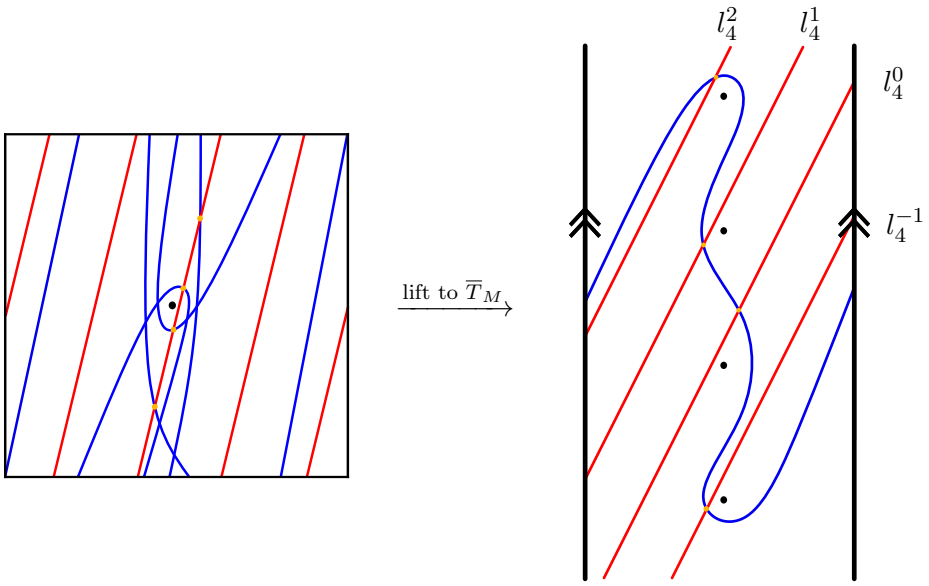

Figure 2.9: The pairing of $\widehat{HF}(S^3 \setminus \nu T(2,5))$ and $h(\widehat{HF}(D^2 \times S^1))$, whose intersection Floer homology is $\widehat{HF}(S^3_4(T(2,5))$.

Definition 2.3.6. Let $l_r^s = h_r(\widehat{HF}(D^2 \times S^1))$ denote the slope-r line in $\widetilde{T}$ that crosses the neighborhood of $\overline{\mu}$ at height $[s]$. These are selected so that each l_r^s crosses at heights congruent to $[s]$ (mod r), with $[s]$ taken to be the representative that falls between $-\frac{r}{2} < [s] \leq \frac{r}{2}$.

In this way, Theorem 2.3.5 implies

$$\widehat{HF}(S^3_r(K), [s]) \cong HF(\widehat{HF}(S^3 \setminus \nu K), l_r^s).$$

After using regular homotopy of curves to remove any possible intersections that do not contribute to homology, we can determine dim $(\widehat{HF}(S^3_r(K), [s])$ as the intersection count between $\widehat{HF}(M)$ and l_r^s. This is easiest to achieve by pulling the components of $\widehat{HF}(M)$ tight to the lifts of z.

Definition 2.3.7. Fix a metric on the torus T_M with $\epsilon > 0$. We say $\widehat{HF}(M)$ is in pegboard form if the immersed curves are homotoped to have minimal length in T_M, where the curves remain outside an ϵ-ball of z. When $M = S^3 \setminus \nu K$, let n_i denote the number of vertical segments of the pegboard representative of $\widehat{HF}(M)$ that are parallel to $\overline{\mu}_i$, the lift of μ at height i.

The result is a pegboard representative for $\widehat{HF}(M)$, and we may lift these to both $\overline{T}_M$ and $\widetilde{T}$, where each lift of z has an ϵ-ball disjoint from the lift(s) of $\widehat{HF}(M)$. Pegboard forms are invaluable for pairing, since pulling curves tight homotopes away pseudo-holomorphic disks that do not contribute to the intersection Floer homology of a pairing. This ensures that the resulting Floer homology is minimal [HRW16, Lemma 47].

When $M = S^3 \setminus \nu K$, the lift $\widehat{HF}(M)$ consists of inessential curves, or curves that are null-homotopic after allowing homotopies through the basepoints, and a single essential curve $\overline{\gamma}$ that is homotopic to the homological longitude when allowing homotopies through the basepoints [HRW18, Corollary 63]. The invariance of $\widehat{HF}(M)$ under the action of the hyperelliptic involution implies that $n_{-i} = n_i$ for its pegboard representative. It will be particularly useful to characterize those knots whose complements have curve invariants with minimal n_i for all $i \in \mathbb{Z}$. Recall that a knot J is an *L-space knot* if it admits an L-space surgery, and that it also satisfies $g(J) = |\tau(J)|$. The following lemma is essentially the immersed curves version of [OS05a, Corollary 1.3].

Lemma 2.3.8. *Let $M = S^3 \setminus \nu J$ with J non-trivial. Then J is an L-space knot if and only if $\widehat{HF}(M, \mathfrak{s})$ pulls tight to a curve with $n_i = 1$ for $|i| < g(J)$ and $n_i = 0$ otherwise.*

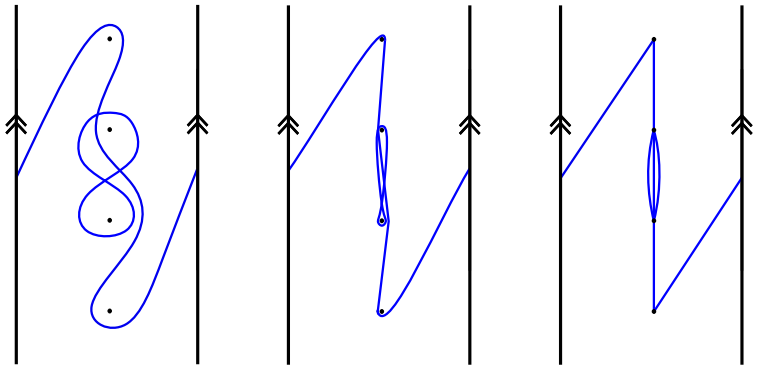

Figure 2.10: Pulling the immersed curve invariant $\widehat{HF}(S^3 \setminus (T(2,3)\#T(2,3)))$ (without grading arrows) tight to pegboard form. The figures from left to right show the stages of homotoping the invariant to lie within a neighborhood of the lifts of the meridian μ.

Proof. When J is a genus g knot with an L-space surgery $S^3_p(J)$, by mirroring if necessary we may take p to be positive. A surgery exact triangle argument shows that $S^3_{p+1}(J)$ is an L-space, and likewise for $S^3_k(J)$ with integral $k > p$. For some $k > 2g-1$, Theorem 2.2.2 then additionally provides that

$$\widehat{HF}(S^3_k(J), [s]) \cong \widehat{A}_s$$

for all $s \in \mathbb{Z}$. Then each $\widehat{A}_s \cong \mathbb{F}$ since $S^3_k(J)$ is an L-space. We can view $S^3_k(J)$ as the $+k$-sloped gluing of $D^2 \times S^1$ to M, so that Theorem 2.3.5 guarantees

$$\widehat{HF}(S^3_k(J)) \cong HF(\widehat{HF}(M), h(\widehat{HF}(D^2 \times S^1))).$$

Analogous to the $S^3_4(T(2,5))$ example, precisely k lifts of the $+k$-sloped curve $\widehat{HF}(D^2 \times S^1)$ are required to lift all intersections in T_M to $\overline{T}_M$, and each lift is in correspondence to precisely one spin^c structure of $\mathrm{Spin}^c(S^3_k(J))$. These differ in height by one in $\overline{T}_M$, and each lift must intersect the essential curve $\overline{\gamma}$ at least once. An inessential curve component contributes an even number of vertical segments to some n_i with $|i| < g(J)$. If the pegboard representative of $\widehat{HF}(M)$ contains such a component, then $\dim \widehat{HF}(S^3_k(J), [s]) > 1$ for some spin^c structure $[s]$ since $k > 2g(J) - 1$ (we are guaranteed that some lift of $h(\widehat{HF}(D^2 \times S^1)$ crosses $\overline{\mu}_i$). As $S^3_k(J)$ is an L-space, we must have not have any inessential curve components. Then $\overline{\gamma}$ is the only component of $\widehat{HF}(S^3 \setminus \nu J)$, and so $n_i = 1$ for $|i| < g(J)$ and $n_i = 0$ otherwise.

If $\widehat{HF}(M, \mathfrak{s})$ has a pegboard representative satisfying $n_i = 1$ for $|i| < g(J)$ and $n_i = 0$

otherwise, then by mirroring if necessary we may suppose $\tau(J) > 0$ since J is non-trivial. The invariant $\widehat{HF}(M, \mathfrak{s})$ is just $\overline{\gamma}$ since no n_i has room to admit an inessential component. Further, $\overline{\gamma}$ has slope $2\tau(J) - \epsilon(J) = 2g(J) - 1$ and pulls tight to vertical segments parallel to $\overline{\mu_i}$ for $|i| < g(J)$. If h is a gluing with slope $k > 2g(J) - 1$, then each lift of $h(\widehat{HF}(D^2 \times S^1))$ intersects $\widehat{HF}(M, \mathfrak{s})$ at most once. Using Theorem 2.3.5, we have dim $\widehat{HF}(S^3_k(J), [s]) = 1$ for each spin^c structure $[s]$. Therefore $S^3_k(J)$ is an L-space, and so J is an L-space knot. □

Remark. For an L-space knot J, we have $|\tau(J)| = g(J)$ and so the pegboard representative of $\widehat{HF}(M)$ takes on one of two mirrored forms depending on the sign of $\tau(J)$. These are illustrated in Figure 2.11 for a genus two knot.

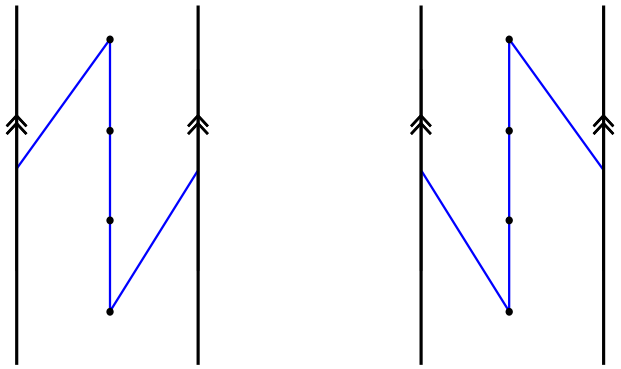

Figure 2.11: The two curve invariants for a genus two L-space knot, placed in pegboard form. Left: $\tau(J) = g(J)$. Right: $\tau(J) = -g(J)$.

To incorporate the relative Maslov grading in pairng, we use a formula from [Han19]. Suppose $\mathbf{x}$ and $\mathbf{y}$ are two intersections belonging to the same $[s] \in \text{Spin}^c(S^3_r(K))$, arising from intersections between $\widehat{HF}(M)$ and l^s_r. Further, let P be the bigon from $\mathbf{x}$ to $\mathbf{y}$ whose boundary consists of a (not necessarily smooth) path from $\mathbf{x}$ to $\mathbf{y}$ in $\widehat{HF}(M)$, concatenated with a path from $\mathbf{y}$ to $\mathbf{x}$ in l^s_r. Defined this way, the boundary of P is a closed path that is smooth apart from right corners at $\mathbf{x}$ and $\mathbf{y}$, and possibly one or more cusps. The following formula follows from the conversion of bordered invariants into immersed curves, keeping track of grading contributions from relevant Reeb chords [HRW18, Section 2.2].

Proposition 2.3.9. Suppose $\mathbf{x}, \mathbf{y}$, and P are defined as above. Let $\mathrm{Rot}(P)$ denote $\frac{1}{2\pi}$ times the total counterclockwise rotation along the smooth sections of P, let $\mathrm{Wind}(P)$ denote the net winding number of P around enclosed basepoints, and finally let $\mathrm{Wght}(P)$ be the sum of weights (counted with sign) of all grading arrows traversed by P. Then

$$M(\mathbf{y}) - M(\mathbf{x}) = 2\mathrm{Wind}(P) + 2\mathrm{Wght}(P) - 2\mathrm{Rot}(P).$$

If l_r^s intersects a simple figure-eight component at height n of $\widehat{HF}(M)$, it does so in two places. These are a *right intersection* y^n and a *left intersection* x^n, taken so that $M(x^n) - M(y^n) = 1$. Figure 2.12 shows off the three types of bigons that will typically appear. The first type has P connecting a right and left intersection of the same simple figure-eight. The bigon encloses a single basepoint with positive winding number, total counterclockwise rotation along smooth sections as π, and no contribution from traversed grading arrows. These traits imply $M(x^n) - M(y^n) = 1$. The second and third types are the more interesting ones, and have the same winding number of enclosed basepoints, but the rotation and grading arrow contributions to $M(y^n) - M(a^s)$ initially appear to be different. We will see in Chapter 5 that the $2\mathrm{Wght}(P) - 2\mathrm{Rot}(P)$ component of the grading difference is the same.

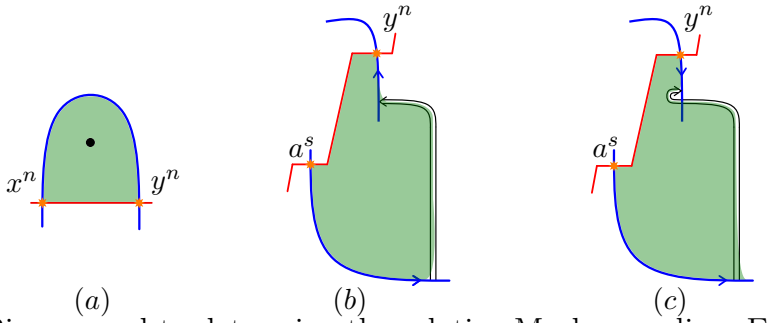

Figure 2.12: Bigons used to determine the relative Maslov grading. Example (a) does not involve a grading arrow, while (b) and (c) (with a cusp) do.

CHAPTER

3

KLEIN BOTTLE SURGERIES

To obstruct integral Dehn surgeries from containing a Klein bottle, we will decompose the surgery along the boundary of N, the twisted I-bundle over the Klein bottle, and involve Heegaard Floer homology via immersed curves techniques. As alluded to in the introduction, if a closed, orientable 3-manifold X contains a Klein bottle, then we may view X as a gluing $X = M \cup_h N$ where M is a rational homology solid torus. Alternatively we can view $M = Y \setminus \nu J$ as a knot manifold, which is the complement of a knot J in Y some rational homology sphere. We specialize to gluings of N to S^3 knot complements, and use immersed curves machinery to determine which knot complements can glue with N to have the Floer homology as that of $S^3_8(K)$ with $g(K) = 2$. The proof of Theorem 1.2.1 involves establishing three main lemmas implying the following:

- In Lemma 3.2.1, we will see that if J is the unknot, then $X = S^3_8(T(2,5))$.
- Afterward, Lemma 3.3.1 will be used to show that if J is non-trivial, then dim $\widehat{HF}(X)$ forces $J = T(2,3)$.
- Finally in the following chapter, we invoke Lemma 4.4.1 to see that if $J = T(2,3)$, then X does not arise as $S^3_8(K)$ with $g(K) = 2$.

The first lemma does not require immersed curves, but does use the Maslov grading information for $\widehat{HF}$ via the d-invariants. The second lemma is where immersed curves are used to constrain J. Finally the third lemma, in Chapter 4, follows using the relative $\mathbb{Q}$-grading on the box tensor product of bordered invariants for $S^3 \setminus \nu T(2,3)$ and N. Afterward we will consider reducible surgeries on thin, hyperbolic knots in Chapters 5 and 6.

3.1 The Gluing Map h

Let us now pin down the possibilities for the gluing map h. Summands of homology will typically be ordered with the summand generated by the rational longitude first, such as in $H_1(\partial N) \cong \mathbb{Z}_{[\phi_0]} \oplus \mathbb{Z}_{[\phi_1]}$.

Definition 3.1.1. Let $X = (S^3 \setminus \nu J) \cup_h N$ be the gluing of N to the complement $S^3 \setminus \nu J$, where the orientation-reversing gluing induces h_* on homology given by

$$[h_*] = \begin{pmatrix} q & a \\ p & b \end{pmatrix}.$$

We say h is a slope p/q gluing, corresponding to the slope of $h_*(\phi_0)$.

Proposition 3.1.2. Let h be defined as above. Then $|H_1(X)| = 8$ if only if $|p| = 2$. Additionally, we have

$$H_1(X) = \begin{cases} \mathbb{Z}/2\mathbb{Z} \oplus \mathbb{Z}/4\mathbb{Z} & b \equiv 0 \pmod 2 \\ \mathbb{Z}/8\mathbb{Z} & b \not\equiv 0 \pmod 2 \end{cases}$$

Proof. Recall the parameterization on ∂N by the rational longitude ϕ_0 and our chosen dual curve ϕ_1, so that $H_1(\partial N) \cong \mathbb{Z}_{[\phi_0]} \oplus \mathbb{Z}_{[\phi_1]}$. As a slight abuse of notation, let ϕ_0 and ϕ_1 also denote the inclusion of these slopes in $H_1(N)$. The dual curve ϕ_1 includes in $H_1(N)$ as twice some primitive curve x since ϕ_0 includes with order two [Wat12, Subsection 3.1], and so $H_1(N) \cong \mathbb{Z}/2\mathbb{Z}_{[\phi_0]} \oplus \mathbb{Z}_{[x]}$. For the knot complement, $H_1(\partial(S^3 \setminus \nu J)) \cong \mathbb{Z}_{[\lambda]} \oplus \mathbb{Z}_{[\mu]}$ and $H_1(S^3 \setminus \nu J) \cong \mathbb{Z}_{[\mu]}$, with the inclusions $[\mu]$ primitive and $[\lambda]$ trivial. Then using the Mayer-Vietoris sequence for homology, we obtain

$$H_1(X) \cong (H_1(S^3 \setminus \nu J) \oplus H_1(N)) \big/ f_*(H_1(\partial N)),$$

where f_* maps $H_1(\partial N)$ into $H_1(N)$ by inclusion and into $H_1(S^3 \setminus \nu J)$ through h_* and inclusion.

The quotient identifies $\phi_0 \sim q\lambda + p\mu$ and $\phi_1 = 2x \sim a\lambda + b\mu$, and so $H_1(X)$ has the following presentation:

$$\begin{aligned} H_1(X) &\cong \langle \lambda, \mu, \phi_0, x \mid \lambda = 0, 2\phi_0 = 0, \phi_0 = q\lambda + p\mu, 2x = a\lambda + b\mu \rangle \\ &\cong \langle \mu, x \mid 2p\mu = 0, 2x = b\mu \rangle. \end{aligned}$$

From this we see that $|H_1(X)| = 8$ if and only if $|p| = 2$, and that $H_1(X)$ is cyclic when $b \not\equiv 0 \pmod 2$. □

A gluing h that satisfies the cyclic condition of Proposition 3.1.2 will be referred to as a *cyclic gluing*. To narrow the amount of cyclic gluings to consider, we can appeal to a form of Dehn twisting invariance enjoyed by $\widehat{HF}(N)$.

Definition 3.1.3. A *Heegaard Floer homology solid torus* M is a rational homology solid torus satisfying

$$\widehat{CFD}(M, \mu_M, \lambda_M) \cong \widehat{CFD}(M, \mu_M + \lambda_M, \lambda_M),$$

with λ_M the rational longitude of M and μ_M any slope dual to λ.

The twisted I-bundle over the Klein bottle is shown to be a Heegaard Floer homology solid torus in [BGW, Proposition 7], and this invariance for $A(\theta_{N,\mathfrak{s}_1})$ is shown in Figure 3.1. The new yellow edge recovering the ρ_3 edge is the result of applying edge reduction [Lev12, Section 2.6]. The case for the loose component $A(\theta_{N,\mathfrak{s}_0})$ is immediate. Equivalently, inspection of $\widehat{HF}(N)$ in Figure 2.6 reveals that the curve invariant can be homotoped (without crossing the basepoint) to lie within a neighborhood of the rational longitude.

Dehn twisting n times along ϕ_0, and then gluing is equivalent to pre-composing $[h_*]$ with

$$[T_n] = \begin{pmatrix} 1 & n \\ 0 & 1 \end{pmatrix}, \text{ yielding } [h_* \circ T_n] = \begin{pmatrix} q & a + nq \\ p & b + np \end{pmatrix}.$$

Gluing by either map yields manifolds with equivalent ranks of $\widehat{HF}(X, \mathfrak{t})$ for each spin^c structure [HRW2, Corollary 27]. The mod p residue class of $[b]$ is preserved for all $n \in \mathbb{Z}$, and so we have to consider an integral family of manifolds X obtained by varying n. This will be more pertinent in Chapter 4 where we appeal to more than just dim $\widehat{HF}(X)$, so let us then restrict attention to the maps h with $-2 < b \leq 0$. We are also interested in cyclic gluings, which means $b \equiv 1 \pmod 2$ due to Proposition 3.1.2. We will show that

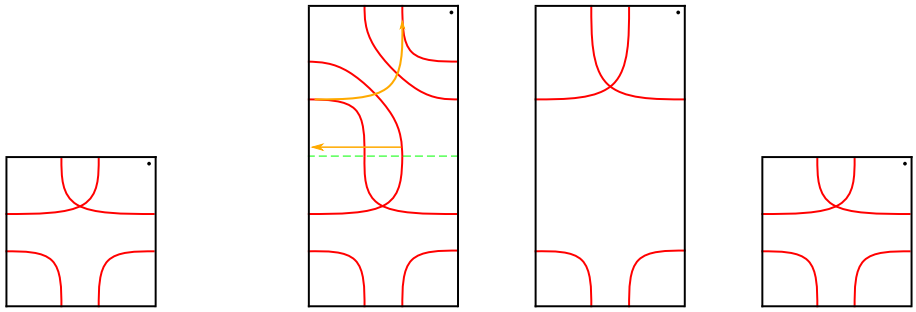

Figure 3.1: Left: The type A realization of $\widehat{CFD}(N, \phi_1, \phi_0, \mathfrak{s}_1)$. Right: Dehn twisting to obtain the type A realization of $\widehat{CFD}(N, \phi_1 + \phi_0, \phi_0, \mathfrak{s}_1)$, and the edge reduction showing homotopy equivalence.

the pairing slope $\pm 2/q$ must be integral when J is non-trivial to provide the right dim $\widehat{HF}(X)$, so we will also take $q = 1$. The Dehn twisting invariance of $\widehat{CFD}(N)$ allows us to choose $b = -1$, and so the prototypical gluing h induces

$$[h_*] = \begin{pmatrix} 1 & 0 \\ 2 & -1 \end{pmatrix}.$$

3.2 Gluings with J Trivial

We now establish the first lemma handling the case when J is trivial, which is when X is a Dehn filling of N. Continuing as before, let M will denote the knot complement $M = S^3 \setminus \nu J$.

Lemma 3.2.1. *Suppose $X = (Y \setminus \nu J) \cup_h N$ contains a Klein bottle and is realized as $S^3_8(K)$ with $g(K) = 2$. If J is trivial, then $Y = S^3$, $K = T(2, 5)$, and $X = (-1; \frac{1}{2}, \frac{1}{2}, \frac{2}{5})$ as a Seifert fibered manifold.*

Proof. We know from Corollary 2.2.5 that M is irreducible, and so $Y = S^3$ and $M = D^2 \times S^1$. Such a gluing X is a Dehn filling $N(\alpha)$, where α is a slope on ∂N. The twisted I-bundle over the Klein bottle N has a Seifert structure with base orbifold $D^2(2, 2)$ [LW14], and we may parametrize ∂N using $\{\phi_0, \phi_1\}$ as before, where $\phi_0 = \lambda_N$ is the rational longitude of N and ϕ_1 is our preferred choice of curve dual to ϕ_0. We have $N(\phi_1) = \mathbb{R}P^3 \# \mathbb{R}P^3$ and $b_1(N(\phi_0)) > 0$, and so we can consider $\alpha \neq \phi_0, \phi_1$. Since N is a Heegaard Floer homology solid torus, X is an L-space for all $\alpha \neq \phi_0$ [HRW18, Theorem 26]. Then if X is realizable as 8-surgery along K with $g(K) = 2$, we must have that K is

an L-space knot. This implies $\widehat{HFK}(K) \cong \widehat{HFK}(T(2,5))$. Any Dehn filling $X = N(\alpha)$ for which $\alpha \neq \phi_0, \phi_1$ admits a pair of Seifert structures with base orbifolds $\mathbb{R}P^2(\Delta(\alpha, \phi_0))$ and $S^2(2, 2, \Delta(\alpha, \phi_1))$. Since ∂N compresses in $S^3 \setminus \nu J$, we see that $\pi_1(X)$ is finite. Thus, X is either a lens space or has $\pi_1(X)$ non-cyclic.

We obstruct $X \cong L(8, q)$ using the d-invariants from [OS03a] using Proposition 2.2.7 from [NW15]. Since K has isomorphic knot Floer homology to that of $T(2, 5)$, we must have $V_s(K) = V_s(T(2, 5))$. With $V_0(K) = V_1(K) = 1$ and $V_s(K) = 0$ for $s \geq 2$, one computes

$$d(S^3_8(K), [s]) = \begin{cases} -1/8 & s \equiv 5 \pmod 8 \\ 1/4 & s \equiv 6 \pmod 8 \\ -9/8 & s \equiv 7 \pmod 8 \\ -1/4 & s \equiv 0 \pmod 8 \\ -9/8 & s \equiv 1 \pmod 8 \\ 1/4 & s \equiv 2 \pmod 8 \\ -1/8 & s \equiv 3 \pmod 8 \\ -1/4 & s \equiv 4 \pmod 8 \end{cases}$$

We have $d(L(8, \pm 1), [t_1]) = \pm 7/4$ and $d(L(8, \pm 3), [t_2]) = \pm 5/8$ for some $t_1, t_2 \in \mathbb{Z}$ from the recursion in [OS03a, Proposition 4.8], but both of these differ from any $d(S^3_8(K), [s])$. Therefore, X cannot be a lens space.

In [Doi15, Theorem 2], Doig classifies finite, non-cyclic surgeries $S^3_r(K)$ for $|r| \leq 9$. Among these, the manifolds with $|H_1(X)| = 8$ are specific dihedral manifolds that are small Seifert fibered with base orbifold S^2. They are $-S^3_8(T(2, 3)) = \left(-1; \frac{1}{2}, \frac{1}{2}, \frac{2}{3}\right)$, and $S^3_8(K) = \left(-1; \frac{1}{2}, \frac{1}{2}, \frac{2}{5}\right)$ for $\widehat{HFK}(K) \cong \widehat{HFK}(T(2, 5))$. However, since eight is a characterizing slope for $T(2, 5)$ due to [NZ18], we have $\left(-1; \frac{1}{2}, \frac{1}{2}, \frac{2}{5}\right) = S^3_8(T(2, 5))$. For $T(2, 3)$ we have $V_1(T(2, 3)) = 0$, and so

$$d(-S^3_8(T(2, 3), [1]) = -d(S^3_8(T(2, 3)), [1]) = -\tfrac{7}{8}.$$

This differs from any $d(S^3_8(K), [s])$ above when K has the same knot Floer homology as $T(2, 5)$, establishing the lemma. □

3.3 Gluings with J Non-trivial

Now suppose that J is a non-trivial knot in S^3. There is a convenient visual way to track Floer homology associated to a given spin^c structure of X, that we have already encountered in both Figure 2.9 and in proving Lemma 2.3.8.

By Theorem 2.3.5, we have $\widehat{HF}(X, \mathfrak{t})$ isomorphic to a summand of $HF(\widehat{HF}(M, \mathfrak{s}), h(\widehat{HF}(N), \mathfrak{s}_k))$ when $\mathfrak{t} \in \pi^{-1}(\mathfrak{s} \times \mathfrak{s}_k)$. Intersections $\mathbf{x}, \mathbf{y}$ in pairing generate Floer homology in the same spin^c structure if and only if there exist paths p_0 from $\mathbf{x}$ to $\mathbf{y}$ in $\widehat{HF}(M, \mathfrak{s})$ and p_1 from $\mathbf{x}$ to $\mathbf{y}$ in $h(\widehat{HF}(N, \mathfrak{s}_k))$, such that the concatenation of p_0 with $-p_1$ lifts to a closed, piecewise smooth path in $\widetilde{T}$ [HRW18, Section 2]. When h has slope $\pm 2/q$, a single lift $h(\widehat{HF}(N, \mathfrak{s}_k))$ of the component of $h(\widehat{HF}(N))$ corresponding to $\mathfrak{s}_k$ will fail to lift all intersections in T_M generated by this component; two lifts of the component are required.

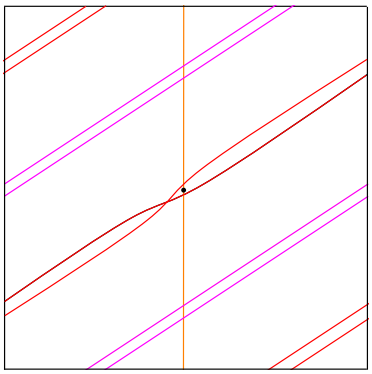

Figure 3.2: The 2/3-sloped curves of N associated to $\mathfrak{s}_1$ in T_M.

This is motivated by Figure 3.2 for $h(\widehat{HF}(N, \mathfrak{s}_1))$ projected to T_M, where h is a cyclic gluing of slope 2/3. A single lift to $\overline{T}_M$ cannot simultaneously lift all intersections by the suggestively colored red and purple pieces of the projection of $h(\widehat{HF}(N, \mathfrak{s}_1))$. A simpler example of this is seen from Figure 2.9, where four lifts of $h(\widehat{HF}(D^2 \times S^1))$ are needed. Additionally, Figure 1.1 provides an example of the four required curves of $h(\widehat{HF}(N, \mathfrak{s}_1))$ with h a cyclic gluing of slope 2. Notice that the lifted curves cannot generate intersections with the same Spin^c grading as there is no path between the curves in $h(\widehat{HF}(N, \mathfrak{s}_k))$. For this reason, we can associate the eight $\mathfrak{t} \in \text{Spin}^c(X)$ with these lifted curves of $h(\widehat{HF}(N, \mathfrak{s}_1))$ and $h(\widehat{HF}(N, \mathfrak{s}_0))$.

Now that we can distinguish intersections generating Floer homology in different Spin^c structures, we establish the second lemma toward proving Theorem 1.2.1. This is the extent to which ignoring the Maslov grading in the immersed curves package can push the case where J is non-trivial. Since we are only interested in X with $H_1(X) \cong \mathbb{Z}/8\mathbb{Z}$ and constrained dim $\widehat{HF}(X, \mathfrak{t})$ from Proposition 2.2.3, we assume these traits.

Lemma 3.3.1. *Let J be non-trivial and consider $X = (S^3 \setminus \nu J) \cup_h N$, where h is any slope $2/q$ cyclic gluing. If dim $\widehat{HF}(X, \mathfrak{t}) = 1$ for at least five $\mathfrak{t} \in$ Spin$^c(X)$, then h has slope ± 2 and $J = T(2, \pm 3)$.*

Proof. Let $M = S^3 \setminus \nu J$, and pull $\widehat{HF}(M)$ tight to pegboard form. From Theorem 2.3.5 we have

$$\widehat{HF}(X, \mathfrak{t}) \cong HF(\widehat{HF}(M), h(\widehat{HF}(N), \mathfrak{s}_k)),$$

where $\mathfrak{t} \in \pi^{-1}(\mathfrak{s} \times \mathfrak{s}_k)$.

Suppose for the sake of contradiction that $|q| > 1$, so that the slope of h satisfies $|2/q| < 1$. Since J is non-trivial, $\widehat{HF}(M)$ must have $n_i \neq 0$ for some i. It is then immediate that all four lifts of the loose curves $h(\widehat{HF}(N, \mathfrak{s}_0))$ intersect the vertical segment(s) at height i of $\widehat{HF}(M)$ more than once (such as in Figure 3.2). Since dim $\widehat{HF}(X, \mathfrak{t}) = 1$ for at least five $\mathfrak{t} \in \text{Spin}^c(X)$, we must have $n_i = 0$ for all $|i| < g(J)$. However this condition is satisfied only by the unknot, which is the desired contradiction. Then we may suppose that h is a slope 2 cyclic gluing, mirroring K if necessary to make the slope positive.

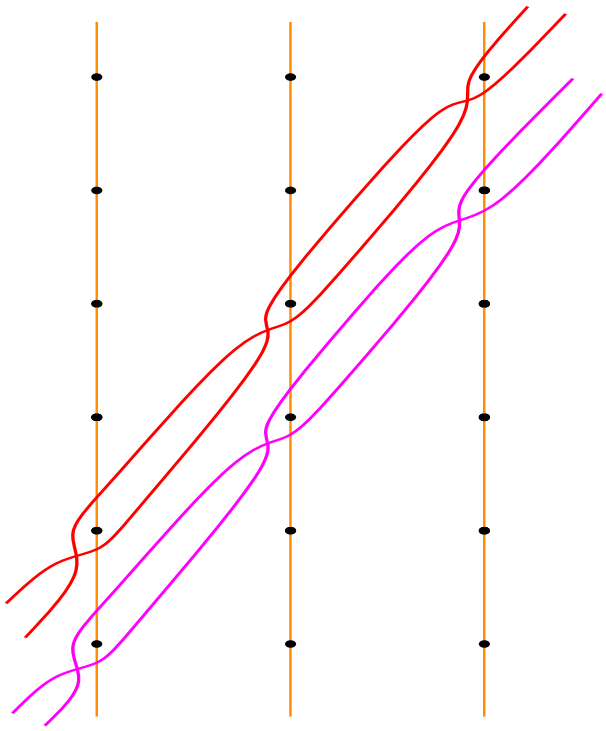

Figure 3.3: Intersections between the lifts of $h(\widehat{HF}(N, \mathfrak{s}_1))$ and potential vertical segments of $\widehat{HF}(M)$.

Notice that each potential vertical segment of $\widehat{HF}(M)$ at height i intersects two of the four lifted curves of $h(\widehat{HF}(N, \mathfrak{s}_1))$, showcased in Figure 3.3. Similarly, the same potential vertical segment intersects two of the four lifted curves of the loose component $h(\widehat{HF}(N, \mathfrak{s}_0))$. Then for all $i \in \mathbb{Z}$, we have n_i contributing to dim $\widehat{HF}(X, \mathfrak{t})$ in at least

four different spin^c structures. We are then forced to have $n_i \leq 1$ for all $i \in \mathbb{Z}$, which is equivalent to $\widehat{HF}(M)$ not containing any inessential curve components. Therefore, J is an L-space knot by Lemma 2.3.8. In the remark following that lemma, we see that the pegboard representative of $\widehat{HF}(M) = \overline{\gamma}$ for an L-space knot complement is completely determined by $\tau(J)$.

If $g(J) > 1$, four lifted components (two for each $\mathfrak{s}_k$) of $h(\widehat{HF}(N))$ intersect $\overline{\gamma}$ more than once. This is shown in Figure 3.4 when $\tau(J) = 2$. Then we must have $g(J) = 1$ since J is non-trivial, and so J is either $T(2,3)$ or $T(2,-3)$. Observe that gluing N to $S^3 \backslash \nu T(2,-3)$ by a $+2$-sloped cyclic gluing yields a manifold with excessive Floer homology since $\tau(T(2,-3)) < 0$. Noting that the same argument would imply $J = T(2,-3)$ if h was a slope -2 cyclic gluing, we have established the lemma. □

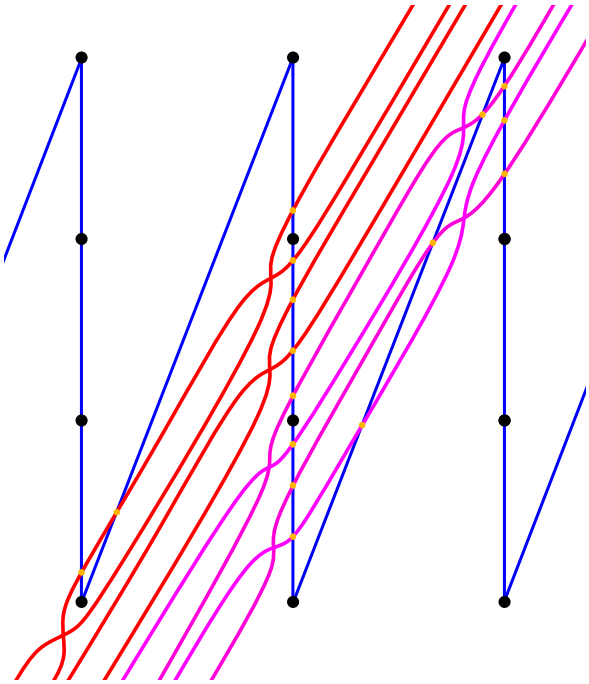

Figure 3.4: The pairing of $h(\widehat{HF}(N))$ with $\widehat{HF}(M)$, where h is a slope 2 cyclic gluing and J is an L-space knot with $\tau(J) = 2$.

CHAPTER

4

REFINED GRADINGS IN PAIRING

In this chapter, we obstruct $(S^3 \setminus \nu T(2,3)) \cup_h N$ from being realized as $S^3_8(K)$ for $g(K) = 2$ using the Maslov grading structure on $\widehat{HF}(X)$. The argument style works identically for $J = T(2,-3)$ when h has slope -2, and so we will proceed only for the positive case. The relative $\mathbb{Z}$-grading on Heegaard Floer homology can be lifted to an absolute $\mathbb{Q}$-grading, and for an L-space surgery the grading of the generator of $\widehat{HF}(S^3_p(K), [s])$ is given by $d(S^3_p(K), [s])$. In general these are easy to determine from $CFK^\infty(K)$, which we did back in Lemma 3.2.1 for 8-surgery along a knot K with $\widehat{HFK}(K) \cong \widehat{HFK}(T(2,5))$.

While the immersed curves framework has been invaluable for ruling out most suitable knot complements $S^3 \setminus \nu J$, it is limited in its capacity to compare grading information across spin^c structures. We will compute the relative $\mathbb{Q}$-grading on $\widehat{HF}(X)$ using train tracks and their associated prototype pairing theorem (Subsection 2.3.2), and then generate the desired obstruction by comparing grading differences. This is possible through the main result of [LOT18a], which we will give after a brief overview of the (refined) grading on bordered invariants (for manifolds with torus boundary).

From [LOT18b, Section 11.1], the refined grading on the algebra $\mathcal{A}(\mathbb{T})$ takes values in a non-commutative group G (arising as a $\mathbb{Z}$-central extension of $H_1(\mathbb{T})$). The group G is generated by triples $(j; p, q)$ with $j, p, q \in \frac{1}{2}\mathbb{Z}$ and $p + q \in \mathbb{Z}$, and has a central element

$\lambda = (1; 0, 0)$ (not to be confused with the homological longitude of $S^3 \setminus \nu J$). We will refer to j as the Maslov component, and (p, q) as the Spin^c component. The group law is given by

$$(j_1; p_1, q_1) \cdot (j_2; p_2, q_2) = \left(j_1 + j_2 + \begin{vmatrix} p_1 & q_1 \\ p_2 & q_2 \end{vmatrix}; p_1 + p_2, q_1 + q_2 \right),$$

and the gradings of the algebra elements are generated from the non-zero products on $\mathcal{A}(\mathbb{T})$ from:

$$\begin{aligned} \mathrm{gr}(\rho_1) &= (-\tfrac{1}{2}; \tfrac{1}{2}, -\tfrac{1}{2}) \\ \mathrm{gr}(\rho_2) &= (-\tfrac{1}{2}; \tfrac{1}{2}, \tfrac{1}{2}) \\ \mathrm{gr}(\rho_3) &= (-\tfrac{1}{2}; -\tfrac{1}{2}, \tfrac{1}{2}) \end{aligned}$$

Let M_1 be a bordered manifold with torus boundary. Given $\mathfrak{s}_1 \in \mathrm{Spin}^c(M_1)$, fix a base generator $\mathbf{x}_0 \in \widehat{CFA}(M_1, \mathfrak{s}_1)$. The module $\widehat{CFA}(M_1, \mathfrak{s}_1)$ is graded by the right G-set $G_A(M_1, \mathfrak{s}_1) := P(\mathbf{x}_0)\backslash G$, with subgroup $P(\mathbf{x_0})$ defined in terms of periodic domains $B \in \pi_2(\mathbf{x}_0, \mathbf{x}_0)$ in a bordered Heegaard diagram for M. While this construction depends on the choice of base generator $\mathbf{x}_0$, different choices give isomorphic grading sets [LOT18b, Section 10.3]. We have $\pi_2(\mathbf{x}_0, \mathbf{x}_0) \cong H_2(M_1) \oplus \mathbb{Z}$ when M_1 has torus boundary, and so $P(\mathbf{x}_0)$ is cyclic if M is a rational homology solid torus.

Since the bordered manifolds in this paper are rational homology solid tori, we have $\widehat{CFA}(M_1, \mathfrak{s}_1)$ graded by $\langle f \rangle \backslash G$ for some $f \in G$. Similarly for another bordered manifold with torus boundary M_2, we have that $\widehat{CFD}(M_2, \mathfrak{s}_2)$ is graded by the left G-set $G_D(M_2, \mathfrak{s}) := G/\langle h \rangle$ for some $h \in G$. The box tensor product $\widehat{CFA}(M_1, \mathfrak{s}_1) \boxtimes \widehat{CFD}(M_2, \mathfrak{s}_2)$ is graded by $G_A(M_1, \mathfrak{s}_1) \times_G G_D(M_2, \mathfrak{s}_2)$, and the grading of $\mathbf{x}_1 \otimes \mathbf{x}_2$ is $\mathrm{gr}(\mathbf{x}_1 \otimes \mathbf{x}_2) = (\mathrm{gr}(\mathbf{x}_1), \mathrm{gr}(\mathbf{x}_2))$.

We can also work with rational periodic domains by extending G and its multiplication over $\mathbb{Q}$ to obtain $G_{\mathbb{Q}}$. We also have quotients by the $\mathbb{Q}$-span of $\langle f \rangle$ and $\langle h \rangle$, given as $G_{A,\mathbb{Q}}(M, \mathfrak{s}) := \langle t \cdot f \rangle \backslash G_{\mathbb{Q}}$ and $G_{D,\mathbb{Q}}(M, \mathfrak{s}) := G_{\mathbb{Q}}/\langle t \cdot h \rangle$ for $t \in \mathbb{Q}$. The main results of [LOT18a] are combined in Theorem 4.0.1 below (in the case of manifolds with torus boundary). It states that the relative $\mathbb{Q}$-grading by $G_{A,\mathbb{Q}}(M_1, \mathfrak{s}_1) \times_{G_{\mathbb{Q}}} G_{D,\mathbb{Q}}(M_2, \mathfrak{s}_2)$ recovers the relative $\mathbb{Q}$-grading on $\widehat{CF}(M_1 \cup_h M_2)$.

Theorem 4.0.1 ([LOT18a, Theorem 1, Corollary 3.2, Remark 3.3])**.** *Consider the pairing $X = M_1 \cup_h M_2$, where the M_i are compact, oriented 3-manifolds with torus boundary and h is an orientation-reversing homeomorphism of boundaries. Suppose that $\mathbf{x}, \mathbf{y} \in \widehat{CFA}(M_1, \alpha_1, \beta_1, \mathfrak{s}_1) \boxtimes \widehat{CFD}(M_2, h^{-1}(\beta_1), h^{-1}(\alpha_1), \mathfrak{s}_2)$ are such that $\mathfrak{s}(\mathbf{x})$ and $\mathfrak{s}(\mathbf{y})$ are torsion and $\mathfrak{s}(\mathbf{x})|_{M_i} = \mathfrak{s}(\mathbf{y})|_{M_i} =: \mathfrak{s}_i$ for $i = 1, 2$. Then $gr_{\mathbb{Q}}(\mathbf{x})$ and $gr_{\mathbb{Q}}(\mathbf{y})$ lie in the same $\mathbb{Q}$-orbit of $G_{A,\mathbb{Q}}(M_1, \mathfrak{s}_1) \times_{G_{\mathbb{Q}}} G_{D,\mathbb{Q}}(M_2, \mathfrak{s}_2)$. In particular, the G-set grading $gr_{\mathbb{Q}}$ determines the relative $\mathbb{Q}$-grading on $\widehat{HF}$.*

Since $\widehat{CFA}(M)$ is an $\mathcal{A}_\infty$-module graded by a right G-set, homogeneous elements $\mathbf{x} \in \widehat{CFD}(M)$ and $\rho_{I_n} \in \mathcal{A}$ satisfy

$$\mathrm{gr}(m_{k+1}(\mathbf{x}, \rho_{I_1}, \dots, \rho_{I_k})) = \lambda^{k-1}\mathrm{gr}(\mathbf{x})\mathrm{gr}(\rho_{I_1}) \cdots \mathrm{gr}(\rho_{I_k}) \text{ if } \mathbf{x} \otimes \rho_{I_1} \otimes \cdots \otimes \rho_{I_k} \neq 0.$$

Similarly, since $\widehat{CFD}(M)$ is a left differential $\mathcal{A}$-module graded by a left G-set, homogeneous elements $\mathbf{x} \in \widehat{CFD}(M)$ and $\rho_I \in \mathcal{A}$ satisfy both

$$\begin{aligned} \mathrm{gr}(\rho_I \otimes \mathbf{x}) &= \mathrm{gr}(\rho_I)\mathrm{gr}(\mathbf{x}) && \text{if } \rho_I \otimes \mathbf{x} \neq 0 \\ \mathrm{gr}(\partial\mathbf{x}) &= \lambda^{-1}\mathbf{x} && \text{if } \partial\mathbf{x} \neq 0. \end{aligned}$$

We can now use these properties to compute the refined gradings on the relevant bordered invariants, and use Theorem 4.0.1 to establish the final lemma to prove Theorem 1.2.1. For the rest of this chapter, let $M = S^3 \setminus \nu T(2, 3)$. For our prototypical gluing h, we have

$$\begin{aligned} \widehat{HF}(X) &= H_*(\widehat{CFA}(M, \mu, \lambda) \boxtimes \widehat{CFD}(N, h^{-1}(\lambda), h^{-1}(\mu))) \\ &= H_*(\widehat{CFA}(M, \mu, \lambda) \boxtimes \widehat{CFD}(N, 2\phi_1 + \phi_0, -\phi_1)). \end{aligned}$$

We first need to determine the refined gradings for $\widehat{CFA}(M, \mu, \lambda)$, and both $\widehat{CFD}(N, 2\phi_1 + \phi_0, -\phi_1, \mathfrak{s}_1)$ and $\widehat{CFD}(N, 2\phi_1 + \phi_0, -\phi_1, \mathfrak{s}_0)$. We begin with the former, and work towards the latter two structures on N.

4.1 Refined Gradings for $\widehat{CFA}(M, \mu, \lambda)$

We will use the decorated graph representation of $\widehat{CFA}(M, \mu, \lambda)$ to determine the refined gradings of its generators. To obtain this, let us reverse-engineer $A(\theta_M)$ from $\widehat{HF}(M, \mathfrak{s})$ by projecting an appropriate representative onto T_M (with z at $(1 - \epsilon, 1 - \epsilon)$). The form

of $\widehat{HF}(M,\mathfrak{s})$ in $\widetilde{T}$ is simple due to Lemma 2.3.8. Seen in $\overline{T}_M$, the curve invariant initially wraps around a lift of z at height $\frac{1}{2}$, then around a lift of z at height $-\frac{1}{2}$ before wrapping back around the cylinder since $\tau(T(2,3)) = 1$ and $\epsilon(T(2,3)) = 1$. The choice representative in $\widetilde{T}$ is shown in Figure 4.2, together with the projection onto T_M yielding the desired $A(\theta_M)$. Recall that the decorated graph representing $\widehat{CFD}(M,\mu,\lambda)$ can be extracted from $A(\theta_M)$ using the edge identifications from Figure 2.5. The result is shown in Figure 4.1.

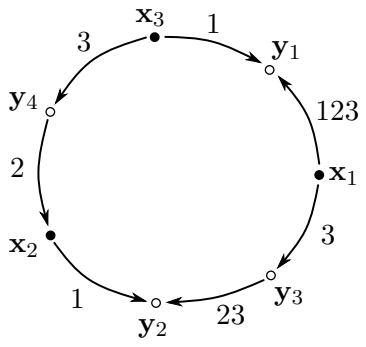

Figure 4.1: The decorated graph representation of $\widehat{CFD}(M,\mu,\lambda)$

Finally, an algorithm of Hedden and Levine may be followed to obtain the decorated graph representation of $\widehat{CFA}(M,\mu,\lambda)$ [HL16]. The idempotent splitting according to vertex labels remains the same, but the edge labels are interpreted differently. First, rewrite them according to the bijection $1 \leftrightarrow 3$. Given a directed path from x to y, construct a sequence $I = I_1, \dots I_k$ and assign the multiplication $m_{k+1}(x \otimes \rho_{I_1} \otimes \cdots \otimes \rho_{I_k}) = y$. Reading the edge labels of the directed path in order, form I by regrouping to find the minimum k so that each I_j is an element of $\{1,2,3,12,13,23,123\}$. For example, the edge labeled $\{23\}$ from $\mathbf{y}_3$ to $\mathbf{y}_2$ in Figure 4.1 gives the sequence $I = \{2,1\}$ and the product $m_3(\mathbf{y}_3,\rho_2,\rho_1) = \mathbf{y}_2$. The resulting decorated graph is shown in Figure 4.3.

Reading the edge labels gives each generator's contribution to the m_k, and allows us to determine their refined gradings taking values in $\langle f \rangle \backslash G$, up to some indeterminacy f. Set $\mathbf{x}_1$ to be the base generator. Since the decorated graph for $\widehat{CFA}(M,\mu,\lambda)$ is valence 2 and connected, we can traverse an oriented path from $\mathbf{x}_1$ to itself through the other generators to simultaneously compute the refined gradings of the remaining generators and the indeterminacy f.

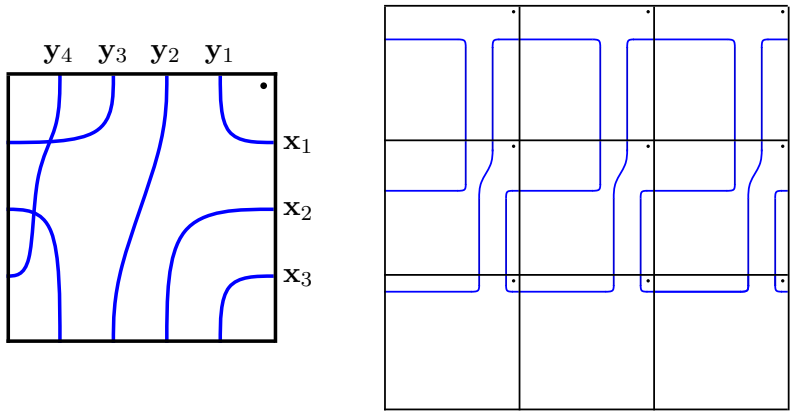

Figure 4.2: Right: A particular representative of $\widehat{HF}(M, \mathfrak{s})$ in $\widetilde{T}$. Left: The type A realization $A(\theta_M)$

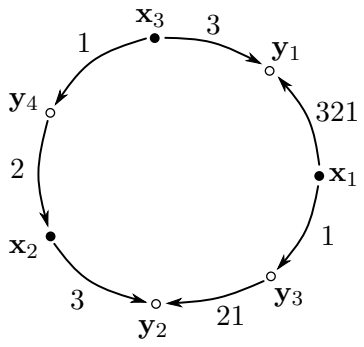

Figure 4.3: The decorated graph representation of $\widehat{CFA}(M, \mu, \lambda)$

The relevant contributions to the m_k are the following:

1) $m_4(\mathbf{x}_1, \rho_3, \rho_2, \rho_1) = \mathbf{y}_1$
2) $m_2(\mathbf{x}_3, \rho_3) = \mathbf{y}_1$
3) $m_2(\mathbf{x}_3, \rho_{123}) = \mathbf{y}_2$
4) $m_3(\mathbf{y}_3, \rho_2, \rho_1) = \mathbf{y}_2$
5) $m_2(\mathbf{x}_1, \rho_1) = \mathbf{y}_3$

For the first term $m_4(\mathbf{x}_1, \rho_3, \rho_2, \rho_1) = \mathbf{y}_1$, we see that

$$\begin{aligned}
\mathrm{gr}(\mathbf{y}_1) &= \lambda^2 \mathrm{gr}(\mathbf{x}_1)\mathrm{gr}(\rho_3)\mathrm{gr}(\rho_2)\mathrm{gr}(\rho_1) \\
&= \mathrm{gr}(\mathbf{x}_1)\lambda^2 \mathrm{gr}(\rho_3) \left(-\tfrac{1}{2}; \tfrac{1}{2}, \tfrac{1}{2}\right) \left(-\tfrac{1}{2}; \tfrac{1}{2}, -\tfrac{1}{2}\right) \\
&= \mathrm{gr}(\mathbf{x}_1)\lambda^2 \left(-\tfrac{1}{2}; -\tfrac{1}{2}, \tfrac{1}{2}\right) \left(-\tfrac{3}{2}; 1, 0\right) \\
&= \mathrm{gr}(\mathbf{x}_1) \left(2; 0, 0\right) \left(-\tfrac{5}{2}; \tfrac{1}{2}, \tfrac{1}{2}\right) \\
&= \langle f \rangle \backslash \left(-\tfrac{1}{2}; \tfrac{1}{2}, \tfrac{1}{2}\right)
\end{aligned}$$

Performing this for the remaining generators, we obtain their (undetermined) refined gradings in $\langle f \rangle \backslash G$:

$$\begin{aligned}
\mathrm{gr}(\mathbf{x}_1) &= \langle f \rangle \backslash (0; 0, 0) & \mathrm{gr}(\mathbf{y}_1) &= \langle f \rangle \backslash \left(-\tfrac{1}{2}; \tfrac{1}{2}, \tfrac{1}{2}\right) \\
\mathrm{gr}(\mathbf{x}_2) &= \langle f \rangle \backslash (-1; 2, 0) & \mathrm{gr}(\mathbf{y}_2) &= \langle f \rangle \backslash \left(-\tfrac{1}{2}; \tfrac{3}{2}, \tfrac{1}{2}\right) \\
\mathrm{gr}(\mathbf{x}_3) &= \langle f \rangle \backslash \left(-\tfrac{1}{2}; 1, 0\right) & \mathrm{gr}(\mathbf{y}_3) &= \langle f \rangle \backslash \left(\tfrac{1}{2}; \tfrac{1}{2}, \tfrac{1}{2}\right) \\
& & \mathrm{gr}(\mathbf{y}_4) &= \langle f \rangle \backslash \left(-\tfrac{3}{2}; \tfrac{3}{2}, -\tfrac{1}{2}\right)
\end{aligned}$$

The final term $m_2(\mathbf{x}_1, \rho_1) = \mathbf{y}_3$ allows us to pin down f:

$$\begin{aligned}
\mathrm{gr}(\mathbf{x}_1)\mathrm{gr}(\rho_1) &= \mathrm{gr}(\mathbf{y}_3) \\
\Rightarrow \mathrm{gr}(\mathbf{x}_1) &= \mathrm{gr}(\mathbf{y}_3)\mathrm{gr}(\rho_1)^{-1} \\
&= \langle f \rangle \backslash \left(\tfrac{1}{2}; \tfrac{1}{2}, \tfrac{1}{2}\right) \left(\tfrac{1}{2}; -\tfrac{1}{2}, \tfrac{1}{2}\right) \\
&= \langle f \rangle \backslash \left(\tfrac{3}{2}; 0, 1\right).
\end{aligned}$$

Thus, $f = \left(\frac{3}{2}; 0, 1\right)$ since it is primitive. The refined gradings for generators of $\widehat{CFA}(M, \mu, \lambda)$ are the following:

$$\begin{aligned}
\mathrm{gr}(\mathbf{x}_1) &= \langle (\tfrac{3}{2}; 0, 1) \rangle \backslash (0; 0, 0) & \mathrm{gr}(\mathbf{y}_1) &= \langle (\tfrac{3}{2}; 0, 1) \rangle \backslash \left(-\tfrac{1}{2}; \tfrac{1}{2}, \tfrac{1}{2}\right) \\
\mathrm{gr}(\mathbf{x}_2) &= \langle (\tfrac{3}{2}; 0, 1) \rangle \backslash (-1; 2, 0) & \mathrm{gr}(\mathbf{y}_2) &= \langle (\tfrac{3}{2}; 0, 1) \rangle \backslash \left(-\tfrac{1}{2}; \tfrac{3}{2}, \tfrac{1}{2}\right) \\
\mathrm{gr}(\mathbf{x}_3) &= \langle (\tfrac{3}{2}; 0, 1) \rangle \backslash \left(-\tfrac{1}{2}; 1, 0\right) & \mathrm{gr}(\mathbf{y}_3) &= \langle (\tfrac{3}{2}; 0, 1) \rangle \backslash \left(\tfrac{1}{2}; \tfrac{1}{2}, \tfrac{1}{2}\right) \\
& & \mathrm{gr}(\mathbf{y}_4) &= \langle (\tfrac{3}{2}; 0, 1) \rangle \backslash \left(-\tfrac{3}{2}; \tfrac{3}{2}, -\tfrac{1}{2}\right)
\end{aligned}$$

4.2 Refined Gradings for $\widehat{CFD}(N, 2\phi_1 + \phi_0, -\phi_1, \mathfrak{s}_0)$

In order to obtain the desired decorated graph representation, we can reverse-engineer its form from $A(\theta_{h(N,\mathfrak{s}_0)})$ (shown on the right side of Figure 2.6 back in Subsection 2.3.2). This involves performing a series of Dehn twists and reflections on T_N for the type A realization of $\widehat{CFD}(N, \phi_1, \phi_0, \mathfrak{s}_0)$, illustrated in Figure 4.4. First, we use the reflection $r(y = \frac{1}{2})$ to obtain $\widehat{CFD}(-N, -\phi_1, \phi_0, \mathfrak{s}_0)$. Second, Dehn twisting -2 times along $-\phi_1$ yields $\widehat{CFD}(-N, -\phi_1, 2\phi_1 + \phi_0, \mathfrak{s}_0)$. Finally we use the reflection $r(y = x)$, giving the bottom-right collection of curves $A(\theta_{h(N,\mathfrak{s}_0)})$ with the proper orientation on ∂N.

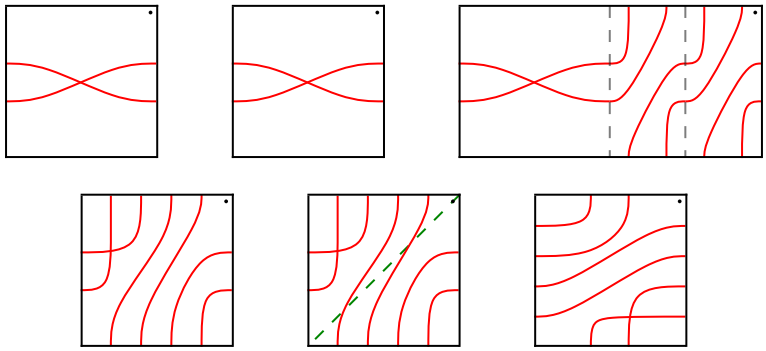

Figure 4.4: The series of Dehn twists and reflections required to obtain the type A realization of $\widehat{CFD}(N, 2\phi_1 + \phi_0, -\phi_1, \mathfrak{s}_0)$.

The corresponding decorated graph representation of $\widehat{CFD}(N, 2\phi_1 + \phi_0, -\phi_1, \mathfrak{s}_0)$ is shown in Figure 4.5. Label the ι_0 generators by $\mathbf{a}_i$ and the ι_1 generaters by $\mathbf{b}_i$. Reading the edge labels gives each generator's contribution to δ^1, and allows us to determine their refined gradings in $G/\langle h_0 \rangle$ up to some indeterminacy h. Set $\mathbf{a}_1$ to be the base generator. Since the decorated graph at hand is valence 2 and connected, we can traverse an oriented path from $\mathbf{a}_1$ to itself through the other generators to simultaneously compute the refined gradings of the remaining generators and the indeterminacy h_0. This is performed below using the properties of the refined grading.

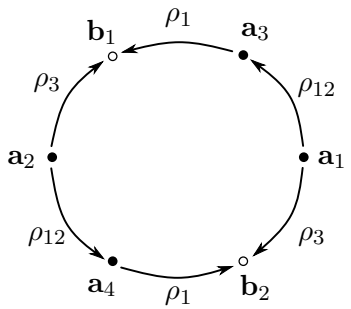

Figure 4.5: The decorated graph representation of $\widehat{CFD}(N, \phi_0 + 2\phi_1, -\phi_1, \mathfrak{s}_0)$

The relevant contributions to δ^1 are

$$\begin{aligned} &1)\ \rho_{12} \otimes \mathbf{a}_3 \in \delta^1 \mathbf{a}_1 && 4)\ \rho_{12} \otimes \mathbf{a}_4 \in \delta^1 \mathbf{a}_2 \\ &2)\ \rho_1 \otimes \mathbf{b}_1 \in \delta^1 \mathbf{a}_3 && 5)\ \rho_1 \otimes \mathbf{b}_2 \in \delta^1 \mathbf{a}_4 \\ &3)\ \rho_3 \otimes \mathbf{b}_1 \in \delta^1 \mathbf{a}_2 && 6)\ \rho_3 \otimes \mathbf{b}_2 \in \delta^1 \mathbf{a}_1 \end{aligned}$$

For the first term $\rho_{12} \otimes \mathbf{a}_3 \in \delta^1 \mathbf{a}_1$, we see that

$$\begin{aligned} \lambda^{-1}\mathrm{gr}(\mathbf{a}_1) &= \mathrm{gr}(\rho_{12})\mathrm{gr}(\mathbf{a}_3) \\ \lambda^{-1}\mathrm{gr}(\mathbf{a}_1) &= \mathrm{gr}(\rho_1)\mathrm{gr}(\rho_2)\mathrm{gr}(\mathbf{a}_3) \\ \Rightarrow \mathrm{gr}(\mathbf{a}_3) &= \mathrm{gr}(\rho_2)^{-1}\mathrm{gr}(\rho_1)^{-1}\lambda^{-1}\mathrm{gr}(\mathbf{a}_1) \\ &= \left(\tfrac{1}{2}; -\tfrac{1}{2}, -\tfrac{1}{2}\right)\left(\tfrac{1}{2}; -\tfrac{1}{2}, \tfrac{1}{2}\right)\lambda^{-1}\mathrm{gr}(\mathbf{a}_1) \\ &= \left(\tfrac{1}{2}; -1, 0\right)(-1; 0, 0)\,\mathrm{gr}(\mathbf{a}_1) \\ &= \left(-\tfrac{1}{2}; -1, 0\right)/\langle h_0 \rangle. \end{aligned}$$

Performing this for the remaining generators, we obtain their (undetermined) refined gradings in $G/\langle h_0 \rangle$.

$$\begin{aligned} &\mathrm{gr}(\mathbf{a}_1) = (0; 0, 0)/\langle h_0 \rangle && \mathrm{gr}(\mathbf{a}_4) = (-1; -3, 1)/\langle h_0 \rangle \\ &\mathrm{gr}(\mathbf{a}_2) = \left(\tfrac{1}{2}; -2, 1\right)/\langle h_0 \rangle && \mathrm{gr}(\mathbf{b}_1) = \left(-\tfrac{1}{2}; -\tfrac{3}{2}, \tfrac{1}{2}\right)/\langle h_0 \rangle \\ &\mathrm{gr}(\mathbf{a}_3) = \left(-\tfrac{1}{2}; -1, 0\right)/\langle h_0 \rangle && \mathrm{gr}(\mathbf{b}_2) = \left(-\tfrac{1}{2}; -\tfrac{7}{2}, \tfrac{3}{2}\right)/\langle h_0 \rangle \end{aligned}$$

The final term $\rho_3 \otimes \mathbf{b}_2 \in \delta^1 \mathbf{a}_1$ allows us to pin down h_0:

$$\begin{aligned}
\lambda^{-1}\mathrm{gr}(\mathbf{a}_1) &= \mathrm{gr}(\rho_3)\mathrm{gr}(\mathbf{b}_2) \\
\Rightarrow \mathrm{gr}(\mathbf{a}_1) &= \lambda \mathrm{gr}(\rho_3)\mathrm{gr}(\mathbf{b}_2) \\
&= (1;0,0)\left(-\tfrac{1}{2};-\tfrac{1}{2},\tfrac{1}{2}\right)\mathrm{gr}(\mathbf{b}_2) \\
&= \left(\tfrac{1}{2};-\tfrac{1}{2},\tfrac{1}{2}\right)\left(-\tfrac{1}{2};-\tfrac{7}{2},\tfrac{3}{2}\right)\mathrm{gr}(\mathbf{a}_1) \\
&= (1;-4,2)\,/\langle h_0\rangle.
\end{aligned}$$

Then h_0 divides $(-1;4,-2)$, and so the two possibilities for h_0 are $(-\frac{1}{2};2,-1)$ or $(-1;4,-2)$. Supposing the former to generate a contradiction, we would have $\mathrm{gr}(\mathbf{a}_2) = \mathrm{gr}(\mathbf{a}_1)$ in $G/\langle h_0\rangle$, which in turn forces $\mathfrak{s}(\mathbf{x}_1 \boxtimes \mathbf{a_1}) = \mathfrak{s}(\mathbf{x}_1 \boxtimes \mathbf{a_2})$. This contradicts the discussion in Subsection 3.3, where these generators correspond to separate spin^c structures because no closed, piecewise smooth path in $\widetilde{T}$ exists to connect them. Then with $h_0 = (-1;4,-2)$, the refined gradings for generators of $\widehat{CFD}(N, 2\phi_1+\phi_0, -\phi_1, \mathfrak{s}_1)$ are the following:

$$\begin{aligned}
\mathrm{gr}(\mathbf{a}_1) &= (0;0,0)\,/\langle(-1;4,-2)\rangle & \mathrm{gr}(\mathbf{a}_4) &= (-1;-3,1)\,/\langle(-1;4,-2)\rangle \\
\mathrm{gr}(\mathbf{a}_2) &= \left(\tfrac{1}{2};-2,1\right)/\langle(-1;4,-2)\rangle & \mathrm{gr}(\mathbf{b}_1) &= \left(-\tfrac{1}{2};-\tfrac{3}{2},\tfrac{1}{2}\right)/\langle(-1;4,-2)\rangle \\
\mathrm{gr}(\mathbf{a}_3) &= \left(-\tfrac{1}{2};-1,0\right)/\langle(-1;4,-2)\rangle & \mathrm{gr}(\mathbf{b}_2) &= \left(-\tfrac{1}{2};-\tfrac{7}{2},\tfrac{3}{2}\right)/\langle(-1;4,-2)\rangle
\end{aligned}$$

It is interesting to note that

$$\begin{aligned}
\mathrm{gr}_{\mathbb{Q}}(\mathbf{a}_2) &= \left(\tfrac{1}{2};-2,1\right)/\langle(-1;4,-2)\rangle \\
&= \left(\tfrac{1}{2};-2,1\right)\left(-\tfrac{1}{2};2,-1\right)/\langle(-1;4,-2)\rangle \\
&= (0;0,0)\,/\langle(-1;4,-2)\rangle \\
&= \mathrm{gr}_{\mathbb{Q}}(\mathbf{a}_1),
\end{aligned}$$

by acting over $\mathbb{Q}$. The same holds true for the other generators, with $\mathrm{gr}_{\mathbb{Q}}(\mathbf{a}_4) = \mathrm{gr}_{\mathbb{Q}}(\mathbf{a}_3)$ and $\mathrm{gr}_{\mathbb{Q}}(\mathbf{b}_1) = \mathrm{gr}_{\mathbb{Q}}(\mathbf{b}_2)$. Generators of $HF(\widehat{HF}(S^3\backslash\nu J), h(\widehat{HF}(N,\mathfrak{s}_0)))$ come in pairs exhibiting this feature, which suggests that they are associated to conjugate spin^c structures on X. That this behavior does not depend on J is enough to show this, but we will not need it for our purposes.

Finally, we will need the corresponding type D realization $D(\theta_{h(N,\mathfrak{s}_0)})$ for pairing in Subsection 4.4, presented now in Figure 4.6.

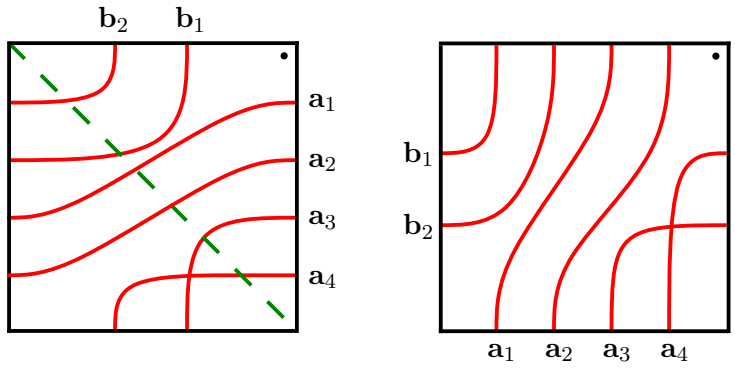

Figure 4.6: Left: $A(\theta_{h(N,\mathfrak{s}_0)})$. Right: Obtaining $D(\theta_{h(N,\mathfrak{s}_0)})$ via $r(y=-x)$.

4.3 Refined Gradings for $\widehat{CFD}(N, 2\phi_1+\phi_0, -\phi_1, \mathfrak{s}_1)$

Recall from Subsection 2.3.2 that the decorated graph on the left side of Figure 2.4 gives rise to $A(\theta_{N,\mathfrak{s}_1})$ shown in Figure 2.6. The same series of Dehn twists and reflections as those in the previous subsection can be applied to obtain $A(\theta_{h(N,\mathfrak{s}_1)})$ and $D(\theta_{h(N,\mathfrak{s}_1)})$. The end results are depicted in Figure 4.7.

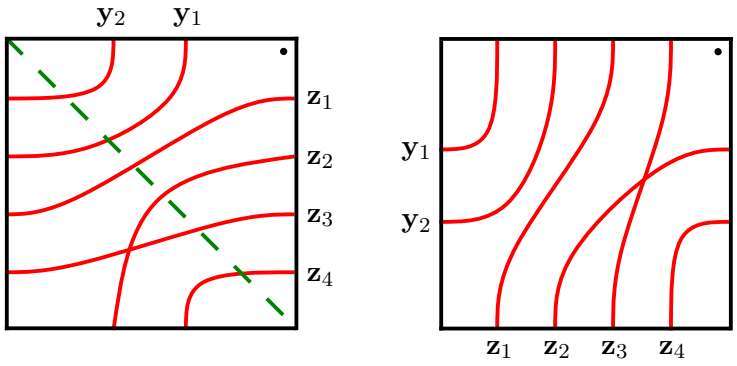

Figure 4.7: Left: $A(\theta_{h(N,\mathfrak{s}_1)})$. Right: Obtaining $D(\theta_{h(N,\mathfrak{s}_1)})$ via $r(y=-x)$.

Label the ι_0 generators by $\mathbf{z}_i$ and the ι_1 generators by $\mathbf{w}_i$. The decorated graph for $\widehat{CFD}(N, 2\phi_1+\phi_0, -\phi_1, \mathfrak{s}_0)$ is then given by Figure 4.8.

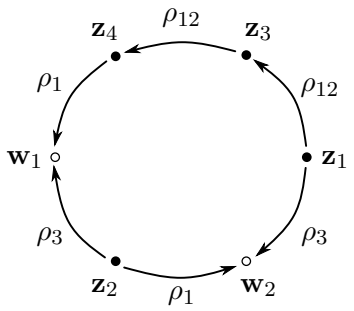

Figure 4.8: The decorated graph representation of $\widehat{CFD}(N, \phi_0 + 2\phi_1, -\phi_1, \mathfrak{s}_0)$

Using similar computations to those in the previous subsection, we have that the refined gradings for generators of $\widehat{CFD}(N, 2\phi_1 + \phi_0, -\phi_1, \mathfrak{s}_1)$ lie in $G/\langle(-3; 4, -2)\rangle$ and are the following:

$$\begin{aligned}
\mathrm{gr}(\mathbf{z}_1) &= (0; 0, 0)\,/\langle(-3; 4, -2)\rangle & \mathrm{gr}(\mathbf{z}_4) &= (-1; -2, 0)\,/\langle(-3; 4, -2)\rangle \\
\mathrm{gr}(\mathbf{z}_2) &= (1; -3, 1)\,/\langle(-3; 4, -2)\rangle & \mathrm{gr}(\mathbf{w}_1) &= \left(-\tfrac{1}{2}; -\tfrac{5}{2}, \tfrac{1}{2}\right)/\langle(-3; 4, -2)\rangle \\
\mathrm{gr}(\mathbf{z}_3) &= \left(-\tfrac{1}{2}; -1, 0\right)/\langle(-3; 4, -2)\rangle & \mathrm{gr}(\mathbf{w}_2) &= \left(\tfrac{3}{2}; -\tfrac{7}{2}, \tfrac{3}{2}\right)/\langle(-3; 4, -2)\rangle
\end{aligned}$$

4.4 Refined Gradings for Generators in Pairing

With $A(\theta_M)$ from Subsection 4.1, and both $D(\theta_{h(N,\mathfrak{s}_0)})$ from Subsection 4.2 and $D(\theta_{h(N,\mathfrak{s}_1)})$ from Subsection 4.3, we can now compute the relative Maslov grading differences for the generators of $\widehat{HF}(X)$. We do this first in detail for those $\mathfrak{t} \in \pi^{-1}(\mathfrak{s} \times \mathfrak{s}_0)$, and then briefly perform the same methods for those $\mathfrak{t} \in \pi^{-1}(\mathfrak{s} \times \mathfrak{s}_1)$ for completeness.

Include $A(\theta_M)$ into the first quadrant of T_M and $D(\theta_{h(N,\mathfrak{s}_1)})$ into the third quadrant of T_M, extending both horizontally and vertically. This results in the configuration shown on the left of Figure 4.9. According to the train track version of the pairing theorem, the summands $\widehat{HF}(X, \mathfrak{t})$ for which $\mathfrak{t} \in \pi^{-1}(\mathfrak{s} \times \mathfrak{s}_0)$ are given by $H_*(\mathcal{C}(A(\theta_M), D(\theta_{h(N,\mathfrak{s}_0)}), d^\theta))$. It is significantly more convenient to lift to $\widetilde{T}$, such as on the right of Figure 4.9, to see which generators are annihilated under Floer homology.

This is done in stages throughout Figures 4.9 and 4.10 to illustrate the homotopy performed to remove most bigons that do not cover a basepoint. Ultimately, the four generators are in correspondence with the four surviving intersections in Figure 4.11. They are $\mathbf{x}_1 \boxtimes \mathbf{a}_1$, $\mathbf{x_1} \boxtimes \mathbf{a}_2$, $\mathbf{y}_1 \boxtimes \mathbf{b}_1$, and $\mathbf{y_1} \boxtimes \mathbf{b}_2$. Their refined gradings lie in $G_{A,\mathbb{Q}}(M, \mathfrak{s}) \times_{G_\mathbb{Q}}$

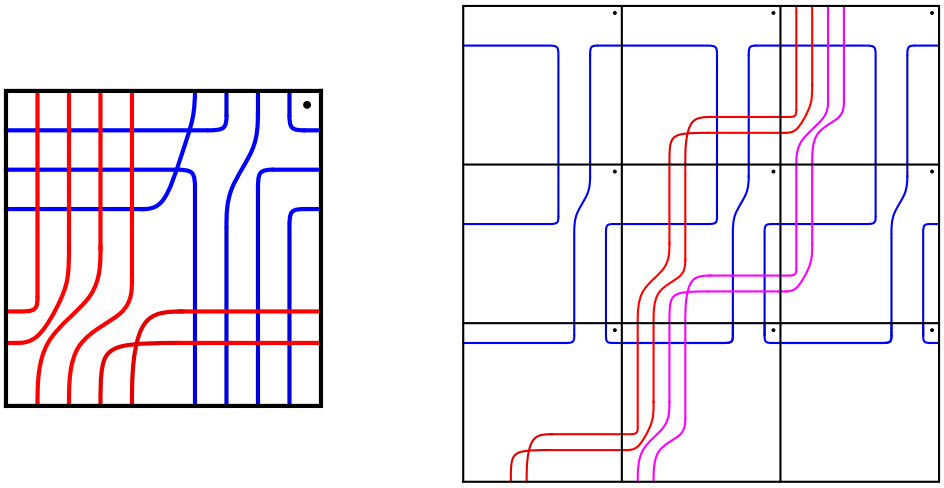

Figure 4.9: Including $A(\theta_M)$ and $D(\theta_{h(N,\mathfrak{s}_0)})$ in T_M, and lifting intersections to $\widetilde{T}$.

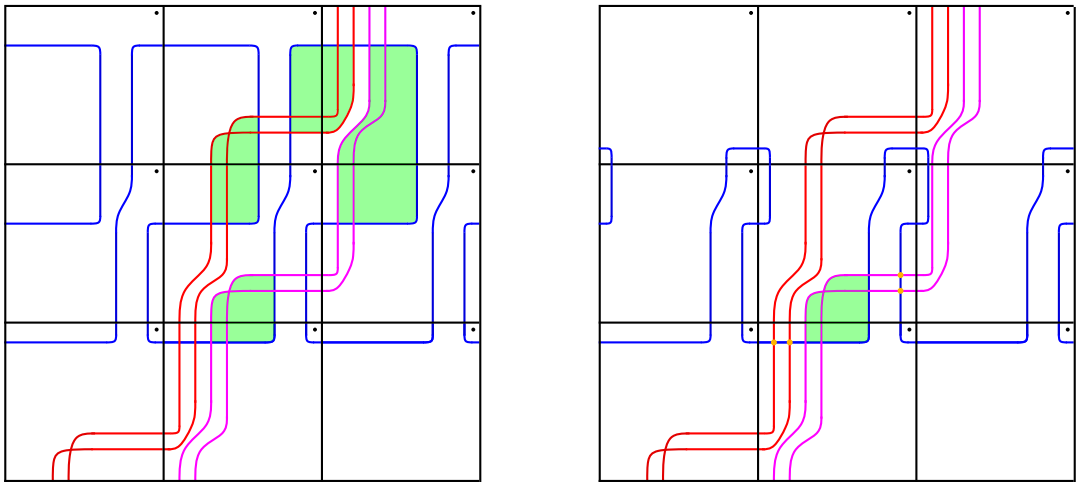

Figure 4.10: Left: Bigons between lifted intersections of $A(\theta_M)$ and $D(\theta_{h(N,\mathfrak{s}_0)})$ to $\widetilde{T}$. Right: Homotoped $A(\theta_M)$, removing most generators annihilated in intersection Floer homology and leaving lifts of four generators that survive.

$G_{D,\mathbb{Q}}(h(N,\mathfrak{s}_0))$, which may be determined using the information from Subsections 4.1 and 4.3 together with Theorem 4.0.1.

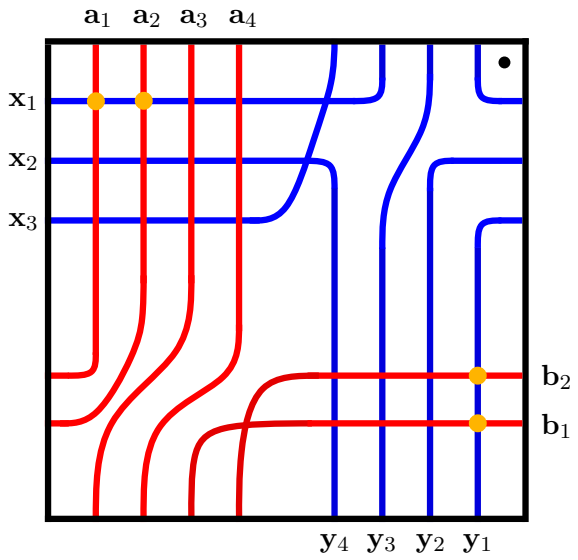

Figure 4.11: The four generators of $H_*(\widehat{CFA}(M,\mu,\lambda)\boxtimes\widehat{CFD}(N,2\phi_1+\phi_0,-\phi_1,\mathfrak{s}_0))$.

The gradings take values in $\langle\left(\frac{3}{2};0,1\right)\rangle\backslash G/\langle(-1;4,-2)\rangle$, and are given by the following:

$$\begin{aligned}
\mathrm{gr}(\mathbf{x}_1\boxtimes\mathbf{a}_1) &= \mathrm{gr}(\mathbf{x}_1)\mathrm{gr}(\mathbf{a}_1)\\
&= \langle\left(\tfrac{3}{2};0,1\right)\rangle\backslash\left(0;0,0\right)/\langle(-1;4,-2)\rangle\\
\mathrm{gr}(\mathbf{x}_1\boxtimes\mathbf{a}_2) &= \mathrm{gr}(\mathbf{x}_1)\mathrm{gr}(\mathbf{a}_2)\\
&= \langle\left(\tfrac{3}{2};0,1\right)\rangle\backslash\left(\tfrac{1}{2};-2,1\right)/\langle(-1;4,-2)\rangle\\
\mathrm{gr}(\mathbf{y_1}\boxtimes\mathbf{b}_1) &= \mathrm{gr}(\mathbf{y_1})\mathrm{gr}(\mathbf{b}_1)\\
&= \langle\left(\tfrac{3}{2};0,1\right)\rangle\backslash\left(-\tfrac{1}{2};\tfrac{1}{2},\tfrac{1}{2}\right)\left(-\tfrac{1}{2};-\tfrac{3}{2},\tfrac{1}{2}\right)/\langle(-1;4,-2)\rangle\\
&= \langle\left(\tfrac{3}{2};0,1\right)\rangle\backslash\left(0;-1,1\right)/\langle(-1;4,-2)\rangle\\
\mathrm{gr}(\mathbf{y_1}\boxtimes\mathbf{b}_2) &= \mathrm{gr}(\mathbf{y_1})\mathrm{gr}(\mathbf{b}_2)\\
&= \langle\left(\tfrac{3}{2};0,1\right)\rangle\backslash\left(-\tfrac{1}{2};\tfrac{1}{2},\tfrac{1}{2}\right)\left(-\tfrac{1}{2};-\tfrac{7}{2},\tfrac{3}{2}\right)/\langle(-1;4,-2)\rangle\\
&= \langle\left(\tfrac{3}{2};0,1\right)\rangle\backslash\left(\tfrac{3}{2};-3,2\right)/\langle(-1;4,-2)\rangle
\end{aligned}$$

Acting over $\mathbb{Q}$ to make each Spin^c component equal to $(0,0)$ yields the following:

$$\begin{aligned}
\mathrm{gr}_{\mathbb{Q}}(\mathbf{x}_1 \boxtimes \mathbf{a}_1) &= \langle (\tfrac{3}{2};0,1)\rangle \backslash (0;0,0)/\langle (-1;4,-2)\rangle \\
\mathrm{gr}_{\mathbb{Q}}(\mathbf{x}_1 \boxtimes \mathbf{a}_2) &= \langle (\tfrac{3}{2};0,1)\rangle \backslash (\tfrac{1}{2};-2,1)/\langle (-1;4,-2)\rangle \\
&= \langle (\tfrac{3}{2};0,1)\rangle \backslash (\tfrac{1}{2};-2,1)(-\tfrac{1}{2};2,-1)/\langle (-1;4,-2)\rangle \\
&= \langle (\tfrac{3}{2};0,1)\rangle \backslash (0;0,0)/\langle (-1;4,-2)\rangle \\
\mathrm{gr}_{\mathbb{Q}}(\mathbf{y_1} \boxtimes \mathbf{b}_1) &= \langle (\tfrac{3}{2};0,1)\rangle \backslash (0;-1,1)/\langle (-1;4,-2)\rangle \\
&= \langle (\tfrac{3}{2};0,1)\rangle \backslash (-\tfrac{3}{4};0,-\tfrac{1}{2})(0;-1,1)(-\tfrac{1}{4};1,-\tfrac{1}{2})/\langle (-1;4,-2)\rangle \\
&= \langle (\tfrac{3}{2};0,1)\rangle \backslash (-\tfrac{5}{4};-1,\tfrac{1}{2})(-\tfrac{1}{4};1,-\tfrac{1}{2})/\langle (-1;4,-2)\rangle \\
&= \langle (\tfrac{3}{2};0,1)\rangle \backslash (-\tfrac{3}{2};0,0)/\langle (-1;4,-2)\rangle \\
\mathrm{gr}_{\mathbb{Q}}(\mathbf{y_1} \boxtimes \mathbf{b}_2) &= \langle (\tfrac{3}{2};0,1)\rangle \backslash (\tfrac{3}{2};-3,2)/\langle (-1;4,-2)\rangle \\
&= \langle (\tfrac{3}{2};0,1)\rangle \backslash (-\tfrac{3}{4};0,-\tfrac{1}{2})(\tfrac{3}{2};-3,2)(-\tfrac{3}{4};3,-\tfrac{3}{2})/\langle (-1;4,-2)\rangle \\
&= \langle (\tfrac{3}{2};0,1)\rangle \backslash (-\tfrac{3}{4};-3,\tfrac{3}{2})(-\tfrac{3}{4};3,-\tfrac{3}{2})/\langle (-1;4,-2)\rangle \\
&= \langle (\tfrac{3}{2};0,1)\rangle \backslash (-\tfrac{3}{2};0,0)/\langle (-1;4,-2)\rangle
\end{aligned}$$

While not necessary to generate the desired surgery obstruction, the grading differences for the other four generators may be of independent interest. Performing the same methods for the pairing of $A(\theta_M)$ and $D(\theta_{h(N,\mathfrak{s}_1)})$ yields the configuration in Figure 4.12. The four surviving generators are $\mathbf{x}_1 \boxtimes \mathbf{z}_1$, $\mathbf{y}_1 \boxtimes \mathbf{w}_1$, $\mathbf{x}_1 \boxtimes \mathbf{z}_3$, and $\mathbf{y_1} \boxtimes \mathbf{w}_2$. Knowing these generators, we now compute their refined gradings in $G_{A,\mathbb{Q}}(M,\mathfrak{s}) \times_{G_{\mathbb{Q}}} G_{D,\mathbb{Q}}(h(N,\mathfrak{s}_1))$ using the information from Subsections 4.1 and 4.2.

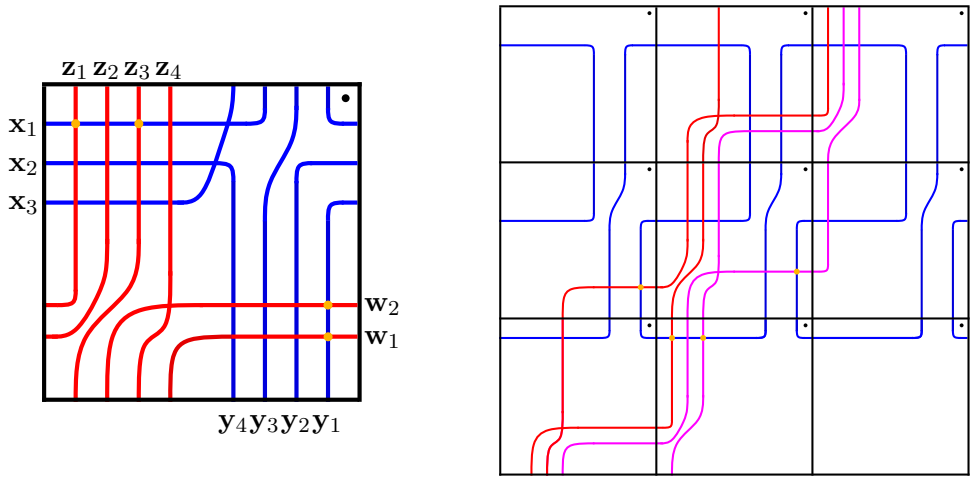

Figure 4.12: The four generators of $H_*(\widehat{CFA}(M,\mu,\lambda) \boxtimes \widehat{CFD}(N, 2\phi_1+\phi_0, -\phi_1, \mathfrak{s}_1))$.

The gradings take values in $\langle(\frac{3}{2};0,1)\rangle\backslash G/\langle(-3;4,-2)\rangle$, and are given by the following:

$$\begin{aligned}
\mathrm{gr}(\mathbf{x}_1 \boxtimes \mathbf{z}_1) &= \mathrm{gr}(\mathbf{x}_1)\mathrm{gr}(\mathbf{z}_1)\\
&= \langle(\tfrac{3}{2};0,1)\rangle\backslash(0;0,0)/\langle(-3;4,-2)\rangle\\
\mathrm{gr}(\mathbf{y}_1 \boxtimes \mathbf{w}_1) &= \mathrm{gr}(\mathbf{y}_1)\mathrm{gr}(\mathbf{w}_1)\\
&= \langle(\tfrac{3}{2};0,1)\rangle\backslash(-\tfrac{1}{2};\tfrac{1}{2},\tfrac{1}{2})(-\tfrac{1}{2};-\tfrac{5}{2},\tfrac{1}{2})/\langle(-3;4,-2)\rangle\\
&= \langle(\tfrac{3}{2};0,1)\rangle\backslash(\tfrac{1}{2};-2,1)/\langle(-3;4,-2)\rangle\\
\mathrm{gr}(\mathbf{x}_1 \boxtimes \mathbf{z}_3) &= \mathrm{gr}(\mathbf{x}_1)\mathrm{gr}(\mathbf{z}_3)\\
&= \langle(\tfrac{3}{2};0,1)\rangle\backslash(-\tfrac{1}{2};-1,0)/\langle(-3;4,-2)\rangle\\
\mathrm{gr}(\mathbf{y}_1 \boxtimes \mathbf{w}_2) &= \mathrm{gr}(\mathbf{y}_1)\mathrm{gr}(\mathbf{w}_2)\\
&= \langle(\tfrac{3}{2};0,1)\rangle\backslash(-\tfrac{1}{2};\tfrac{1}{2},\tfrac{1}{2})(\tfrac{3}{2};-\tfrac{7}{2},\tfrac{3}{2})/\langle(-3;4,-2)\rangle\\
&= \langle(\tfrac{3}{2};0,1)\rangle\backslash(\tfrac{7}{2};-3,2)/\langle(-3;4,-2)\rangle
\end{aligned}$$

Acting over $\mathbb{Q}$ to make each Spin^c component equal to $(0,0)$ yields the following:

$$\begin{aligned}
\mathrm{gr}_{\mathbb{Q}}(\mathbf{x}_1 \boxtimes \mathbf{z}_1) &= \langle(\tfrac{3}{2};0,1)\rangle \backslash (0;0,0)/\langle(-3;4,-2)\rangle \\
\mathrm{gr}_{\mathbb{Q}}(\mathbf{y}_1 \boxtimes \mathbf{w}_1) &= \langle(\tfrac{3}{2};0,1)\rangle \backslash (\tfrac{1}{2};-2,1)/\langle(-3;4,-2)\rangle \\
&= \langle(\tfrac{3}{2};0,1)\rangle \backslash (\tfrac{1}{2};-2,1)(-\tfrac{3}{2};2,-1)/\langle(-3;4,-2)\rangle \\
&= \langle(\tfrac{3}{2};0,1)\rangle \backslash (-1;0,0)/\langle(-3;4,-2)\rangle \\
\mathrm{gr}_{\mathbb{Q}}(\mathbf{x}_1 \boxtimes \mathbf{z}_3) &= \langle(\tfrac{3}{2};0,1)\rangle \backslash (-\tfrac{1}{2};-1,0)/\langle(-3;4,-2)\rangle \\
&= \langle(\tfrac{3}{2};0,1)\rangle \backslash (\tfrac{3}{4};0,\tfrac{1}{2})(-\tfrac{1}{2};-1,0)(-\tfrac{3}{4};1,-\tfrac{1}{2})/\langle(-3;4,-2)\rangle \\
&= \langle(\tfrac{3}{2};0,1)\rangle \backslash (\tfrac{3}{4};-1,\tfrac{1}{2})(-\tfrac{3}{4};1,-\tfrac{1}{2})/\langle(-3;4,-2)\rangle \\
&= \langle(\tfrac{3}{2};0,1)\rangle \backslash (0;0,0)/\langle(-3;4,-2)\rangle
\end{aligned}$$

$$\begin{aligned}
\mathrm{gr}_{\mathbb{Q}}(\mathbf{y}_1 \boxtimes \mathbf{w}_2) &= \langle(\tfrac{3}{2};0,1)\rangle \backslash (\tfrac{7}{2};-3,2)/\langle(-3;4,-2)\rangle \\
&= \langle(\tfrac{3}{2};0,1)\rangle \backslash (-\tfrac{3}{4};0,-\tfrac{1}{2})(\tfrac{7}{2};-3,2)(-\tfrac{9}{4};3,-\tfrac{3}{2})/\langle(-3;4,-2)\rangle \\
&= \langle(\tfrac{3}{2};0,1)\rangle \backslash (\tfrac{5}{4};-3,\tfrac{3}{2})(-\tfrac{9}{4};3,-\tfrac{3}{2})/\langle(-3;4,-2)\rangle \\
&= \langle(\tfrac{3}{2};0,1)\rangle \backslash (-1;0,0)/\langle(-3;4,-2)\rangle
\end{aligned}$$

With the desired grading differences at hand, we now establish the third lemma.

Lemma 4.4.1. *Let $X = (S^3 \setminus \nu T(2,3)) \cup_h N$, where h is any slope 2 cyclic gluing. Then there exist generators $\mathbf{x}, \mathbf{y}$ of $\widehat{HF}(X)$ such that $\mathfrak{s}(\mathbf{x}), \mathfrak{s}(\mathbf{y}) \in \pi^{-1}(\mathfrak{s} \times \mathfrak{s}_0)$ and $gr_{\mathbb{Q}}(\mathbf{x}) - gr_{\mathbb{Q}}(\mathbf{y}) = \frac{3}{2}$.*

Proof. Recall that any slope 2 gluing satisfying the cyclic condition of Proposition 3.1.2 induces

$$[(h^n)_*] = \begin{pmatrix} 1 & n \\ 2 & 2n-1 \end{pmatrix}.$$

on homology for some $n \in \mathbb{Z}$. We saw from Section 3.1 that it is obtained from the base slope 2 gluing h by the pre-composition

$$[(h^n)_*] = [h_* \circ T^n] = \begin{pmatrix} 1 & 0 \\ 2 & -1 \end{pmatrix} \begin{pmatrix} 1 & n \\ 0 & 1 \end{pmatrix}.$$

For $X^n = M \cup_{h^n} N$, the pairing theorem implies

$\widehat{HF}(X^n, \mathfrak{t}) \cong H_*(\widehat{CFA}(M, \mu, \lambda) \boxtimes \widehat{CFD}(N, (h^n)_*^{-1}(\lambda), (h^n)_*^{-1}(\mu), \mathfrak{s}_0))$ for $\mathfrak{t} \in \pi^{-1}(\mathfrak{s} \times \mathfrak{s}_0)$. The required type D structure for pairing is $\widehat{CFD}(N, 2\phi_1 + (1-2n)\phi_0, -\phi_1 + n\phi_0, \mathfrak{s}_0)$, whose type A realization can be obtained from that of $\widehat{CFD}(N, \phi_1 - n\phi_0, \phi_0, \mathfrak{s}_0)$ by using precisely the same series of Dehn twists and reflections from Subsection 4.2. Since $\widehat{CFD}(N, \phi_1 - n\phi_0, \phi_0, \mathfrak{s}_0) \cong \widehat{CFD}(N, \phi_1, \phi_0, \mathfrak{s}_0)$ because N is a Heegaard Floer homology solid torus, we have that the type A realizations of $\widehat{CFD}(N, 2\phi_1 + (1-2n)\phi_0, -\phi_1 + n\phi_0, \mathfrak{s}_0)$ and $\widehat{CFD}(N, 2\phi_1 + \phi_0, -\phi_1, \mathfrak{s}_0)$ agree. Further, the decorated graph representations and refined gradings from Subsection 4.2, as well as the relative $\mathbb{Q}$-grading differences (between generators belonging to the same pre-image $\pi^{-1}(\mathfrak{s} \times \mathfrak{s}_i)$) from Subsection 4.4 all hold for each gluing h^n, regardless of $n \in \mathbb{Z}$.

These grading differences were computed using the prototype pairing theorem for train tracks, whose use is currently unjustified. They will correspond to grading differences of $\widehat{HF}(X)$ if the bordered invariants in pairing satisfy the mild hypotheses of [HRW16, Theorem 16]. Specifically, we require that $A(\theta_M)$ is reduced and that $D(\theta_{h(N,\mathfrak{s}_0)})$ is special bounded. The realization $A(\theta_M)$ is reduced since it is generated from a decorated graph for which no edges are labeled with $\varnothing$. A train track is special bounded if it is bounded and almost reduced, meaning that its underlying decorated graph does not contain an oriented cycle and any edges labeled with $\varnothing$ occur in specific configurations. The underlying decorated graph for $D(\theta_{h(N,\mathfrak{s}_0)})$ does not have any edges labeled with $\varnothing$, and also does not contain an oriented cycle (even though $D(\theta_{N,\mathfrak{s}_0})$ does).

With equal spin^c components, we can recover the $\mathbb{Q}$-grading difference between $\mathbf{x}_1 \boxtimes \mathbf{a}_1$ and $\mathbf{y}_1 \boxtimes \mathbf{b}_1$ as the difference between their Maslov components: $\mathrm{gr}_{\mathbb{Q}}(\mathbf{x}_1 \boxtimes \mathbf{a}_1) - \mathrm{gr}_{\mathbb{Q}}(\mathbf{y}_1 \boxtimes \mathbf{b}_1) = \frac{3}{2}$. Together with the Dehn twisting invariance of $\widehat{CFD}(N, \phi_1, \phi_0, \mathfrak{s}_0)$, this establishes the lemma. □

Remark. We caution the reader that the techniques used to prove this lemma do **not** show that the Dehn twisting invariance of $\widehat{CFD}(N, \phi_1, \phi_0)$ in pairing provides an integral family of manifolds with relatively-graded, isomorphic $\widehat{HF}$. All that we show is that the relative $\mathbb{Q}$-grading differences between generators $\mathbf{x}, \mathbf{y}$ with $\mathfrak{s}(\mathbf{x}), \mathfrak{s}(\mathbf{y}) \in \pi^{-1}(\mathfrak{s} \times \mathfrak{s}_i)$ are independent of Dehn twisting N along ϕ_0. We should expect to see the relative $\mathbb{Q}$-grading differences grow between generators providing Floer homology supported in spin^c structures belonging to different spin^c pre-images of π.

4.5 Proof of Theorem 1.2.1

Proof. Suppose $X = (S^3 \setminus \nu J) \cup_h N$ is realized as 8-surgery along K with $g(K) = 2$. If J is the unknot, then Lemma 3.2.1 using Doig's classification together with [NZ18, Theorem 1.6] implies that $X = S^3_8(T(2,5))$. This manifold is an L-space, and is the Seifert fibered manifold $(-1; \frac{1}{2}, \frac{1}{2}, \frac{2}{5})$ with base orbifold S^2.

Suppose for the sake of contradiction that some non-trivial $J \subset S^3$ gives rise to X. Then Lemma 3.3.1 implies $J = T(2,3)$, and so X is an L-space as large surgery along an L-space knot. As an L-space, the relative $\mathbb{Q}$-grading differences for generators of $\widehat{HF}(X)$ are given by differences of the d-invariants. Since K is a genus two L-space knot, we have $\widehat{HFK}(K) = \widehat{HFK}(T(2,5))$ and so the d-invariants of surgery are

$$d(S^3_8(K), [s]) = \begin{cases} -1/8 & s \equiv 5 \pmod 8 \\ 1/4 & s \equiv 6 \pmod 8 \\ -9/8 & s \equiv 7 \pmod 8 \\ -1/4 & s \equiv 0 \pmod 8 \\ -9/8 & s \equiv 1 \pmod 8 \\ 1/4 & s \equiv 2 \pmod 8 \\ -1/8 & s \equiv 3 \pmod 8 \\ -1/4 & s \equiv 4 \pmod 8 \end{cases}$$

Lemma 4.4.1 shows that there must be generators $\mathbf{x}, \mathbf{y}$ for $\widehat{HF}(X)$ such that $\mathrm{gr}_{\mathbb{Q}}(\mathbf{x}) - \mathrm{gr}_{\mathbb{Q}}(\mathbf{y}) = \frac{3}{2}$. This is impossible given $d(S^3_8(K), [s])$ above, which is the contradiction we sought. □

CHAPTER

5

REDUCIBLE SURGERIES AND THIN KNOTS

For both this chapter and the next, let K be a thin, hyperbolic knot and let M denote $S^3 \setminus \nu K$. We aim to show K can admit a reducible surgery only if it is an L-space knot. It is unknown whether such a knot K exists. Recall that a reducing slope for K is integral, and satisfies the Matignon-Sayari genus bound $1 < |r| \leq 2g(K) - 1$. As mentioned in the introduction, we will only consider positive reducing slopes by mirroring K if necessary.

5.1 Gradings via Immersed Curves

We saw toward the end of the previous chapter that involving Maslov grading differences in tandem with dim $\widehat{HF}$ leads to strong restrictions on the surgery knot. Our approach will use this idea together with the periodicity enjoyed by the Floer homology of a reducible manifold with an L-space summand (Lemma 2.2.6). The analysis will involve a few cases, each with their own subcases, depending on $\tau(K)$ relative to r and $g(K)$. Most of these are addressed in this chapter, with the remaining ones relegated to Chapter 6 where we

appeal to the d invariants once more.

To enable swift grading comparisons later on, let us designate a reference intersection associated to $[s] \in \text{Spin}^c(S^3_r(K))$, recalling our conventions for the range that $[s]$ falls in. Notice that the essential curve $\overline{\gamma}$ has vertical segments if $\tau(K) \neq 0$. We will define a *vertical intersection* to be an intersection between l^s_r and a vertical segment of $\overline{\gamma}$ within a neighborhood of $\overline{\mu}$. If $[s]$ satisfies $0 \leq |[s]| < |\tau(K)|$, then such an intersection occurs and we will denote it using a^s. Alternatively, if $|[s]| \geq \tau(K) \geq 0$ then any intersection between l^s_r and $\overline{\gamma}$ is outside any neighborhood of the lifts of the marked point in $\overline{T}_M$. In this case l^s_r intersects $\overline{\gamma}$ once if $\tau(K) \geq 0$, and so a^s will denote this lone intersection. When $\tau(K) < 0$ and $[s] \geq 0$, we let a^s denote the intersection between l^s_r and $\overline{\gamma}$ to the left of $\overline{\mu}$. Analogously when $\tau(K) < 0$ and $[s] < 0$, we will have a^s be the intersection between l^s_r and $\overline{\gamma}$ to the right of $\overline{\mu}$. It is likely helpful to reference Figure 5.1 for these different possibilities. While cumbersome, this scheme allows us to label the interesction that often corresponds via the Pairing theorem to a generator with the least Maslov grading.

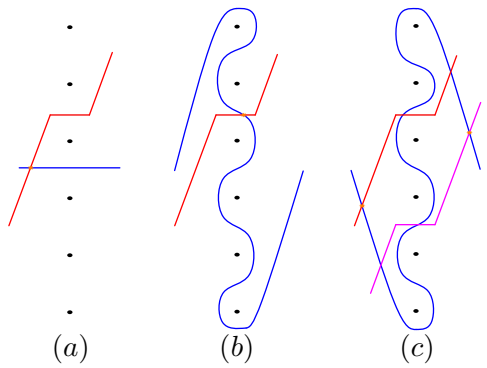

Figure 5.1: The possibilities for the reference intersection a^s. (a) has $\tau(K) = 0$, (b) has $\tau(K) > 0$ and $|s| < \tau(K)$, and (c) has $\tau(K) < 0$ with two curves representing $s \geq 0$ in red and $s < 0$ in purple. The case when $\tau(K) > 0$ and $|s| \geq \tau(K)$ is similar to (a).

It will also be particularly useful to know the winding number of enclosed lifts of the marked point of specific regions. Consider the neighborhood of $\overline{\mu}$ in $\overline{T}_M$ that contains the lifts of the marked points, which is also wide enough to enclose the vertical segments of $\overline{\gamma}$. Intersect $\overline{\gamma}$ with a horizontal line l^s_0 slightly longer than this neighborhood at height s, so that these segments together bound regions enclosing basepoints. We will define $\widetilde{H}_s$ to be the number of enclosed lifts of the marked point in the region bounded above by l^s, on the

side(s) by the neighborhood of $\overline{\mu}$, and elsewhere by $\overline{\gamma}$. If the region is empty, then $\widetilde{H}_s = 0$. This number coincides with the invariant H_s from the mapping cone formula, but we will use this alternate notation to make the geometric distinction clear. Analogously, there is often a region where l^s bounds from below and the number of enclosed lifts of the marked point of such a region will be denoted by $\widetilde{V}_s$. These are depicted in Figure 5.2. Due to Theorem 2.3.3, we recover both $\widetilde{H}_{-s} = \widetilde{V}_s$ and $\widetilde{H}_s - \widetilde{V}_s = \widetilde{H}_s - \widetilde{H}_{-s} = \frac{1}{2}(s - (-s)) = s$.

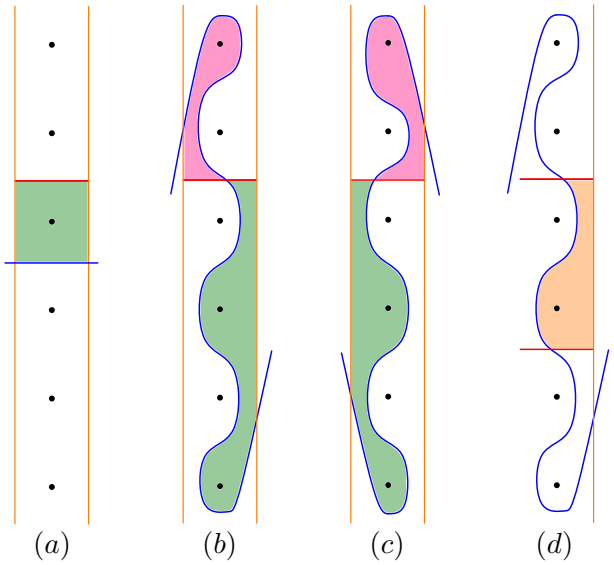

Figure 5.2: $\widetilde{H}_s$ is the number of marked points enclosed in green regions, and $\widetilde{V}_s$ is the number of marked points enclosed in pink regions. (a) shows $\tau(K) = 0$, (b) shows $\tau(K) > 0$, (c) shows $\tau(K) < 0$, and (d) shows $\widetilde{H}_s - \widetilde{V}_s = s$.

From the discussion in the previous section, we know that the form of $\widehat{HF}(M)$ is very restricted. Our goal is to leverage this to constrain gradings on $\widehat{HF}(S^3_r(K), [s]) \cong HF(\widehat{HF}(M), l^s_r)$ to obstruct reducible surgeries. We use multisets, which are sets with repitition allowed, to collect these relative Maslov gradings.

Definition 5.1.1. Let $[s] \in \mathrm{Spin}^c(S^3_r(K))$ be arbitrary with reference intersection a^s. For any intersection y of $HF(\widehat{HF}(M), l^s_r)$, let $M_{rel}(y)$ denote the grading difference $M(y) - M(a^s)$. We define the desired multiset by

$$MR^{[s]} \coloneqq \left\{ M_{rel}(y) \mid y \in \widehat{HF}(M) \pitchfork l^s_r \right\}.$$

Further, let $\mathrm{Width}(MR^{[s]})$ denote the difference between the largest and smallest elements of this multiset.

As defined, $MR^{[s]}$ is only an invariant up to translation, which means its width is an invariant. We can now look at computing grading differences between intersections, using Proposition 2.3.9. For a bigon P, we will first determine the contribution due to $2\mathrm{Wght}(P) - 2\mathrm{Rot}(P)$ using the knot Floer homology of K. This is performed using an analogous bigon P_K for $\widehat{HFK}$, and then we show that the same properties hold for the bigon P for $\widehat{HF}$. If l_r^s intersects a simple figure-eight of $\widehat{HF}(M)$ at height n, it does so in two places x^n and y^n. We will label them as *left* (x^n) and *right* (y^n) intersections,

Lemma 5.1.2. *Let y^n be a right intersection belonging to a simple figure-eight at height n of $\widehat{HF}(M)$, let a be an intersection of $\widehat{HF}(M) \pitchfork l_r^s$, and suppose P is a bigon between them. If K is thin, then $2\,Wght(P) - 2Rot(P) = -1 - \tau(K) - |n|$.*

Proof. In the infinite cylinder $\overline{T}_M$, we can represent $\overline{\mu}$, the lift of the meridian of T_M, as the vertical line that pierces each lift of the marked point in $\overline{T}_M$. Let $a^{-\tau(K)}$ be the last intersection that $\overline{\gamma}$ makes with $\overline{\mu}$ before wrapping around $\overline{T}_M$. Because $\widehat{HF}(M)$ is invariant under the action by the hyperelliptic involution, the weights of the grading arrows connecting $\overline{\gamma}$ to the simple figure-eights at heights n and $-n$ are equivalent. From this we can assume that n is non-negative, and use $|n|$ in future formulas otherwise.

Lift $\widehat{HF}(M)$ to $\overline{T}$ for convenience, and intersect it with $\overline{\mu}$. If we place z and w basepoints to the left and right, respectively, of every lift of the marked point, then $\widehat{HFK}(K) \cong HF(\widehat{HF}(M), \overline{\mu})$ due to [HRW18, Theorem 51]. This pairing is depicted in Figure 5.3. The formula in Proposition 2.3.9 still holds with the adjustment that Wind is modified to count the net winding number of enclosed w basepoints, denoted Wind_w.

Since $\widehat{HF}(M)$ has a simple figure-eight component at height n, there must be a generator η of $\widehat{HFK}(K)$ with $A(\eta) = n + 1$. Let P_K be the bigon from $a^{-\tau(K)}$ to η that traverses the grading arrow connecting the relevant components of $\widehat{HF}(M)$, visible in Figure 5.3 with $\tau(K) \geq 0$ and $\tau(K) < 0$, respectively. To determine $\mathrm{Wght}(P_K)$ directly would require care for the orientations of the grading arrow. However since we are after a different term, we can abuse notation by having every grading arrow connect to the right side of a simple figure-eight, regardless of its orientation. Essentially, any change that $\mathrm{Wght}(P_K)$ experiences between the two ways of attaching the grading arrow is inverted and absorbed by $\mathrm{Rot}(P)$, so that $2\mathrm{Wght}(P_K) - 2\mathrm{Rot}(P_K)$ remains unchanged.

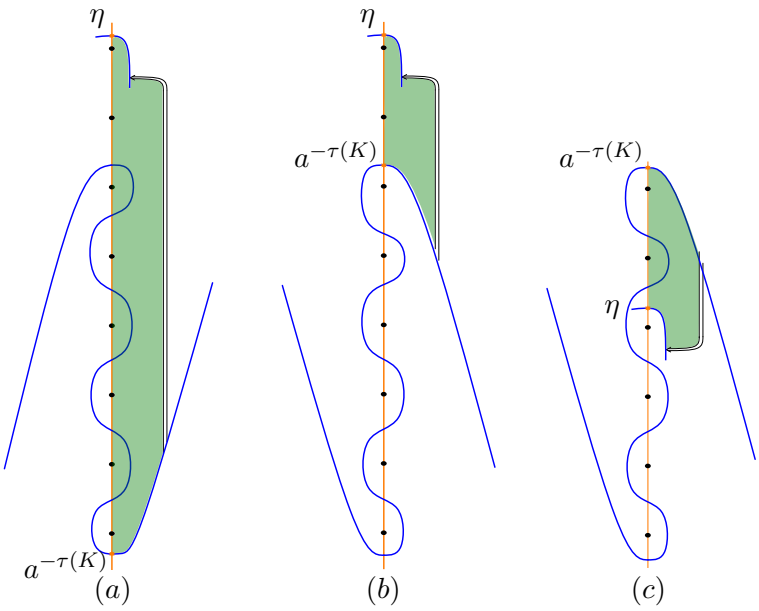

Figure 5.3: The bigon P_K between $a^{-\tau(K)}$ and η, formed from path components in $\widehat{HF}(M)$ and $\widetilde{\mu}$. (a) shows this for $\tau(K) \geq 0$ and (b) shows this for $A(\eta) > -\tau(K) > 0$. However for (c) with $A(\eta) \geq -\tau(K) > 0$, the bigon P_K runs from η to $a^{-\tau(K)}$.

If $\tau(K) \geq 0$ so that $A(a^{-\tau(K)}) < n$, we have

$$M(\eta) - M(a^{-\tau(K)}) = 2\text{Wind}_w(P_K) + 2\text{Wght}(P_K) - 2\text{Rot}(P_K).$$

However since K is thin, it follows that

$$M(\eta) - M(a^{-\tau(K)}) = A(\eta) - A(a^{-\tau(K)}) = A(\eta) + \tau(K).$$

Then $2\text{Wght}(P_K) - 2\text{Rot}(P_K) = A(\eta) - 2\text{Wind}(P_K) + \tau(K)$. Since $\text{Wind}(P_K) = A(\eta) + \tau(K)$, we have $2\text{Wght}(P_K) - 2\text{Rot}(P_K) = -A(\eta) - \tau(K) = -1 - \tau(K) - n$.

If $\tau(K) < 0$, the above computation follows through for $A(\eta) > -\tau(K)$, but the case for $A(\eta) \leq -\tau(K)$ differs slightly. In this situation P_K is a bigon from η to $a^{-\tau(K)}$ that also traverses the grading arrow in reverse, visible in Figure 5.3. Traveling the grading arrow in reverse means that we have $M(a^{-\tau(K)}) - M(\eta) = 2\text{Wind}_w(P_K) - 2\text{Wght}(P_K) - 2\text{Rot}(P_K)$,

and so

$$\begin{aligned}-2\text{Wght}(P_K) - 2\text{Rot}(P_K) &= M(a^{-\tau(K)}) - M(a^\eta) - 2\text{Wind}_w(P) \\ &= -\tau(K) - (n+1) - 2(-\tau(K) - (n+1)) \\ &= 1 + \tau(K) + n.\end{aligned}$$

Due to the shape of P_K, the bigon has a cusp near the grading arrow regardless of how it connects these components, and so $\text{Rot}(P_K) = 0$. Then we have $2\text{Wght}(P_K) - 2\text{Rot}(P_K) = 2\text{Wght}(P_K) + 2\text{Rot}(P_K) = -1 - \tau(K) - n$, as claimed.

With the formula established for P_K, we will now show that it is satisfied for a bigon between generators of $HF(\widehat{HF}(M), l_r^s)$ with similar attributes. Let y^n be a right intersection from the simple figure-eight at height n and let a be an intersection from a vertical segment of $\overline{\gamma}$ and l_r^s. With P denoting the bigon from a to y^n, we see that P must traverse the same grading arrow that P_K traversed, and so $\text{Wght}(P) = \text{Wght}(P_K)$. Additionally, it is straightforward to see that $\text{Rot}(P) = \text{Rot}(P_K)$ after tilting the bigons as well, with visual given in Figure 5.4. This completes the proof. □

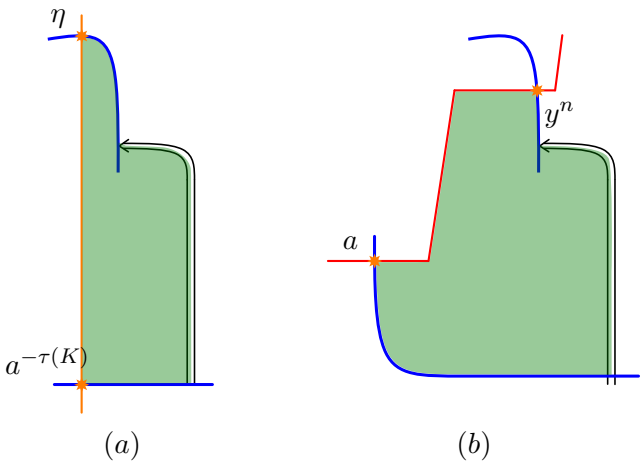

Figure 5.4: Tilting bigons to show they have equivalent net clockwise rotation along their boundaries. (a) The bigon P_K from $a^{-\tau(K)}$ to η. (b) The bigon P from a to y^n.

The following proposition considers left and right intersections of a simple figure-eight whose height n is less than $|\tau(K)|$. There is then a nearby vertical intersection a^n, and we will see that these three intersections have little difference in grading.

Proposition 5.1.3. Let K be thin and have M denote $S^3 \setminus \nu K$. Further, let x^n and y^n be left and right intersections belonging to a simple figure-eight of $\widehat{HF}(M)$ with height $0 \leq n < |\tau(K)|$, and let a^n be the nearby vertical generator. Then $-1 \leq M(y^n) - M(a^n) \leq 0$ and $0 \leq M(x^n) - M(a^n) \leq 1$.

Proof. If P is the bigon between a^n and y^n, we have $2\text{Wght}(P) - 2\text{Rot}(P) = -1 - \tau(K) - |n|$ due to Lemma 5.1.2. Due to the hyperelliptic involution invariance of $\widehat{HF}(M)$, we can take $0 \leq n < |\tau(K)|$. We have $\text{Wind}(P)$ is $\widetilde{H}_n$ if $\tau(K) \geq 0$ or $\widetilde{V}_n$ if $\tau(K) < 0$, the values of which depend on the parity of n and $\tau(K)$ when K is thin. The simple structure of $\overline{\gamma}$ for a thin knot together with a counting argument for $\tau(K) > 0$ yields

$$\widetilde{H}_n = \begin{cases} \dfrac{n + \tau(K)}{2} & \text{parity}(n) = \text{ parity}(\tau(K)) \\ \dfrac{n + \tau(K) + 1}{2} & \text{parity}(n) \neq \text{ parity}(\tau(K)). \end{cases}$$

Then for $\tau(K) > 0$ we have $M(y^n) - M(a^n) = 2\widetilde{H}_n - 1 - \tau(K) - n$ implies $M(y^n) - M(a^n)$ is either -1 or 0. Since $M(x^n) - M(y^n) = 1$, we see that $M(x^n) - M(a^n)$ is either 0 or 1, handling the $\tau(K) > 0$ case.

When $\tau(K) < 0$, the bigon P runs from y^n to a^n, encloses $\widetilde{V}_n$ lifts of the marked points, traverses the grading arrow in reverse, and has $\text{Rot}(P) = 0$. Figure 5.2 shows that $\widetilde{V}_n$ with $\tau(K) < 0$ is the same as $\widetilde{V}_n = \widetilde{H}_{-n}$ with $\tau(K) \geq 0$, except using $-\tau(K)$ or $-\tau(K) - 1$ in the formula above. Using Lemma 5.1.2 and the $-\tau(K)$ modified formula for $\widetilde{H}_{-n}$, we have $M(a^n) - M(y^n) = 2\widetilde{H}_{-n} + 1 + \tau(K) + n$. This is either 1 or 0, and so $M(y^n) - M(a^n)$ is either -1 or 0 and analogously $M(x^n) - M(a^n)$ is either 0 or 1. □

Because $M(x^n) - M(y^n) = 1$, these possibilities happen in pairs. A simple figure-eight at height $n < |\tau(K)|$ contributes either $\{M_{rel}(a^n), M_{rel}(a^n) - 1, M_{rel}(a^n)\} \subseteq MR^{[s]}$ or $\{M_{rel}(a^n), M_{rel}(a^n), M_{rel}(a^n) + 1\} \subseteq MR^{[s]}$. An example of this to keep in mind is when looking at large surgery on the figure-eight knot 4_1. In this situation we have $\{0, -1, 0\} = MR^{[0]}$, and the right intersection contributing -1 to $MR^{[0]}$ actually has the smallest relative Maslov grading. This proposition then allows us to determine which intersection associated to $[s] \in \text{Spin}^c(S^3_r(K))$ has the smallest relative Maslov grading depending on $\text{parity}(\tau(K))$:

- If $\tau(K) \geq 0$, $\text{parity}(s) = \text{parity}(\tau(K))$, and there is a right intersection y^s, then $M_{rel}(y^s) = -1$ is the smallest relative grading of $MR^{[s]}$.

- If $\tau(K) \geq 0$, parity(s) = parity$(\tau(K))$, and there is no simple figure-eight at height s, then $M_{rel}(a^s) = 0$ is the smallest relative grading of $MR^{[s]}$.

- If $\tau(K) \geq 0$ and parity$(s) \neq$ parity$(\tau(K))$, then $M_{rel}(a^s) = 0$ is the smallest relative grading of $MR^{[s]}$.

- If $\tau(K) < 0$, then $M_{rel}(a^s) = 0$ is the smallest relative grading of $MR^{[s]}$.

The last component of the grading difference formula to handle is Wind(P). Lift both $\widehat{HF}(M)$ and each l_r^s to the tiled plane $\widetilde{T}$, and let the 0th column be the neighborhood of the lift $\widetilde{\mu}$ for which each l_r^s intersects $\widetilde{\mu}$ at height $[s]$. For $[s] \in \mathbb{Z}/r\mathbb{Z}$ define $w_s = \dfrac{n - [s]}{r}$, with n the largest natural number satisfying $0 \leq n \leq g(K) - 1$ and $n \equiv [s] \pmod{r}$. This number represents the number of columns of marked points in $\widetilde{T}$ between a^s and a potential furthest right intersection y^n. Further, because the slopes we consider satisfy $r \leq 2g(K) - 1$, we have $w_s \geq 0$. While it is certainly possible that a simple figure-eight component may not exist at this height, it is still sufficient for the following strategy to suppose otherwise.

Proposition 5.1.4. For a given $[s] \in \mathbb{Z}/r\mathbb{Z}$, let a^s be the chosen reference intersection and y^n be a right intersection of a furthest possible figure-eight component. If $\tau(K) \geq 0$, then

$$\text{Wind}(P) = \widetilde{H}_s + \sum_{i=1}^{w_s} (s + ir).$$

If $\tau(K) < 0$, then

$$\text{Wind}(P) = \begin{cases} \displaystyle\sum_{i=0}^{w_s} (s + ir) & [s] \geq 0 \\ \displaystyle\sum_{i=1}^{w_s} (s + ir) & [s] < 0, \end{cases}$$

where all sums are taken to be zero if empty.

When $\tau(K) \geq 0$, the contribution to Wind(P) from the 0th column of $\widetilde{T}$ is $\widetilde{H}_s$. The contribution from the ith column is $\widetilde{H}_{s+ir} - \widetilde{V}_{s+ir} = s + ir$, and is shown in Figure 5.5. When $\tau(K) < 0$, we have the different choices for a^s depending on s influencing

whether the contribution from the 0th column is non-trivial. However in every column, the contribution to $\mathrm{Wind}(P)$ is $\widetilde{H}_{s+ir} - \widetilde{V}_{s+ir} = s + ir$. Since these terms are always non-negative, it follows that the smallest relative grading belongs to an intersection in the 0th column.

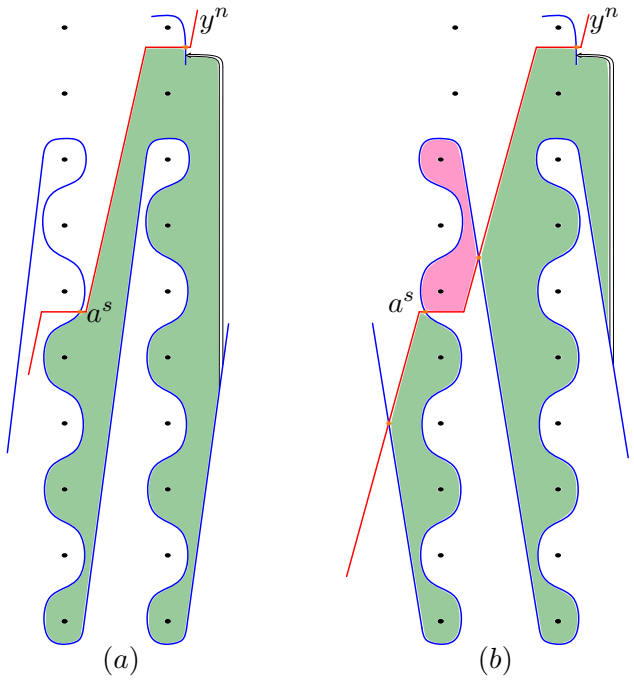

Figure 5.5: Example bigons P between a^s and y^n, showing the contributions from each column to $\mathrm{Wind}(P)$ for (a) $\tau(K) \geq 0$ and (b) $\tau(K) < 0$ with $s \geq 0$.

5.2 Cases with $|\tau(K)| < g(K)$

Our objective is to build a collection of lemmas required to prove the main theorem. These vary depending on r in relation to $g(K)$, and on $\tau(K)$ and its parity. The primary technique involves comparing the various $\mathrm{Width}(MR^{[s]})$ to obstruct periodicity, typically done by showing that $\mathrm{Width}(MR^{[s']})$ is maximal if $[s']$ is the spin^c structure associated to the line that crosses height $g(K) - 1$. At other times the widths will agree up to translation, but the multiplicity of specific elements of the grading multisets will not.

Use Theorem 2.3.5 to identify $\widehat{HF}(S^3_r(K), [s]) \cong HF(\widehat{HF}(M), l^s_r)$. In order to halve the

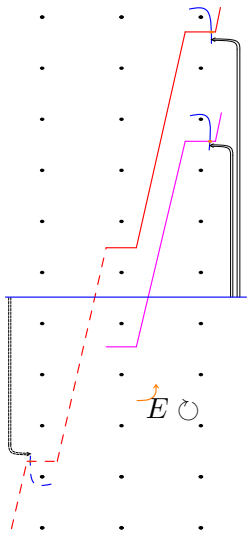

Figure 5.6: The correspondence between intersections of $\widehat{HF}(M)$ and l_r^s in negative columns of $\widetilde{T}$ and intersections of $\widehat{HF}(M)$ and l_r^{-s} in positive columns.

amount of comparisons to make, we leverage the fact that $\widehat{HF}(S^3_r(K),[s]) \cong \widehat{HF}(S^3_r(K),[-s])$ [OS04c]. In immersed curves form, Theorem 2.3.3 implies that intersections between $\widehat{HF}(M)$ and l_r^s in negative columns of $\widetilde{T}$ are in correspondence with intersections of $\widehat{HF}(M)$ and l_r^{-s} that belong to positive columns of $\widetilde{T}$ (see Figure 5.6). Also, the self-conjugate spin^c structure(s) [0] (and possibly $[r/2]$) are symmetric in this way by default.

Recall that the smallest element of $MR^{[s]}$ is the relative grading of an intersection belonging to the 0th column of $\widetilde{T}$, which is either the reference intersection a^s or a nearby right/left intersection. This means that we can capture $\text{Width}(MR^{[s]})$ by considering non-negative intersections associated to both $[s]$ and $[-s]$. Note that since $\text{parity}(s) = \text{parity}(-s)$, the need to translate a multiset by 1 is consistent if it arises.

Definition 5.2.1. The multiset $MR^{[s]}_+$ consists of the relative gradings of intersections between $\widehat{HF}(M)$ and l_r^s that belong to non-negative columns of $\widetilde{T}$. We define $MR^{[s]}_-$ analogously, and notice that $\text{Width}(MR^{[s]}) = \max\left\{\text{Width}(MR^{[s]}_+), \text{Width}(MR^{[s]}_-)\right\}$.

Due to how genus detection is expressed by $\widehat{HF}(M)$, either $\overline{\gamma}$ achieves height $g(K)$ (equivalent to $|\tau(K)| = g(K)$), or only a simple figure-eight at height $g(K)-1$ achieves this desired height (equivalent to $|\tau(K)| < g(K)$). We will divide the problem among these two cases, starting with the latter.

Case A: $|\tau(\mathbf{K})| < \mathbf{g(K)}$. Since $|\tau(K)| < g(K)$, there exists a simple figure-eight component at height $g(K)-1$. Let $[s']$ be the spin^c structure for which $l_r^{s'}$ intersects this simple figure-eight, which means $w_{s'} = \frac{g(K)-1-s'}{r}$. Our potential reducing slopes divide this case into two subcases. We see that $[s'] = g(K)-1$ when $r \geq 2(g(K)-1)$, which implies $w_{s'} = 0$. Otherwise $w_{s'} > 0$, which is the easier starting point.

Case A1: $\mathbf{w_{s'} > 0}$. In this situation, we will show that Width$(MR^{[s']})$ is maximal.

Lemma 5.2.2. *Suppose K is thin, $|\tau(K)| < g(K)$, and $1 < r < 2(g(K)-1)$. Then there exists an $[s'] \in Spin^c(S^3_r(K))$ for which every $[s] \neq [\pm s']$ satisfies $MR^{[s]} \ncong MR^{[s']}$ up to translation.*

Proof. For some $[s] \neq [\pm s']$, the largest possible relative grading that $MR_+^{[s]}$ can achieve is associated to an intersection of some hypothetical simple figure-eight at largest height. Looking at the terms in the grading difference formula for a bigon from a^s to such a generator, we see that the $2\text{Wind}(P)$ term satisifes $2\text{Wind}(P) \geq 2n$ while the other term is $-1-\tau(K)-n$. For this reason, we will suppose that $\widehat{HF}(M)$ has a simple figure-eight at height n, taken to be the largest integer satisfying both $n < g(K)-1$ and $n \equiv s \pmod r$. Let P' be the bigon between $a^{s'}$ and y^{g-1}, and P the bigon between a^s and y^n. Because the choice of $a^{s'}$ depends on $\tau(K)$, we will handle the $\tau(K) \geq 0$ subcase first before handling the $\tau(K) < 0$ subcase.

Subcase A1a: $\tau(\mathbf{K}) \geq \mathbf{0}$. Due to Lemma 5.1.2, Proposition 5.1.3, and Proposition 5.1.4, Width$(MR_+^{[s]})$ is nearly determined by $M_{rel}(y^n)$. We have $M_{rel}(y^n) \leq \text{Width}(MR_+^{[s]}) \leq M_{rel}(y^n)+1$, with either equality depending on whether a^s is the smallest relatively graded intersection. To compare widths, we compute

$$M_{rel}(y^{g-1}) = 2\left(\widetilde{H}_{s'} + \sum_{i=1}^{w_{s'}}(s'+ir)\right) - 1 - (s'+w_{s'}r),$$

and likewise

$$M_{rel}(y^n) = 2\left(\widetilde{H}_{s} + \sum_{i=1}^{w_{s}}(s+ir)\right) - 1 - (s+w_{s}r).$$

Their difference is then

$$\begin{aligned} M_{rel}(y^{g-1}) - M_{rel}(y^n) &= 2\left(\widetilde{H}_{s'} + \sum_{i=1}^{w_{s'}}(s'+ir) - \left(\widetilde{H}_s + \sum_{i=1}^{w_s}(s+ir)\right)\right) \\ &\qquad - (s' + w_{s'}r - (s + w_s r)) \\ &= 2\left((\widetilde{H}_{s'} - \widetilde{H}_s) + \sum_{i=1}^{w_{s'}}(s'+ir) - \sum_{i=1}^{w_s}(s+ir)\right) \\ &\qquad - (s'-s) - r(w_{s'} - w_s). \end{aligned}$$

If $s < s'$ so that $w_s = w_{s'}$, then

$$\begin{aligned} M_{rel}(y^{g-1}) - M_{rel}(y^n) &= 2((\widetilde{H}_{s'} - \widetilde{H}_s) + w_{s'}(s'-s)) - (s'-s) \\ &= 2(\widetilde{H}_{s'} - \widetilde{H}_s) + (2w_{s'} - 1)(s'-s) \\ &\geq 1, \end{aligned}$$

since $w_{s'} > 0$ and $s' > s$ implies that $\widetilde{H}_{s'} \geq \widetilde{H}_s$.

If $s > s'$ so that $w_s = w_{s'} - 1$, then shifting P one column to the right in $\widetilde{T}$ (see Figure 5.7) provides

$$\begin{aligned} M_{rel}(y^{g-1}) - M_{rel}(y^n) &= 2\left((\widetilde{H}_{s'} - \widetilde{H}_s) + \sum_{i=1}^{w_{s'}}(s'+ir) - \sum_{i=1}^{w_s}(s+ir)\right) \\ &\qquad - (s'-s) - r(w_{s'} - w_s) \\ \text{(column shift)} \quad &= 2\left((\widetilde{H}_{s'} - \widetilde{H}_s) + \sum_{i=1}^{w_{s'}}(s'+ir) - \sum_{i=2}^{w_{s'}}(s+(i-1)r)\right) \\ &\qquad - (s'+r-s) \\ &= 2\left((\widetilde{H}_{s'} - \widetilde{H}_s) + (s'+r) + \sum_{i=2}^{w'_s}(s'+ir) - \sum_{i=2}^{w_{s'}}(s+(i-1)r)\right) \\ &\qquad - (s'+r-s) \\ &= 2\Big((\widetilde{H}_{s'} + s - \widetilde{H}_s) + (s'+r-s) + (w_{s'}-1)(s'+r-s)\Big) \\ &\qquad - (s'+r-s) \end{aligned}$$

$$
\begin{aligned}
&= 2(\widetilde{H}_{s'} + (s - \widetilde{H}_s)) + (2w_{s'} - 1)(s' + r - s) \\
&= 2(\widetilde{H}_{s'} - \widetilde{V}_s) + (2w_{s'} - 1)(s' + r - s) \\
&= 2(\widetilde{H}_{s'} - \widetilde{H}_{-s}) + (2w_{s'} - 1)(s' + r - s).
\end{aligned}
$$

Notice that $s' + s - 1 \leq 2(\widetilde{H}_{s'} - \widetilde{H}_{-s}) \leq s' + s$ depending on the parities of s and s' together with $s > s'$. Then we have

$$
\begin{aligned}
M_{rel}(y^{g-1}) - M_{rel}(y^n) &= 2(\widetilde{H}_{s'} - \widetilde{H}_{-s}) + (2w_{s'} - 1)(s' + r - s) \\
&\geq s' + s - 1 + (2w_{s'} - 1)(s' + r - s) \\
&\geq s' + s - 1 + s' + r - s \\
&= 2s' - 1 + r \\
&> 1,
\end{aligned}
$$

since $w_{s'} > 0$ and $s' < \frac{r-1}{2}$ if there exists an $s > s'$.

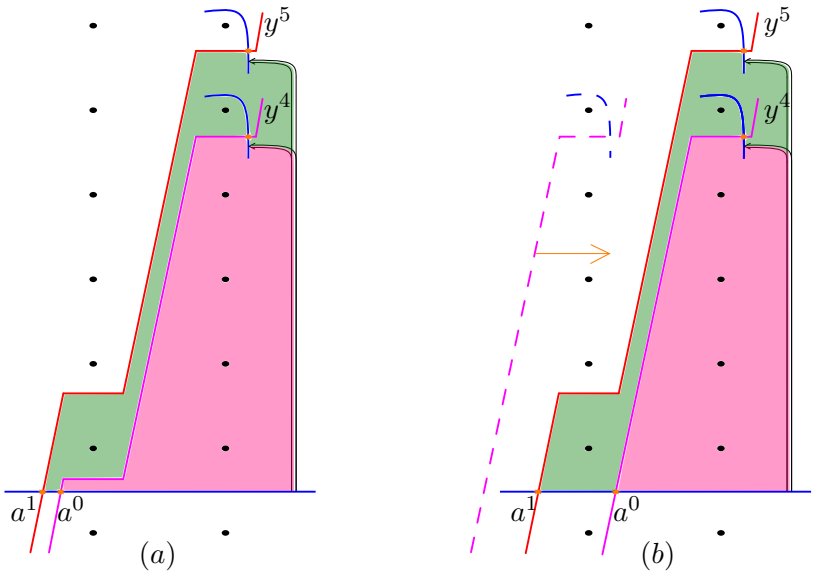

Figure 5.7: Example bigons P' (split-shaded green and pink) and P (shaded pink) when $w_{s'} = 1$. (a) has $s < s'$, while (b) has $s > s'$ together with the single column shift to the right.

In both situations, we see that $M_{rel}(y^{g-1}) - M_{rel}(y^n) \geq 1$. If this difference is greater than one, then

$$\text{Width}(MR^{[s']}) \geq \text{Width}(MR_+^{[s']}) \geq M_{rel}(y^{g-1}) > M_{rel}(y^n) + 1 \geq \text{Width}(MR_+^{[s]}).$$

This already handles the possibility where we need to translate $MR_+^{[s]}$ by 1, so suppose $M_{rel}(y^{g-1}) - M_{rel}(y^n) = 1$. This is possible only if $\widetilde{H}_s = \widetilde{H}_{s'}$, $w_{s'} = 1$, and $s = s' - 1$, which altogether imply that $s = \tau(K)$. However, the widths only match if $\text{Width}(MR_+^{[s]}) = M_{rel}(y^n) + 1$. This condition is equivalent to having parity$(s) \neq$ parity$(\tau(K))$, which is a contradiction. Therefore $\text{Width}(MR^{[s']}) > \text{Width}(MR_\pm^{[s]})$, which completes the $\tau(K) \geq 0$ subcase.

Subcase A1b: $\tau(\mathbf{K}) < \mathbf{0}$. Recall that the reference intersection a^s has no nearby left/right intersections belonging to a simple figure-eight. This means that a^s has the smallest relative grading of $MR^{[s]}$, and so $\text{Width}(MR_+^{[s]}) = M_{rel}(y^n) + 1$. From Proposition 5.1.4 we see

$$\text{Wind}(P) = \begin{cases} s + \sum_{i=1}^{w_s}(s+ir) & s \geq 0, \\ \sum_{i=1}^{w_s}(s+ir) & s < 0. \end{cases}$$

If $0 \leq s < s'$, then proceeding as before we have

$$\begin{aligned} M_{rel}(y^{g-1}) - M_{rel}(y^n) &= 2\left(s' + \sum_{i=1}^{w_{s'}}(s'+ir) - \left(s + \sum_{i=1}^{w_s}(s+ir)\right)\right) \\ &\qquad - (s'-s) - r(w_{s'} - w_s) \\ &= 2(s' - s + w_{s'}(s'-s)) - (s'-s) \\ &= (2w_{s'} + 1)(s'-s) \\ &\geq 3. \end{aligned}$$

If $s < s' \leq 0$, then

$$\begin{aligned} M_{rel}(y^{g-1}) - M_{rel}(y^n) &= (2w_{s'} - 1)(s'-s) \\ &\geq 1. \end{aligned}$$

If $s > s'$, then as before we have $w_s = w_{s'} - 1$. If $s > s' \geq 0$, then

$$\begin{aligned} M_{rel}(y^{g-1}) - M_{rel}(y^n) &= 2\left((s'-s) + \sum_{i=1}^{w_{s'}}(s'+ir) - \sum_{i=1}^{w_s}(s+ir)\right) \\ &\qquad - (s'-s) - r(w_{s'} - w_s) \\ \text{(column shift)} \quad &= 2\left((s'-s) + \sum_{i=1}^{w_{s'}}(s'+ir) - \sum_{i=2}^{w_{s'}}(s+(i-1)r)\right) - (s'+r-s) \\ &= 2(s' + (s'+r-s) + (w_{s'}-1)(s'+r-s)) - (s'+r-s) \\ &= 2s' + (2w_{s'}-1)(s'+r-s) \\ &\geq 1. \end{aligned}$$

In the event that $0 \geq s > s'$, we get

$$\begin{aligned} M_{rel}(y^{g-1}) - M_{rel}(y^n) &= 2\left(\sum_{i=1}^{w_{s'}}(s'+ir) - \sum_{i=1}^{w_s}(s+ir)\right) - (s'-s) - r(w_{s'} - w_s) \\ \text{(column shift)} \quad &= 2\left(\sum_{i=1}^{w_{s'}}(s'+ir) - \sum_{i=2}^{w_{s'}}(s+(i-1)r)\right) - (s'+r-s) \\ &= 2(s'+r+(w_{s'}-1)(s'+r-s)) - (s'+r-s) \\ &= 2(s + w_{s'}(s'+r-s)) - (s'+r-s) \\ &= 2s + (2w_{s'}-1)(s'+r-s) \\ &\geq 2s + s' + r - s \\ &\geq (s'+s) + r \\ &\geq 1. \end{aligned}$$

In every inequality we have $M_{rel}(y^{g-1}) > M_{rel}(y^n)$. Then

$$\text{Width}(MR^{[s']}) \geq \text{Width}(MR^{[s']}_+) = M_{rel}(y^{g-1}) + 1 > M_{rel}(y^n) + 1 = \text{Width}(MR^{[s]}_+),$$

for each $[s] \in \text{Spin}^c(S^3_r(K))$. This completes the $\tau(K) < 0$ subcase, and the proof. □

Case A2: $\mathbf{w_{s'} = 0}$. Recall that in this case we have $r \geq 2(g(K)-1)$, so let us consider $r = 2g(K) - 1$ first. When $\tau(K) \geq 0$, the surgery slope is large enough so that every intersection lies in the 0th column of $\widetilde{T}$. Width alone as an invariant won't be enough, so we will also need to appeal to the multiplicities of the elements of the relative grading

multisets. They will be used to show that only spin^c structures with the same parity are unobstructed. When we assume that $S^3_r(K)$ is reducible later on, the fact that r is odd will provide a contradiction with periodicity. When $\tau(K) < 0$, we need far less sublety.

Lemma 5.2.3. *Suppose K is thin, $0 \leq \tau(K) < g(K)$, and $r = 2g(K) - 1$. Then there exists an $[s'] \in Spin^c(S^3_r(K))$ for which $[s] \neq [\pm s']$ satisfies $MR^{[s]} \cong MR^{[s']}$ up to translation only if parity$([s])$ = parity$([s'])$.*

Proof. The spin^c structure $[s']$ we want to consider has $[s'] = g(K) - 1$. Suppose for the sake of contradiction that some $[s] \neq [\pm s']$ satisfies $MR^{[s]} \cong MR^{[s']}$ up to translation and parity$(s) \neq$ parity(s'). We know that $r > 1$ forces $g(K) > 1$, and also that each l^s_r intersects $\widehat{HF}(M)$ exactly once due to this large surgery slope. Because the choice of reference generator $a^{s'}$ depends on $\tau(K)$, let us split into two cases: $\tau(K) \geq 0$ and $\tau(K) < 0$.

Assume $\tau(K) \geq 0$. Because all intersections lie within the 0th column of $\widetilde{T}$, we will instead use the hyperelliptic involution invariance of $\widehat{HF}(M)$ to only consider $s \geq 0$. If $\widehat{HF}(M)$ has no simple figure-eight at height s, then Width$(MR^{[s]}) = 0$ immediately does not match Width$(MR^{[s']}) \geq 1$, so we may as well assume that there is a simple figure-eight at height s. We have $M_{rel}(y^{s'}) = 2\widetilde{H}_{s'} - 1 - \tau(K) - s' = s' - 1 - \tau(K)$ by Lemma 5.1.2 and Proposition 5.1.4, since $\widetilde{H}_{s'} = s'$ when $\tau(K) \leq g(K) - 1 = s'$. Further,

$$\begin{aligned} M_{rel}(y^{s'}) - M_{rel}(y^s) &= 2\widetilde{H}_{s'} - 1 - \tau(K) - s' - (2\widetilde{H}_s - 1 - \tau(K) - s) \\ &= 2(\widetilde{H}_{s'} - \widetilde{H}_s) - (s' - s). \end{aligned}$$

If $s > \tau(K)$, then $\widetilde{H}_s = s$ implies that $M_{rel}(y^{s'}) - M_{rel}(y^s) = s' - s \geq 1$. But then

$$\text{Width}(MR^{[s']} = M_{rel}(y^{s'}) + 1 > M_{rel}(y^s) + 1 \geq \text{Width}(MR^{[s]}),$$

so we must have $s \leq \tau(K)$ together with Width$(MR^{[s]}) = 1$. Notice that Width$(MR^{[s']}) = M_{rel}(y^{s'}) + 1 = s' - \tau(K) > 1$ if $\tau(K) < s' - 1$, and so we are also forced to have either $\tau(K) = s' - 1$ or $\tau(K) = s'$. In both cases we have Width$(MR^{[s']}) = 1$. Since using width as an invariant has been exhausted, let us count multiplicities of elements of the $MR^{[s]}$'s next.

Recall that e_n denotes the number of simple figure-eights at height n of $\widehat{HF}(M)$. Further, we need $e_s = e_{s'}$ in order to have $|MR^{[s]}| = |MR^{[s']}|$. We have assumed that parity$([s]) \neq$ parity$([s'])$, so one of these two multisets contains -1 and must be translated

by 1 to make 0 the smallest element. This translated multiset will then contain 0 with multiplicity $e_{s'}$, while the other multiset will contain 0 with multiplicity $e_{s'}+1$. This is the desired contradiction. □

When $r = 2(g(K)-1)$, we will end up having $\text{Width}(MR^{[s]}) = 1$ for every $[s]$ if $\tau(K)$ is large enough. This means relative grading information alone will not be enough, and so we will return to such cases in Chapter 6.

Lemma 5.2.4. *Suppose K is thin, $0 \leq \tau(K) < g(K)-2$, and $r = 2(g(K)-1)$. Then there exists an $[s'] \in Spin^c(S^3_r(K))$ for which every $[s] \neq [\pm s']$ satisfies $MR^{[s]} \ncong MR^{[s']}$ up to translation.*

Proof. We again use $s' = g(K)-1$, and notice that when $\tau(K) < g(K)-2$, we have

$$M_{rel}(y^{s'}) = 2(g(K)-1) - 1 - \tau(K) - (g(K)-1) = g(K) - 2 - \tau(K) > 0.$$

This shows that $\text{Width}(MR^{[s']}) = M_{rel}(y^{s'}) + 1 > 1$. Any $[s] \neq [\pm s']$ with $|s| \leq \tau(K)$ has $\text{Width}(MR^{[s]}) = 1$ due to Proposition 5.1.3, so suppose $\tau(K) < |s| < s'$. In this case, $\text{Width}(MR^{[s]}) \leq M_{rel}(y^s) + 1$, but we also have $M_{rel}(y^{s'}) - M_{rel}(y^s) = s' - |s| > 0$. Then $\text{Width}(MR^{[s]}) < \text{Width}(MR^{[s']})$, which completes the proof. □

When $\tau(K) < 0$, the fact that the reference intersection a^s lies outside of the neighborhood of $\widetilde{\mu}_0$ is very convenient. This is an example of a *non-vertical intersection*, which is an intersection between l^s_r and $\overline{\gamma}$ that lies outside of a neighborhood of a lift $\widetilde{\mu}$.

Lemma 5.2.5. *Suppose K is thin, $-g(K) < \tau(K) < 0$, and $r \geq 2(g(K)-1)$. Then there exists an $[s'] \in Spin^c(S^3_r(K))$ for which every $[s] \neq [\pm s']$ satisfies $MR^{[s]} \ncong MR^{[s']}$ up to translation.*

Proof. Since $w_{s'} = 0$, we again have $[s'] = g(K)-1$. Notice that each l^s_r gives rise to only two non-vertical intersections around the 0th column and intersections at height s when $[s] \neq [\pm s']$. We have s' maximal when $w_{s'} = 0$, so use hyperelliptic involution invariance to assume $0 \leq s < s'$. Recall that $\text{Width}(MR^{[s]}) = M_{rel}(y^s) + 1$ under the assumptions that $\tau(K) < 0$. The formula for $\text{Wind}(P)$ does not depend on $\tau(K)$, which means

$$\begin{aligned} M_{rel}(y^{s'}) - M_{rel}(y^s) &= 2s' - 1 - \tau(K) - s' - (2s - 1 - \tau(K) - s) \\ &= s' - s. \end{aligned}$$

Then $\mathrm{Width}(MR^{[s']}) = M_{rel}(y^{s'}) + 1 > M_{rel}(y^s) + 1 = \mathrm{Width}(MR^{[s]})$, which implies $MR^{[s]} \ncong MR^{[s']}$. □

In the following chapter we address the remaining cases involving $|\tau(K)| = g(K)$, as well as the few unresolved cases of this chapter. In particular, the cases with $g(K) - 2 \leq \tau(K) < g(K)$ and $r = 2(g(K) - 1)$ are handled in Lemma 6.2.2.

CHAPTER

6

REMAINING CASES AND ABSOLUTE GRADINGS

With the case analysis for $|\tau(K)| < g(K)$ out of the way, we turn to the more difficult part.

6.1 Cases with $|\tau(K)| = g(K)$

Case B: $|\tau(\mathbf{K})| = \mathbf{g}(\mathbf{K})$. When $|\tau(K)|$ is at its largest, the essential curve $\overline{\gamma}$ suffices to indicate $g(K)$ and we are not guaranteed a simple figure-eight at height $g(K) - 1$. For these cases we still choose $[s']$ so that $g - 1 \equiv s' \pmod{r}$ and continue to use w_s, except now modifying it to just be the largest multiple of r so that $s + w_s r < g(K)$. The $\tau(K) = -g(K)$ case is easier, so we start there.

Case B1: $\tau(\mathbf{K}) = -\mathbf{g}(\mathbf{K})$.

Lemma 6.1.1. *Suppose K is thin with $\tau(K) = -g(K)$, and let $1 < r \leq 2g(K) - 1$. Then there exists an $[s'] \in Spin^c(S^3_r(K))$ for which every $[s] \neq [\pm s']$ satisfies $MR^{[s]} \ncong MR^{[s']}$*

up to translation.

Proof. Recall the labeling scheme from Figure 5.1. The reference intersection a^s is immediately to the left of the $0th$ column if $s \geq 0$, and is similarly immediately to the right of the $0th$ column if $s > 0$. In general we will label these generators x_s^l and x_s^r, respectively. Let us dispense with the $w_{s'} = 0$ case first.

Notice that each $MR^{[s]}$ contains two elements whose difference is precisely $2|s|$. These arise from $M_{rel}(x_s^r) - M_{rel}(x_s^l) = 2\widetilde{H}_s - 1 - (2\widetilde{V}_s - 1) = 2(\widetilde{H}_s - \widetilde{V}_s) = 2s$. We also see that $2\widetilde{H}_s - 1 \leq \text{Width}(MR^{[s]}) \leq 2\widetilde{H}_s$ if $s \leq 0$ and $2\widetilde{V}_s - 1 \leq \text{Width}(MR^{[s]}) \leq 2\widetilde{V}_s$ if $s > 0$, with the even equalities achieved if an appropriate generator from a simple figure-eight exists at height s. So if some $[s] \neq [\pm s']$ is to achieve $MR^{[s]} \cong MR^{[s']}$ up to translation, we should see that the widths of these multisets agree and that there exist pairs with grading differences $2|s|$ and $2|s'|$. These are only possibly simultaneously true if $\widetilde{V}_s = \widetilde{H}_{s'}$ and $\widetilde{H}_s = \widetilde{V}_{s'}$, which forces $s = -s'$ with K thin. Thus, $w_{s'} > 0$.

If $w_{s'} > 0$, we can appeal to $MR^{[s']}$ achieving maximal width once again. Due to the formula for $\text{Wind}(P)$ when $\tau(K) < 0$, the grading difference between consecutive vertical intersections between $\overline{\gamma}$ and l_r^s around the ith column is $2(s + ir)$. As before this happens as $2\widetilde{H}_{s+ir} - 1 - (2\widetilde{V}_{s+ir} - 1) = 2(\widetilde{H}_{s+ir} - \widetilde{V}_{s+ir}) = 2(s + ir)$, and is positive. For this reason it is often the case that the vertical intersection on the left side of the w_sth column, which we now denote by b^s, has the largest relative grading in $MR^{[s]}$. As before, by appealing to the hyperelliptic involution invariance of $\widehat{HF}(M)$ we see that $\text{Width}(MR^{[s]})$ is either $M_{rel}(b^s)$ or $M_{rel}(b^{-s})$ when $w_s > 0$. We will obtain our desired contradiction by comparing $M_{rel}(b^{s'})$ to every $M_{rel}(b^s)$ with $s \neq \pm s'$, just as in the lemmas of the previous chapter.

Chaining the grading differences of vertical intersection pairs from b^s back to a^s, we see that

$$M_{rel}(b^s) = \begin{cases} 2\left(\sum_{i=0}^{w_s-1}(s+ir) + \widetilde{H}_{s+w_s r}\right) - 1 & \text{if } s \geq 0 \\ 2\left(\sum_{i=1}^{w_s-1}(s+ir) + \widetilde{H}_{s+w_s r}\right) - 1 & \text{if } s \leq 0, \end{cases}$$

with empty sums taken to be zero as before. Since it can be hectic determining when such a sum is empty, we break into more cases.

When $s < s'$ we have $w_s = w_{s'}$, and it is straightforward to check that

$$M_{rel}(b^{s'}) - M_{rel}(b^s) \geq 2(\widetilde{H}_{s'+w_{s'}r} - \widetilde{H}_{s+w_{s'}r}) > 0.$$

This follows because the various multiples of $(s' - s)$ are positive if they appear, and because $\widetilde{H}_{s'+w_{s'}r} > \widetilde{H}_{s+w_{s'}r}$ when $s < s'$.

Let us begin the $s' < s$ cases with $w_{s'} = 1$. For $0 \leq s' < s$ we can once again use a column shift to see

$$M_{rel}(b^{s'}) - M_{rel}(b^s) = 2(s' + H_{s'+r} - H_s) > 0,$$

since $s' \geq 0$ and $H_{s'+r} > H_s$. The same inequality holds if $s' \leq 0 < s$, together with dropping the s' term. For $s' < s \leq 0$ with $w_s = 0$, we are forced to have $\text{Width}(MR^{[s]}) = 2\widetilde{H}_s - 1$ if $s \geq 0$ and $\text{Width}(MR^{[s]}) = 2\widetilde{V}_s - 1$ if $s \leq 0$, since $\text{Width}(MR^{[s']})$ is guaranteed to be odd. For the former we get

$$M_{rel}(b^{s'}) - M_{rel}(b^s) = 2(\widetilde{H}_{s'+r} - \widetilde{H}_s) > 0,$$

since $s < s' + r$. The latter yields

$$M_{rel}(b^{s'}) - M_{rel}(b^s) = 2(\widetilde{H}_{s'+r} - \widetilde{V}_s) > 0,$$

since $s > s'$.

Finally we are left with $w_{s'} > 1$ with $s' < s$. If we have $0 \leq s' < s$, then the fact that $\widetilde{H}_{s'+w_{s'}r}$ is maximal ensures

$$\begin{aligned}
M_{rel}(b^{s'}) - M_{rel}(b^s) &= 2\left(\sum_{i=0}^{w_{s'}-1}(s' + ir) - \sum_{i=0}^{w_s-1}(s + ir)\right) + 2(\widetilde{H}_{s+w_{s'}r} - \widetilde{H}_{s+(w_{s'}-1)r}) \\
\text{(column shift)} \quad &= 2\left(s' + \sum_{i=1}^{w_{s'}-1}(s' + ir) - \sum_{i=1}^{w_{s'}-1}(s + (i-1)r)\right) \\
&\qquad + 2(\widetilde{H}_{s+w_{s'}r} - \widetilde{H}_{s+(w_{s'}-1)r}) \\
&= 2s' + 2(w_{s'} - 1)(s' + r - s) + 2(\widetilde{H}_{s+w_{s'}r} - \widetilde{H}_{s+(w_{s'}-1)r}) \\
&> 0,
\end{aligned}$$

Analogously, the same inequality holds true if $s' \leq 0 < s$ by dropping the $2s'$ term. For $s' < s \leq 0$ a single $(s'+r-s)$ term disappears, but the inequality holds since $s'+r-s > 0$ and $\widetilde{H}_{s+w_{s'}r} - \widetilde{H}_{s+(w_{s'}-1)r} > 0$.

Then since $M_{rel}(b^{s'}) > M_{rel}(b^s)$ for every configuration of s relative to s' for $w_{s'} > 0$, we have $\text{Width}(MR^{[s']}) > \text{Width}(MR^{[s]})$. Together with the argument for $w_{s'} = 0$, this

completes the proof. □

Case B2: $\tau(\mathbf{K}) = \mathbf{g}(\mathbf{K})$. Let us consider $1 < r < 2(g(K)-1)$ first, delaying the penultimate slope to Lemma 6.2.2 and the maximal slope to Lemma 6.1.3. If $r < 2(g(K)-1)$, then $l_r^{s'}$ intersects $\overline{\gamma}$ more than once for $s' \equiv g(K)-1 \pmod r$. Our approach involves different arguments depending on whether $l_r^{s'}$ makes vertical intersections on both sides of the 0th column.

Lemma 6.1.2. *Suppose K is thin with $\tau(K) = g(K)$, the surgery slope satisfies $1 < r < 2(g(K)-1)$, and that there exists a k properly dividing r so that every $[s] \in Spin^c(S^3_r(K))$ satisfies $MR^{[s]} \cong MR^{[s+k]}$ up to translation.*

- *If $r < g(K)-1$, then $MR^{[s]} \cong MR^{[s']}$ up to translation only if $[s] = [-s']$.*
- *If $r \geq g(K)-1$, then $\tau(K) = g(K) = r = 3$.*

Proof. If $r < g(K)-1$, then the slope of $l_r^{s'}$ is small enough so that intersecting it with $\overline{\gamma}$ produces vertical intersections in at least 3 columns of $\widetilde{T}$. We know $w_{s'} > 0$ since $r < 2(g(K)-1)$, so suppose $w_{s'} = 1$. We have vertical intersections with $\overline{\gamma}$ to the left and right of this column, which we can label $c^{s'}$ and $b^{s'}$, respectively. Then $M_{rel}(c^{s'}) = 2\widetilde{V}_{s'} - 1$ and $M_{rel}(b^{s'}) = 2\widetilde{H}_{s'} - 1$, and so $2\widetilde{H}_{s'} - 1 \leq \text{Width}(MR^{[s']}) \leq 2\widetilde{H}_{s'}$ since $s' > 0$ yields $\widetilde{H}_{s'} > \widetilde{V}_{s'}$. If some $[s] \neq [\pm s']$ satisfies $MR^{[s]} \cong MR^{[s']}$ up to translation then the parities of their widths must agree. Under the same labeling convention for intersections associated to $[s]$, we see that $2\widetilde{V}_s - 1 \leq \text{Width}(MR^{[s]}) \leq 2\widetilde{V}_s$ if $s \leq 0$ and $2\widetilde{H}_s - 1 \leq \text{Width}(MR^{[s]}) \leq 2\widetilde{H}_s$ if $s \geq 0$.

For $0 < s' < s$, we compute for either parity of width that

$$\text{Width}(MR^{[s']}) - \text{Width}(MR^{[s]}) = 2(\widetilde{H}_{s'} - \widetilde{V}_s).$$

This implies that $\widetilde{V}_s = \widetilde{H}_{s'}$, which is impossible when $s' > 0$. Similarly, if $s < -s'$ then the analogous statement holds true using $\widetilde{H}_s$.

When $-s' < s < s'$, something interesting occurs. In addition to $l_r^{s'}$, we see that l_r^s successfully makes two non-vertical intersections on both sides of the 0th column. Also since K is thin, it follows that $\widetilde{V}_s \leq \widetilde{H}_{s'}$ and $\widetilde{H}_s \leq \widetilde{H}_{s'}$, with equality only possible when $s = -s'+1$ or $s = s'-1$, respectively. However, this results in the configuration shown for the latter situation in Figure 6.1. We see that while the widths of $MR^{[s]}$ and $MR^{[s']}$ can agree if $\widetilde{H}_s = \widetilde{H}_{s'}$, this necessarily results in $\widetilde{V}_s \neq \widetilde{V}_{s'}$ since K is thin. This is true vice

versa as well, and so the multisets cannot both contain the same relative gradings for their respective vertical intersection pairs. Thus we must consider $w_{s'} > 1$, and we will do so following similar computations to those in Lemma 6.1.1.

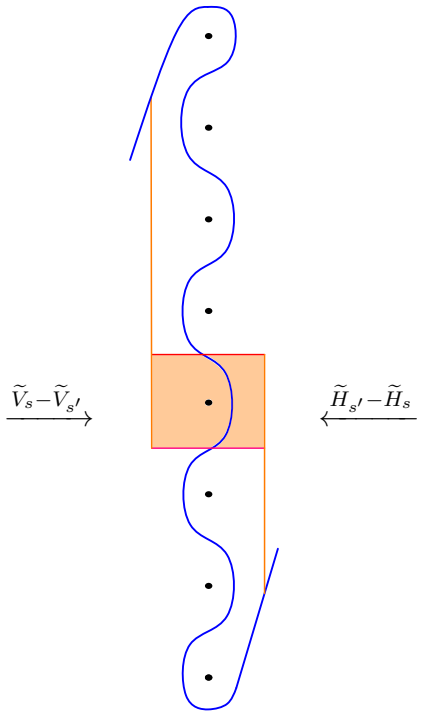

Figure 6.1: If $\widetilde{H}_s = \widetilde{H}_{s'}$ and $s = s' - 1$, then $\widetilde{V}_s - \widetilde{V}_{s'} = 1$ when K is thin.

When $w_{s'} > 1$ the intersection with largest relative grading in $MR^{[s]}$ comes from the furthest non-vertical intersection, which is b^s when $s \geq 0$ or c^s if $s \leq 0$. Since we can use the hyperelliptic involution invariance of $\widehat{HF}(M)$ to treat such a c^s as b^{-s}, let us only compare $M_{rel}(b^{s'})$ to the various $M_{rel}(b^s)$. Chaining grading differences between adjacent non-vertical intersections from b^s back to a^s, we have

$$M_{rel}(b^s) = 2\left(\widetilde{H}_s + \sum_{i=1}^{w_s - 1}(s + ir)\right) - 1.$$

If $s < s'$ then $w_s = w_{s'}$, and we compute

$$\begin{aligned} M_{rel}(b^{s'}) - M_{rel}(b^s) &= 2\left(\widetilde{H}_{s'} - \widetilde{H}_s + \sum_{i=1}^{w_s-1}(s+ir) - \sum_{i=1}^{w_s-1}(s+ir)\right) \\ &= 2(\widetilde{H}_{s'} - \widetilde{H}_s + (w_{s'}-1)(s'-s)) \\ &\geq 1. \end{aligned}$$

We have equality only if $\widetilde{H}_{s'} = \widetilde{H}_s$, $s = s' - 1$, and $w_{s'} = 2$. In this case, we have $\text{parity}(s' + 2r) = \text{parity}(s')$ regardless of r. However $\text{parity}(s' + 2r) \neq \text{parity}(\tau(K))$, and so $\text{parity}(s) = \text{parity}(\tau(K))$. This implies $\text{Width}(MR^{[s]}) \leq M_{rel}(b^s)$, which means we cannot have $s < s'$.

If $s > s'$, then with $w_s = w_{s'} - 1$ we obtain

$$\begin{aligned} M_{rel}(b^{s'}) - M_{rel}(b^s) &= 2\left(\widetilde{H}_{s'} - \widetilde{H}_s + \sum_{i=1}^{w_s-1}(s+ir) - \sum_{i=1}^{w_s-1}(s+ir)\right) \\ \text{(column shift)} \quad &= 2\left(s' + r + \widetilde{H}_{s'} - \widetilde{H}_s + \sum_{i=2}^{w_s-1}(s+ir) - \sum_{i=2}^{w_{s'}-1}(s+ir)\right) \\ &= 2(s'+r) - 2(\widetilde{H}_s - \widetilde{H}_{s'}) + 2(w_{s'}-2)(s'+r-s). \end{aligned}$$

Now $s - s' \leq 2(\widetilde{H}_s - \widetilde{H}_{s'}) \leq s - s' + 1$ when K is thin by careful inspection of these regions. This implies

$$\begin{aligned} M_{rel}(b^{s'}) - M_{rel}(b^s) &= 2(s'+r) + 2(\widetilde{H}_{s'} - \widetilde{H}_s) + 2(w_{s'}-2)(s'+r-s) \\ &\geq 2(s'+r) - (s-s'+1) + 2(w_{s'}-2)(s'+r-s) \\ &= 2s' + r - 1 + (2w_{s'}-3)(s'+r-s) \\ &> 1. \end{aligned}$$

Altogether, these grading comparisons are enough to see that $MR^{[s]} \ncong MR^{[s']}$ up to translation when $r < g(K) - 1$. Next we look at the cases with larger surgery slopes.

If $r = g(K)-1$, then $w_{s'} = 1$ and $s' = 0$. Due to hyperelliptic involution invariance, we can assume $s \neq s'$ satisfies $s < 0$. Notice that $MR^{[s']}$ contains $2\widetilde{H}_{s'} - 1$ with multiplicity at least two since $l_r^{s'}$ generates non-vertical intersections on both sides of the 0th column and $\widetilde{V}_{s'} = \widetilde{H}_{s'}$. The only way that $MR^{[s]}$ could contain this grading with multiplicity greater

than one is if a simple figure-eight component in the 1st column has an intersection with l_r^s. The nearby vertical intersection a^{s+r} has $M_{rel}(a^{s+r}) = 2\widetilde{H}_{s'} - 2$, and so we would require parity$(s+r) \neq$ parity$(\tau(K))$ in order for an intersection with a simple figure-eight to have the desired grading. However $s + r = \tau(K) - 2$, and so $MR^{[s]}$ cannot contain $2\widetilde{H}_{s'} - 1$ more than once. Thus, no $[s] \neq [s']$ satisfies $MR^{[s]} \cong MR^{[s']}$ up to translation when $r = g(K) - 1$.

We still have $w_{s'} = 1$ if $r > g(K) - 1$, but now $s' < 0$. The crux of the argument in the previous case relied on $\widetilde{H}_{s'} > 1$. This holds more generally when $r < 2g(K) - 3$, except now $MR^{[s']}$ need only contain $2\widetilde{H}_{s'} - 1$ once. Since Width$(MR^{[s']}) \geq 3$, the above argument still applies to show that $MR^{[s]} \cong MR^{[s']}$ up to translation only if $[s] = [s' \pm 1]$. This forces $k = 1$, which in turn forces $r \leq 3$ so that there cannot exist $[s' + \alpha k]$ with Width$(MR^{[s'+\alpha k]}) = 1$. The possibility $r = 2$ is handled exactly as in the $r = g(K) - 1$ argument, and so we must have $r = 3$. This means $s' = -1$, and so $\tau(K) = g(K) = r = 3$.

If $r = 2g(K) - 3$, then only $l_r^{\pm s'}$ generates non-vertical intersections between columns of $\widetilde{T}$. All other l_r^s intersect $\widehat{HF}(M)$ only in the 0th column, which means that every Width$(MR^{[s]}) = 1$. Since parity(s') = parity$(\tau(K))$ when $r = 2g(K) - 3$, we must have $e_{s'} = 0$. This is because a simple figure-eight component at this height would contribute an intersection with relative grading -1 to $MR^{[s']}$, which would yield Width$(MR^{[s']}) = 2$ and prevent periodicity. We have dim $\widehat{HF}(S_r^3(K), [s']) = 3+2e_{s'+r}$, and so some $[s'+k]$ satisfying $MR^{[s'+k]} \cong MR^{[s']}$ up to translation forces $1 + 2e_{s'+k} = 3 + 2e_{s'+r}$, or $e_{s'+k} = e_{s'+r} + 1$. If necessary, translate $MR^{[s'+k]}$ so that 0 is the smallest element. The only way that the multiplicities of 0 and 1 agree is if $MR^{[s]}$ contains more 0's than 1's, which happens only when parity$(s' + k)$ = parity$(\tau(K))$. But parity(s') = parity$(\tau(K))$ as well, which is a contradiction since k is odd when r odd. □

We return to the two unhandled cases of $\tau(K) = g(K) = r = 3$ and $r = 2(g(K) - 1)$ shortly in Section 6.2, and for now are left with the case where $r = 2g(K) - 1$. Because $\tau(K) = g(K)$, there is no guaranteed simple figure-eight at height $g(K) - 1$. This small difference is enough of an issue if K is an L-space knot, since each $MR^{[s]} = \{0\}$ means $\widehat{HF}$ cannot provide an obstruction. With existing techniques, we can only show the following:

Lemma 6.1.3. *Suppose K is thin with $\tau(K) = g(K)$, and let $r = 2g(K) - 1$. If there exists a k properly dividing r such that every $[s] \in Spin^c(S_r^3(K))$ satisfies $\widehat{HF}(S_r^3(K), [s]) \cong \widehat{HF}(S_r^3(K), [s + k])$, then K is an L-space knot.*

Proof. Suppose for the sake of contradiction that K is not an L-space knot, meaning that dim $\widehat{HF}(S_r^3(K), [s]) > 1$ for some $[s] \in \text{Spin}^c(S_r^3(K))$. Each l_r^s intersects $\overline{\gamma}$ precisely once

since $r \geq 2g(K) - 1$. In order to have dim $\widehat{HF}(S^3_p(K), [s]) > 1$ for some $[s]$, we need for $\widehat{HF}(M)$ to have a simple figure-eight component at height s due to Lemma 2.3.8. Let t be the height of the lowest simple figure-eight component. We have e_t many simple figure-eights at height t, and so we must also have $e_{t+k} = e_t$ many simple figure-eight components at height $t + k$ to satisfy

$$\text{dim } \widehat{HF}(S^3_r(K), [t]) = \text{ dim } \widehat{HF}(S^3_r(K), [t + k]).$$

If parity$([t]) \neq$ parity$([t + k])$, then one of $MR^{[t]}$ or $MR^{[t+k]}$ contains -1 and would need to be translated by 1 to make 0 the smallest element by Proposition 5.1.3. However, this results in both multisets having unequal multiplicities of 0's and 1's. This would lead to $MR^{[t]} \ncong MR^{[t+k]}$ up to translation, and so we must have parity$([t + k])$ = parity$([t])$. However this condition implies that k is even, which contradicts $r = 2g(K) - 1$ being odd. Therefore, K must be an L-space knot. □

6.2 Obstructions from Absolute Gradings

Until now, we have primarily appealed to information carried by $\widehat{HF}(S^3_r(K))$ as this is currently the only flavor of Heegaard Floer homology computable by immersed curves techniques. When considering $S^3_r(K) = Y\#Z$ with $|H^2(Y)| = k < \infty$, we will use properties of the d-invariants mentioned in Subsection 2.2.1 in order to obtain a relationship between r, k, and the V's associated to K. We initially settle the curious $\tau(K) = g(K) = r = 3$ case, and afterwards assemble the proof of Theorem 1.2.3.

Lemma 6.2.1. *Let K be a thin knot with $\tau(K) = g(K) = 3$. Then $S^3_3(K)$ is irreducible.*

Proof. If $S^3_3(K)$ is reducible, it must admit an integer homology sphere connected summand Y since $r = 3$ is prime. Using the additivity of the d-invariants, we have

$$d(S^3_3(K), [s]) = d(L(3, \pm 1), [s]) + d(Y).$$

Proposition 2.2.7 then implies $d(Y) = -2V_0(K) = -2V_1(K)$, which in turn forces $V_0(K) = V_1(K)$. However this is true only for thin knots with even $\tau(K)$, which can be seen using the formula in Proposition 5.1.3 together with $V_s = H_{-s}$. This forms the desired contradiction. □

Lemma 6.2.2. *Let K be a thin knot with $\tau(K) \geq g(K) - 2$. Then $S^3_r(K)$ is irreducible when $r = 2(g(K) - 1)$.*

Proof. Let $\tau(K) \geq g(K) - 2$, and suppose for the sake of contradiction that $S^3_r(K)$ is reducible for $r = 2(g(K) - 1)$. Then $S^3_r(K)$ admits connected summands Y a lens space and Z with $|H^2(Z)| = k < \infty$. Since $H_1(S^3_r(K))$ is cyclic and r is even, one of $|H_1(Y)| = \frac{r}{k}$ or k is even. We will show the latter must be true.

Using the immersed curves techniques of the previous section, we see that $\text{Width}(MR^{[s]}) = 1$ for all $[s]$ when K is thin and $\tau(K) \geq g(K) - 2$. Using $s' \equiv g(K) - 1 (\text{ mod } r)$ again, we are guaranteed to have $\dim \widehat{HF}(S^3_r(K), [s']) > 1$ since $l^{s'}_r$ either intersects a simple figure-eight at height $g(K) - 1$ when $\tau(K) < g(K)$ or intersects $\overline{\gamma}$ multiple times when $\tau(K) = g(K)$. In order for some $[s' - k]$ to satisfy $MR^{[s'-k]} \cong MR^{[s']}$ up to translation, we also require $\text{parity}(s' - k) = \text{parity}(s')$ so that the multiplicities of 0 and 1 agree. This implies k is even.

Let $\pi_Y([s])$ and $\pi_Z([s])$ denote the restrictions of $[s]$ to $\text{Spin}^c(Y)$ and $\text{Spin}^c(Z)$, respectively. Since $\text{Spin}^c(S^3_r(K)) \cong \mathbb{Z}/r\mathbb{Z}$ is $\mathbb{Z}/r\mathbb{Z}$-equivariant [OS08], we have both

$$\pi_Y([s + \tfrac{r}{k})]) = \pi_Y([s]) \text{ and } \pi_Z([s + k]) = \pi_Z([s]).$$

The two self-conjugate spin^c structures of $S^3_r(K)$ must project onto the lone self-conjugate structure of $L(\frac{r}{k}, q)$, and so

$$\pi_Y([0]) = \pi_Y([\tfrac{r}{2}]) \in \text{Spin}^c(L(\tfrac{r}{k}, q)).$$

Their respective restrictions on Z are distinct, and so let $\pi_Z([0]) = \mathfrak{u}_e$ and $\pi_Z([\frac{r}{k}]) = \mathfrak{u}_o$. Due to the additivity of d-invariants, we have

$$d(S^3_r(K), [s]) = d(L(\tfrac{r}{k}, q), \pi_Y([s])) + d(Z, \pi_Z([s])).$$

Since k is even, we may apply this to the self-conjugate structures to see

$$\begin{aligned} d(S^3_r(K), [0]) - d(S^3_r(K), [\tfrac{r}{2}]) &= (d(L(\tfrac{r}{k}, q), [0]) + d(Z, \mathfrak{u}_e)) - (d(L(\tfrac{r}{k}, q), [0]) + d(Z, \mathfrak{u}_o)) \\ &= d(Z, \mathfrak{u}_e) - d(Z, \mathfrak{u}_o). \end{aligned}$$

Observe that $\pi_Z([\frac{k}{2}]) = \mathfrak{u}_0$, and so $\pi_Z([\frac{r+k}{2}]) = \mathfrak{u}_e$. We likewise have $\pi_Y([\frac{k}{2}]) = \pi_Y([\frac{r+k}{2}])$,

and so

$$d(S^3_r(K),[\tfrac{k}{2}]) - d(S^3_r(K),[\tfrac{r+k}{2}]) = d(Z,\mathfrak{u}_o) - d(Z,\mathfrak{u}_e).$$

Using the inductive formula for $d(L(p,q))$ [OS03a, Proposition 4.8], it follows that $d(L(r,1),[s]) = \frac{s^2}{r} - s + \frac{r-1}{4}$. Summing the prior two equations and using Proposition 2.2.7 (with $V_{\frac{r-k}{2}} = \max\{V_{\frac{r+k}{2}}, V_{r-\frac{r+k}{2}}\}$) yields

$$\begin{aligned} 2\left(V_0 - V_{\frac{r}{2}} + V_{\frac{k}{2}} - V_{\frac{r-k}{2}}\right) &= d(L(r,1),[0]) - d(L(r,1),[\tfrac{r}{2}]) + d(L(r,1),[\tfrac{k}{2}]) \\ &\qquad - d(L(r,1),[\tfrac{r+k}{2}]) \\ &= -\left(\frac{r^2}{4r} - \frac{r}{2}\right) + \left(\frac{k^2}{4r} - \frac{k}{2}\right) - \left(\frac{(r+k)^2}{4r} - \frac{r+k}{2}\right) \\ &= \frac{r-k}{2}, \end{aligned}$$

Therefore, we have the following relationship between r, k, and the V's associated to K:

$$\frac{r-k}{4} = (V_0 - V_{\frac{r}{2}}) + (V_{\frac{k}{2}} - V_{\frac{r-k}{2}}). \tag{6.1}$$

Notice that when K is thin and $\tau(K) \geq 0$, we have that

$$V_0 = \begin{cases} \dfrac{\tau(K)+1}{2} & \text{if parity}(\tau(K)) = 1 \\ \dfrac{\tau(K)}{2} & \text{if parity}(\tau(K)) = 0 \end{cases}$$

We will use this to generate contradictions, and break into cases since the values of $V_{\frac{r}{2}}$ and $V_{\frac{r-k}{2}}$ depend on $\tau(K)$. It will also be useful to use the fact that $k \leq \frac{r}{3}$.

Case C1: $\tau(\mathbf{K}) = \mathbf{g}(\mathbf{K})$. Here we have $V_{\frac{r}{2}} = 1$ and $V_{\frac{r-k}{2}} > 0$. We see that $V_{\frac{k}{2}} - V_{\frac{r-k}{2}}$ is given by half the distance between $\frac{r-k}{2} - \frac{k}{2}$ since K is thin. Thus,

$$V_{\frac{k}{2}} - V_{\frac{r-k}{2}} = \frac{r}{4} - \frac{k}{2}.$$

This together with Equation 6.1 above then yields

$$V_0 = \frac{k}{4} + 1.$$

If parity$(\tau(K)) = 1$, then we have

$$\begin{aligned}
&\frac{\tau(K)+1}{2} = \frac{k}{4} + 1 \\
\Leftrightarrow\ &\frac{\tau(K)-1}{2} = \frac{k}{4} \\
\Leftrightarrow\ &\frac{\tau(K)-1}{2} \leq \frac{r}{12} \\
\Leftrightarrow\ &6(\tau(K)-1) \leq 2(g(K)-1) \\
\Leftrightarrow\ &6(\tau(K)-1) \leq 2(\tau(K)-1) \\
\Rightarrow\ &4\tau(K) \leq 4.
\end{aligned}$$

However this would imply $g(K) = \tau(K) = 1 \Rightarrow r = 0$, a clear contradiction. If parity$(\tau(K)) = 0$, then similar reasoning yields $\tau(K) \leq 2$, which forces $r = \tau(K) = g(K) = 2$. We return to immersed curves techniques to rule out this case by comparing the multiplicity of elements of $MR^{[0]}$ and $MR^{[1]}$. Since parity$(\tau(K)) = 0$, we must translate $MR^{[0]}$ by one so that 0 is its smallest element. The multiplicity of 0 in the translated $MR^{[0]}$ is e_0, and the multiplicity of 0 in $MR^{[1]}$ is $2e_1 + 2$. However if $S^3_2(K)$ is reducible then Lemma 2.2.6 forces $e_0 = 2e_1 + 1$ in order for dim $\widehat{HF}(S^3_2(K), [1]) =$ dim $\widehat{HF}(S^3_2(K), [0])$, generating the desired contradiction.

Case C2: $\tau(\mathbf{K}) = \mathbf{g(K)} - \mathbf{1}$. Once again $V_{\frac{r-k}{2}} > 0$, and in this case we obtain $V_0 = \frac{k}{4}$ since $V_{\frac{r}{2}} = 0$. Together with $r = 2\tau(K)$, the argument of the previous case yields the contradiction $4\tau(K) \leq -4$ when parity$(\tau(K)) = 1$ or $4\tau(K) \leq 2$ when parity$(\tau(K)) = 0$.

Case C3: $\tau(\mathbf{K}) = \mathbf{g(K)} - \mathbf{2}$. We still have $V_{\frac{r}{2}} = 0$, and things are more interesting here since it is possible for $V_{\frac{r-k}{2}} = 0$. This happens only if $k = 2$, in which case Equation 6.1 becomes

$$\frac{r-2}{4} = V_0 + V_1.$$

Curiously enough $\tau(K) = V_0 + V_1$ for a thin knot, and so this would force $\tau(K) = \frac{r-2}{4} = \frac{2(\tau(K)+1)-2}{4} \Leftrightarrow 4\tau(K) = 2\tau(K) \Rightarrow \tau(K) = 0$. However this forces $r = k$, a contradiction. Then we cannot have $k = 2$, and so $V_{\frac{r-k}{2}} > 0$ and we once again have $V_0 = \frac{k}{4}$. As with the previous cases, having $r = 2(\tau(K)+1)$ would yield the contradictions $6(\tau(K)+1) \leq 2(\tau(K)+1)$ if parity$(\tau(K)) = 1$ or $4\tau(K) \leq 2$ if parity$(\tau(K)) = 0$. This completes the proof. □

6.3 Proof of Theorem 1.2.3

Proof. Suppose $S^3_r(K)$ is reducible for K thin and hyperbolic. The Matignon-Sayari bound implies that $1 < r \leq 2g(K) - 1$, after mirroring the knot if necessary to make the surgery slope positive. Reducibility also gives $S^3_r(K) \cong Y \# Z$ for some lens space Y and some Z with $|H^2(Z)| = k < \infty$. By Lemma 2.2.6, we have $\widehat{HF}(S^3_r(K), [s + \alpha k]) \cong \widehat{HF}(S^3_r(K), [s])$ for arbitrary $[s], \alpha \in \mathbb{Z}/r\mathbb{Z}$. When $r < 2(g(K) - 1)$, Lemmas 5.2.2, 6.1.1, and 6.1.2 apply to show that there exists an $[s'] \in \mathrm{Spin}^c(S^3_r(K))$ such that either $\widehat{HF}(S^3_r(K), [s'])$ is relatively-graded isomorphic only to $\widehat{HF}(S^3_r(K), [-s'])$, or $\tau(K) = g(K) = r = 3$. The latter is prevented by Lemma 6.2.1, so we proceed with the former. Since $Y \ncong S^3$, we see that $[s']$ cannot be self-conjugate and also that $|H_1(Y)| = 2$. This implies $Y = \mathbb{R}P^3$, as well as $k = |[s'] - [-s']| = 2|[s']|$. However, together this means 4 divides r, which is impossible when $S^3_r(K)$ admits an $\mathbb{R}P^3$ summand with $H_1(S^3_r(K))$ cyclic.

Therefore, we must have $r \geq 2(g(K) - 1)$. Lemmas 5.2.4 and 5.2.5 cover $-g(K) < \tau(K) < g(K) - 2$ and Lemma 6.2.2 covers $\tau(K) \geq g(K) - 2$ for the possibility that $r = 2(g(K) - 1)$, and so we must have $r = 2g(K) - 1$. In this situation k is odd since r is odd, which means periodicity will cycle through spin^c structures with different parities. Then Lemmas 5.2.3, 5.2.5, and 6.1.1 apply to fully obstruct reducibility via the above argument if $\tau(K) \neq g(K)$. If $\tau(K) = g(K)$, our techniques have been exhausted and leave just the conclusion of Lemma 6.1.3, showing that K must be an L-space knot. □

REFERENCES

[BGH08] Kenneth L. Baker, J. Elisenda Grigsby, and Matthew Hedden. Grid diagrams for lens spaces and combinatorial knot Floer homology. *Int. Math. Res. Not. IMRN*, (10):Art. ID rnm024, 39, 2008.

[BGW13] Steven Boyer, Cameron McA. Gordon, and Liam Watson. On L-spaces and left-orderable fundamental groups. *Math. Ann.*, 356(4):1213–1245, 2013.

[BW69] Glen E. Bredon and John W. Wood. Non-orientable surfaces in orientable 3-manifolds. *Invent. Math.*, 7:83–110, 1969.

[BZ98] S. Boyer and X. Zhang. On Culler-Shalen seminorms and Dehn filling. *Ann. of Math. (2)*, 148(3):737–801, 1998.

[Dey19] Subhankar Dey. Cable knots are not thin. *https://arxiv.org/abs/1904.11591*, 2019.

[Doi15] Margaret I. Doig. Finite knot surgeries and Heegaard Floer homology. *Algebr. Geom. Topol.*, 15(2):667–690, 2015.

[Gab87] David Gabai. Foliations and the topology of 3-manifolds. III. *J. Differential Geom.*, 26(3):479–536, 1987.

[GAnS86] Francisco González-Acuña and Hamish Short. Knot surgery and primeness. *Math. Proc. Cambridge Philos. Soc.*, 99(1):89–102, 1986.

[Ghi08] Paolo Ghiggini. Knot Floer homology detects genus-one fibred knots. *Amer. J. Math.*, 130(5):1151–1169, 2008.

[GL87] C. McA. Gordon and J. Luecke. Only integral Dehn surgeries can yield reducible manifolds. *Math. Proc. Cambridge Philos. Soc.*, 102(1):97–101, 1987.

[GL89] C. McA. Gordon and J. Luecke. Knots are determined by their complements. *J. Amer. Math. Soc.*, 2(2):371–415, 1989.

[GL95] C. McA. Gordon and J. Luecke. Dehn surgeries on knots creating essential tori. I. *Comm. Anal. Geom.*, 3(3-4):597–644, 1995.

[Gor83] C. McA. Gordon. Dehn surgery and satellite knots. *Trans. Amer. Math. Soc.*, 275(2):687–708, 1983.

[Gre15] Joshua Evan Greene. L-space surgeries, genus bounds, and the cabling conjecture. *J. Differential Geom.*, 100(3):491–506, 2015.

[Han19] Jonathan Hanselman. Heegaard Floer homology and cosmetic surgeries in S^3. *https://arxiv.org/abs/1906.06773*, 2019.

[Hed11] Matthew Hedden. On Floer homology and the Berge conjecture on knots admitting lens space surgeries. *Trans. Amer. Math. Soc.*, 363(2):949–968, 2011.

[HL16] Matthew Hedden and Adam Simon Levine. Splicing knot complements and bordered Floer homology. *J. Reine Angew. Math.*, 720:129–154, 2016.

[HLZ15] Jennifer Hom, Tye Lidman, and Nicholas Zufelt. Reducible surgeries and Heegaard Floer homology. *Math. Res. Lett.*, 22(3):763–788, 2015.

[How02] James Howie. A proof of the Scott-Wiegold conjecture on free products of cyclic groups. *J. Pure Appl. Algebra*, 173(2):167–176, 2002.

[HRW16] Jonathan Hanselman, Jacob Rasmussen, and Liam Watson. Bordered Floer homology for manifolds with torus boundary via immersed curves. *https://arxiv.org/abs/1604.03466*, 2016.

[HRW18] Jonathan Hanselman, Jacob Rasmussen, and Liam Watson. Heegaard Floer homology for manifolds with torus boundary: properties and examples. *https://arxiv.org/abs/1810.10355*, 2018.

[HW15] Jonathan Hanselman and Liam Watson. A calculus for bordered Floer homology. *https://arxiv.org/abs/1508.05445*, 2015.

[IT03] Kazuhiro Ichihara and Masakazu Teragaito. Klein bottle surgery and genera of knots. *Pacific J. Math.*, 210(2):317–333, 2003.

[IT05] Kazuhiro Ichihara and Masakazu Teragaito. Klein bottle surgery and genera of knots. II. *Topology Appl.*, 146/147:195–199, 2005.

[Jab15] S. Jabuka. Heegaard Floer groups of Dehn surgeries. *J. Lond. Math. Soc. (2)*, 92(3):499–519, 2015.

[Joh79] Klaus Johannson. *Homotopy equivalences of* 3*-manifolds with boundaries*, volume 761 of *Lecture Notes in Mathematics*. Springer, Berlin, 1979.

[JS79] William H. Jaco and Peter B. Shalen. Seifert fibered spaces in 3-manifolds. *Mem. Amer. Math. Soc.*, 21(220):viii+192, 1979.

[KL08] Bruce Kleiner and John Lott. Notes on Perelman's papers. *Geom. Topol.*, 12(5):2587–2855, 2008.

[Lev12] Adam Simon Levine. Knot doubling operators and bordered Heegaard Floer homology. *J. Topol.*, 5(3):651–712, 2012.

[Lic62] W. B. R. Lickorish. A representation of orientable combinatorial 3-manifolds. *Ann. of Math. (2)*, 76:531–540, 1962.

[LOT18a] Robert Lipshitz, Peter Ozsváth, and Dylan P. Thurston. Relative $\mathbb{Q}$-gradings from bordered Floer theory. *Michigan Math. J.*, 67(4):827–838, 2018.

[LOT18b] Robert Lipshitz, Peter S. Ozsvath, and Dylan P. Thurston. Bordered Heegaard Floer homology. *Mem. Amer. Math. Soc.*, 254(1216):viii+279, 2018.

[LW14] Tye Lidman and Liam Watson. Nonfibered L-space knots. *Pacific J. Math.*, 267(2):423–429, 2014.

[Mos71] Louise Moser. Elementary surgery along a torus knot. *Pacific J. Math.*, 38:737–745, 1971.

[MS03] Daniel Matignon and Nabil Sayari. Longitudinal slope and Dehn fillings. *Hiroshima Math. J.*, 33(1):127–136, 2003.

[MT92] William W. Menasco and Morwen B. Thistlethwaite. Surfaces with boundary in alternating knot exteriors. *J. Reine Angew. Math.*, 426:47–65, 1992.

[Ni07] Yi Ni. *Knot Floer homology detects fibred knots*. ProQuest LLC, Ann Arbor, MI, 2007. Thesis (Ph.D.)–Princeton University.

[NW15] Yi Ni and Zhongtao Wu. Cosmetic surgeries on knots in S^3. *J. Reine Angew. Math.*, 706:1–17, 2015.

[NZ18] Yi Ni and Xingru Zhang. Finite Dehn surgeries on knots in S^3. *Algebr. Geom. Topol.*, 18(1):441–492, 2018.

[OS03a] Peter Ozsváth and Zoltán Szabó. Absolutely graded Floer homologies and intersection forms for four-manifolds with boundary. *Adv. Math.*, 173(2):179–261, 2003.

[OS03b] Peter Ozsváth and Zoltán Szabó. Heegaard Floer homology and alternating knots. *Geom. Topol.*, 7:225–254, 2003.

[OS04a] Peter Ozsváth and Zoltán Szabó. Holomorphic disks and genus bounds. *Geom. Topol.*, 8:311–334, 2004.

[OS04b] Peter Ozsváth and Zoltán Szabó. Holomorphic disks and knot invariants. *Adv. Math.*, 186(1):58–116, 2004.

[OS04c] Peter Ozsváth and Zoltán Szabó. Holomorphic disks and three-manifold invariants: properties and applications. *Ann. of Math. (2)*, 159(3):1159–1245, 2004.

[OS04d] Peter Ozsváth and Zoltán Szabó. Holomorphic disks and topological invariants for closed three-manifolds. *Ann. of Math. (2)*, 159(3):1027–1158, 2004.

[OS04e] Peter Ozsváth and Zoltán Szabó. Holomorphic triangle invariants and the topology of symplectic four-manifolds. *Duke Math. J.*, 121(1):1–34, 2004.

[OS05a] Peter Ozsváth and Zoltán Szabó. Heegaard Floer homology and contact structures. *Duke Math. J.*, 129(1):39–61, 2005.

[OS05b] Peter Ozsváth and Zoltán Szabó. On knot Floer homology and lens space surgeries. *Topology*, 44(6):1281–1300, 2005.

[OS05c] Peter Ozsváth and Zoltán Szabó. On the Heegaard Floer homology of branched double-covers. *Adv. Math.*, 194(1):1–33, 2005.

[OS08] Peter S. Ozsváth and Zoltán Szabó. Knot Floer homology and integer surgeries. *Algebr. Geom. Topol.*, 8(1):101–153, 2008.

[OS11] Peter S. Ozsváth and Zoltán Szabó. Knot Floer homology and rational surgeries. *Algebr. Geom. Topol.*, 11(1):1–68, 2011.

[Pet13] Ina Petkova. Cables of thin knots and bordered Heegaard Floer homology. *Quantum Topol.*, 4(4):377–409, 2013.

[Ras03] Jacob Andrew Rasmussen. *Floer homology and knot complements*. ProQuest LLC, Ann Arbor, MI, 2003. Thesis (Ph.D.)–Harvard University.

[Say98] Nabil Sayari. The reducibility of surgered 3-manifolds and homology 3-spheres. *Topology Appl.*, 87(1):73–78, 1998.

[Sch90] Martin Scharlemann. Producing reducible 3-manifolds by surgery on a knot. *Topology*, 29(4):481–500, 1990.

[Sei35] H. Seifert. Über das Geschlecht von Knoten. *Math. Ann.*, 110(1):571–592, 1935.

[Sma61] Stephen Smale. Generalized Poincaré's conjecture in dimensions greater than four. *Ann. of Math. (2)*, 74:391–406, 1961.

[Ter01] Masakazu Teragaito. Creating Klein bottles by surgery on knots. volume 10, pages 781–794. 2001. Knots in Hellas '98, Vol. 3 (Delphi).

[Thu78] William P. Thurston. The geometry and topology of three-manifolds. *Available at http://msri.org/publications/books/gt3m/*, 1978.

[Thu82] William P. Thurston. Three-dimensional manifolds, Kleinian groups and hyperbolic geometry. *Bull. Amer. Math. Soc. (N.S.)*, 6(3):357–381, 1982.

[VS99] Luis Gerardo Valdez Sánchez. Dehn fillings of 3-manifolds and non-persistent tori. volume 98, pages 355–370. 1999. II Iberoamerican Conference on Topology and its Applications (Morelia, 1997).

[Wal60] Andrew H. Wallace. Modifications and cobounding manifolds. *Canadian J. Math.*, 12:503–528, 1960.

[Wan06] Jiajun Wang. Cosmetic surgeries on genus one knots. *Algebr. Geom. Topol.*, 6:1491–1517, 2006.

[Wat12] Liam Watson. Surgery obstructions from Khovanov homology. *Selecta Math. (N.S.)*, 18(2):417–472, 2012.